

Report No. BMI-1381

UC-25 Metallurgy and Ceramics  
(TID-4500, 15th Ed.)

Contract No. W-7405-eng-92

PROGRESS RELATING TO CIVILIAN APPLICATIONS  
DURING SEPTEMBER, 1959

by

Russell W. Dayton  
Clyde R. Tipton, Jr.

October 1, 1959

BATTELLE MEMORIAL INSTITUTE  
505 King Avenue  
Columbus 1, Ohio

## **DISCLAIMER**

**This report was prepared as an account of work sponsored by an agency of the United States Government. Neither the United States Government nor any agency Thereof, nor any of their employees, makes any warranty, express or implied, or assumes any legal liability or responsibility for the accuracy, completeness, or usefulness of any information, apparatus, product, or process disclosed, or represents that its use would not infringe privately owned rights. Reference herein to any specific commercial product, process, or service by trade name, trademark, manufacturer, or otherwise does not necessarily constitute or imply its endorsement, recommendation, or favoring by the United States Government or any agency thereof. The views and opinions of authors expressed herein do not necessarily state or reflect those of the United States Government or any agency thereof.**

## **DISCLAIMER**

**Portions of this document may be illegible in electronic image products. Images are produced from the best available original document.**



TABLE OF CONTENTS

	<u>Page</u>
REPORTS RELATING TO CIVILIAN APPLICATIONS ISSUED DURING SEPTEMBER, 1959 . . . . .	5
A. ASSISTANCE TO HAPO . . . . .	7
Mechanical Properties of Zirconium Alloys . . . . .	7
A Photographic Study of the Corrosion of Defected Fuel Elements in High-Temperature Water . . . . .	7
Development of a Fuel-Element Leak Detector . . . . .	9
Thermal-Neutron-Flux Monitoring System . . . . .	9
Development of Corrosion-Resistant Welding Alloys for Use With Hastelloy F to Contain Decladding Solutions . . . . .	10
B. DEVELOPMENTS FOR ALUMINUM-CLAD FUEL ELEMENTS . . . . .	13
Preparation of Aluminum-Uranium Alloys . . . . .	13
C. RADIOISOTOPE AND RADIATION APPLICATIONS . . . . .	15
Development of Radioactive-Tracer Quality-Control Systems . . . . .	15
Use of Intrinsic Radioactive Tracers for Process Control . . . . .	17
Graft-Polymerization Studies . . . . .	18
Nitration of Hydrocarbons . . . . .	19
F. RESEARCH FOR AEC REACTOR DEVELOPMENT DIVISION PROGRAM . . . . .	23
REACTOR MATERIALS AND COMPONENTS . . . . .	23
Valence Effects of Oxide Additions to Uranium Dioxide . . . . .	24
High-Pressure High-Temperature Solid-State Studies . . . . .	24
Irradiation-Surveillance Program on Type 347 Stainless Steel . . . . .	26
Development of Niobium-Base Alloys . . . . .	29
Development of Corrosion-Resistant Niobium Alloys . . . . .	31
Investigation of the Creep Properties of Zircaloy-2 During Irradiation at Elevated Temperatures . . . . .	35
Determination of Oxygen in Sodium at Concentrations Below 10 PPM . . . . .	37
STUDIES OF ALLOY FUELS . . . . .	37
Development of Niobium-Uranium Alloys . . . . .	38
Development of Thorium-Uranium Alloys . . . . .	39
FISSION-GAS RELEASE FROM REFRACTORY FUELS . . . . .	42
Characterization of Sintered UO <sub>2</sub> and Model of Gas Release . . . . .	43
Diffusion in UO <sub>2</sub> . . . . .	44
Preparation for In-Pile Study . . . . .	45
GENERAL FUEL-ELEMENT DEVELOPMENT . . . . .	45
Fabrication of Cermet Fuel Elements . . . . .	45
Gas-Pressure Bonding of Molybdenum- and Niobium-Clad Fuel Elements . . . . .	46
Factors Affecting Pressure Bonding . . . . .	48
FF. FUEL-CYCLE PROGRAM STUDIES . . . . .	51
GAS-PRESSURE BONDING OF CERAMIC, CERMET, AND DISPERSION FUEL ELEMENTS . . . . .	51
DEVELOPMENT OF URANIUM CARBIDE-TYPE FUEL MATERIALS . . . . .	55
Alternate Fabrication Methods for UC . . . . .	56
Melting and Casting Techniques for Uranium-Carbon Alloys . . . . .	57
Metallurgical and Engineering Properties of Uranium Monocarbide . . . . .	58
Uranium Monocarbide Diffusion Studies . . . . .	58
Irradiation Effects in UC . . . . .	60
GG. VOID-DISTRIBUTION AND HEAT-TRANSFER STUDIES . . . . .	61
H. PHYSICAL RESEARCH . . . . .	63
Thermal Migration of Hydrogen in Zirconium . . . . .	63
I. SOLID HOMOGENEOUS FUELED REACTORS . . . . .	65
LABORATORY EVALUATIONS OF FUELED-GRAPHITE SPHERES . . . . .	65
EVALUATION OF METAL-COATED UO <sub>2</sub> PARTICLES . . . . .	65
FABRICATION DEVELOPMENT OF AL <sub>2</sub> O <sub>3</sub> -CLAD UO <sub>2</sub> FUEL PARTICLES . . . . .	65
FISSION-PRODUCT RELEASE FROM FUELED-GRAPHITE SPHERES . . . . .	66
Neutron-Activation Studies . . . . .	66
In-Pile Capsule Experiments . . . . .	67
J. PROBLEMS ASSOCIATED WITH THE RECOVERY OF SPENT REACTOR FUEL ELEMENTS . . . . .	69
Corrosion Studies of the Fluoride-Volatility Process . . . . .	69
Study of the Effect of Irradiation on Cladding- and Core-Dissolution Processes . . . . .	70
K. DEVELOPMENTS FOR SRE, OMRE, AND OMR . . . . .	73
EVALUATION OF URANIUM MONOCARBIDE AS A REACTOR FUEL . . . . .	73
Irradiation of Uranium Monocarbide . . . . .	73
Postirradiation Examination of Irradiated Uranium Monocarbide . . . . .	73
Preparation of UC Pins for Irradiation in the SRE . . . . .	74

TABLE OF CONTENTS  
(Continued)

	<u>Page</u>
L. TANTALUM AND TANTALUM-ALLOY STUDIES . . . . .	75
Development of Container Materials for LAMPRE Applications . . . . .	75
Effect of Irradiation on Tantalum . . . . .	78
N. DEVELOPMENTS FOR THE MGCR . . . . .	79
FABRICATION AND CHARACTERIZATION OF FUEL MATERIALS . . . . .	79
UO <sub>2</sub> Dispersions in BeO . . . . .	80
UC and UC <sub>2</sub> Dispersions in Graphite . . . . .	80
Cladding of UO <sub>2</sub> Particles With BeO . . . . .	80
Carburization Studies in the BeO-Graphite System . . . . .	81
Preliminary Characterization by Neutron Activation . . . . .	81
STUDIES OF FISSION-GAS RELEASE FROM FUEL MATERIALS . . . . .	82
Detailed Neutron-Activation Studies . . . . .	82
In-Pile Studies . . . . .	82
HIGH-BURNUP IRRADIATION EFFECTS IN FUEL MATERIALS . . . . .	84
DIFFUSION OF FISSION PRODUCTS IN CLADDING MATERIALS . . . . .	85
CARBON-TRANSPORT CORROSION STUDIES . . . . .	86
O. ENGINEERING ASSISTANCE TO KAISER ENGINEERS . . . . .	87
Reactor-Flow Studies . . . . .	87
P. DEVELOPMENTAL STUDIES FOR THE SM-2 . . . . .	89
Materials Development . . . . .	89
Encapsulation Studies . . . . .	91
Q. GAS-COOLED REACTOR PROGRAM . . . . .	93
MATERIALS DEVELOPMENT PROGRAM . . . . .	93
Fabrication of UO <sub>2</sub> Pellets . . . . .	93
Fabrication of BeO-UO <sub>2</sub> Fuel Pellets . . . . .	95
Encapsulation Studies . . . . .	96
Effects of Irradiation . . . . .	98
GCRE Critical-Assembly Experiments . . . . .	101
IN-PILE-LOOP PROGRAM . . . . .	102
BRR Loop Program . . . . .	102
ETR Loop Program . . . . .	103

REPORTS RELATING TO CIVILIAN APPLICATIONS  
ISSUED DURING SEPTEMBER, 1959

- BMI-1365 "Development of Uranium Nitride-Stainless Steel Dispersion Fuel Elements", by Stan J. Paprocki, Donald L. Keller, George W. Cunningham, and Andrew K. Foulds, Jr.
- BMI-1371 "Spray Deposition of Calcium Metal on Nickel or Inconel", by Albert F. Haskins and Robert M. Evans.
- BMI-1372 "Progress on the Use of Gas-Pressure Bonding for Fabricating Low-Cost Ceramic, Cermets, and Dispersion Fuels", work done by Donald L. Keller, Edwin S. Hodge, Charles B. Boyer, John B. Fox, and Donald E. Kizer.
- BMI-1373 "The Diffusion of Hydrogen in Beta Zirconium", by William M. Albrecht and W. Douglas Goode, Jr.
- BMI-1377 "Progress Relating to Civilian Applications During August, 1959", by Russell W. Dayton and Clyde R. Tipton, Jr.



THE UNIVERSITY OF CHICAGO  
DEPARTMENT OF CHEMISTRY

REPORT OF THE  
COMMISSION ON THE  
STRUCTURE OF THE  
ATOMIC NUCLEUS

BY  
R. F. B. AND  
M. J. S.

CHICAGO, ILLINOIS  
1952

UNIVERSITY OF CHICAGO PRESS



## A-1

## A. ASSISTANCE TO HAPO

F. R. Shober

The creep properties of annealed and 15 per cent cold-worked Zircaloy-2 are being determined at 290, 345, and 400 C for times as long as 15,000 hr. The effects of a cyclic exposure at 290 and 345 C on the creep properties of annealed and cold-worked material are also being investigated. Additional work to determine the rate of dissolution of AgBr as a function of the flow rate has been done in the investigation to develop an isotopic-exchange fuel-element leak-detection system.

Work on a thermal-neutron-flux monitoring system has been concerned with development of fabrication techniques for tubular ceramic specimens. Methods to attach electrical contacts to ceramic bodies are being investigated to obtain a bond which is both electrically and mechanically sound over the 100 to 1200 F temperature range. A new program to develop corrosion-resistant welding alloys for use with Hastelloy has been initiated. The alloys are to be resistant to boiling Niflex and Sulflex solutions used for decladding fuel elements.

Mechanical Properties of Zirconium Alloys

L. P. Rice and J. A. VanEcho

The creep properties of annealed and 15 per cent cold-worked Zircaloy-2 are being determined at elevated temperatures. Long-time creep tests (15,000 hr) are being conducted at 290, 345, and 400 C on 15 per cent cold-worked material. Both annealed and cold-worked Zircaloy-2 are also being tested under cyclic-temperature conditions. Some tests on cold-worked Zircaloy-2 are still in progress.

Creep data accumulated to date on specimens of annealed Zircaloy-2 sheet are presented in Table A-1. These tests are tentatively set for 5000 hr. It is readily apparent from the data presented that very little creep occurs in annealed Zircaloy-2 sheet at 290 and 345 C. Nearly all of the deformation took place on loading, and only limited creep occurred thereafter regardless of the stress. At 400 C, on the other hand, deformation occurred by creep rather than on initial loading. These tests are continuing.

A Photographic Study of the Corrosion of Defected  
Fuel Elements in High-Temperature Water

E. F. Stephan and F. W. Fink

The individual films for the different specimens studied have been combined into a single reel. All experimental work has been completed. A topical report is in preparation.

TABLE A-1. TENTATIVE CREEP DATA ON ANNEALED ZIRCALOY-2 SHEET

Specimen	Stress, psi	Deformation at Indicated Time, per cent				Time in Progress, hr	Minimum Creep Rate, per cent per hr	
		On Loading	100 Hr	500 Hr	1500 Hr			Final
<u>290 C (550 F)</u>								
Zr-A-7	27,500	--	--	--	--	20.3	0.9 <sup>(a)</sup>	8.0
Zr-A-6	25,000	--	--	--	--	44.3	0.3 <sup>(a)</sup>	--
Zr-A-10	22,500	3.180	4.250	4.260	4.270	4.286	4500	0.00001
Zr-A-13	20,000	1.54	2.800	2.817	2.825	2.825	1500	0.00001
Zr-A-14	17,500	1.250	1.940	1.940	1.946	1.946	1500	--
Zr-A-18	15,000 <sup>(b)</sup>	0.635	0.960	0.960	0.959	0.959	1500	--
<u>345 C (650 F)</u>								
Zr-A-8	25,000	--	3.18	5.41	--	--	857.8 <sup>(a)</sup>	0.004
Zr-A-3	22,500	4.27	4.95	5.00	5.10	5.82	4000	0.0001
Zr-A-15	20,000	2.24	4.13	4.19	--	--	1000	0.00006
Zr-A-17	17,500	1.778	1.860	1.890	1.924	--	1500	0.00003
Zr-A-25	15,000 <sup>(b)</sup>	0.971	1.008	--	--	--	100	--
<u>400 C (750 F)</u>								
Zr-A-9	21,860	--	--	--	--	36.6	Failed on loading	--
Zr-A-2	21,800	--	--	--	--	21.3	48.7 <sup>(a)</sup>	0.15
Zr-A-12	17,500	2.20	3.32	11.96	--	45.7	1035.7 <sup>(a)</sup>	0.025
Zr-A-5	15,000	0.896	2.10	5.40	12.4	20.4	2500	0.006
Zr-A-16	12,500	0.447	0.681	1.005	1.686	--	1500	0.00055
Zr-A-21	10,000 <sup>(c)</sup>	0.113	0.227	0.356	--	--	500	0.00028

Note: Specimens Zr-A-1 through Zr-A-12 were from one batch of material. Balance of specimens starting with Zr-A-13 were from a second batch. Each batch was annealed separately.

(a) Rupture time; all other tests are in progress.

(b) A stress of 12,500 psi is scheduled.

(c) A stress of 9,000 psi is scheduled.

A-3

Development of a Fuel-Element Leak Detector

J. E. Howes, Jr., T. S. Elleman, and D. N. Sunderman

This report summarizes the progress on the development of an isotopic-exchange fuel-element leak-detection system.

During the past month, the rate of dissolution of AgBr as a function of flow rate was investigated. Water at 180 F was flowed through a column of silver-110-tagged AgBr at rates of 0.4, 1, and 1.5 gal per min. Rate of dissolution of AgBr was measured as described in BMI-1377. The rate of dissolution under these conditions was found to vary from 29 mg per hr at 0.4 gal per min to 77 mg per hr at 1.5 gal per min.

Experiments are now in progress to determine the exchange between iodine-131 and AgBr as a function of AgBr column size and flow rate. AgBr was selected as the exchange material since the rate of dissolution of AgCl was too great to be usable. From the exchange experiments the optimum column size and flow rate will be selected for use in the prototype system.

Thermal-Neutron-Flux Monitoring System

P. M. Steinback, J. W. Lennon, M. J. Snyder, and D. R. Grieser

A thermal-neutron-flux monitoring system is being developed for Hanford reactors. The system will be an improved version of a device previously produced (BMI-1083) for neutron-flux measurement. Operation is based on the measurement of the electrical power required to maintain the temperature of a dummy element at the same level as that of an adjacent element containing a fissionable material.

The present study of ceramic-element fabrication techniques has progressed to the extent that tubular specimens have been produced by extrusion. Recent experiments indicate that slight adjustments can be made in composition and firing temperature to yield extruded specimens which have the desired resistivity and  $UO_2$  content. Additional extruded specimens will be produced, and the study of the effects of composition and processing variables on the reproducibility and stability of properties will be continued.

An investigation of the attachment of electrical contacts to the ceramic bodies is being made. Contacts having limited reliability have been produced by silver painting platinum-wire loops onto element faces. Although these junctions are not mechanically as strong as either the wire or the ceramic body, their electrical stability has permitted extensive testing of the electrical characteristics of the ceramic bodies. Other methods of contact attachment, such as Microbrazing, are being investigated in order to obtain a bond which is both electrically and mechanically sound over the anticipated operating-temperature range of 100 to 1200 F.

The electrical characteristics of the ceramic elements are being studied in detail. The data so far show that element resistivities remain fairly reproducible over the temperature range of 100 to 1500 F. The exaggerated change in resistivity with time at elevated temperatures which was encountered in previous studies has not been encountered in the present investigations. It is not yet known whether this is a result of a difference in measuring technique or of improved control in the fabrication process. Continued study of the electrical properties of both dust-pressed and extruded specimens will be made to determine the range of variability of resistance with composition, fabrication technique, temperature, induced current, and time. Additional theoretical calculations will be made to determine the electrical and mechanical tolerances which will be allowable in the production of flux-measuring probes.

Development of Corrosion-Resistant Welding Alloys for Use  
With Hastelloy F to Contain Decladding Solutions

M. E. Langston and A. M. Hall

A program directed toward the development of corrosion-resistant welding alloys for use with vacuum-melted low-carbon Hastelloy F to contain HAPO spent-fuel-element decladding solutions was initiated. The program is to be conducted in the following sequence: (1) vacuum-induction melting of 12 initial alloy compositions, (2) processing of the ingots to 1/8-in. -thick strip, (3) preparation and evaluation of weldments, and (4) evaluation of the corrosion resistance of weldments as well as of solution-annealed unwelded alloys in boiling Niflex and Sulfex decladding solutions. Based on the results obtained for the initial alloys with respect to forming, welding, and corrosion properties, a second series of alloy compositions will be selected and evaluated.

Vacuum-induction melting of 15-lb heats of the alloy compositions listed in Table A-2 is in progress. The heats are being poured into Zirconite sand molds to produce a tapered rectangular ingot weighing about 8 to 9 lb, a small pilot ingot of similar shape weighing about 1 to 1-1/2 lb, and a tapered circular hot top weighing about 5 to 6 lb. The pilot ingot will be used to determine suitable forging-temperature ranges for each of the alloys.

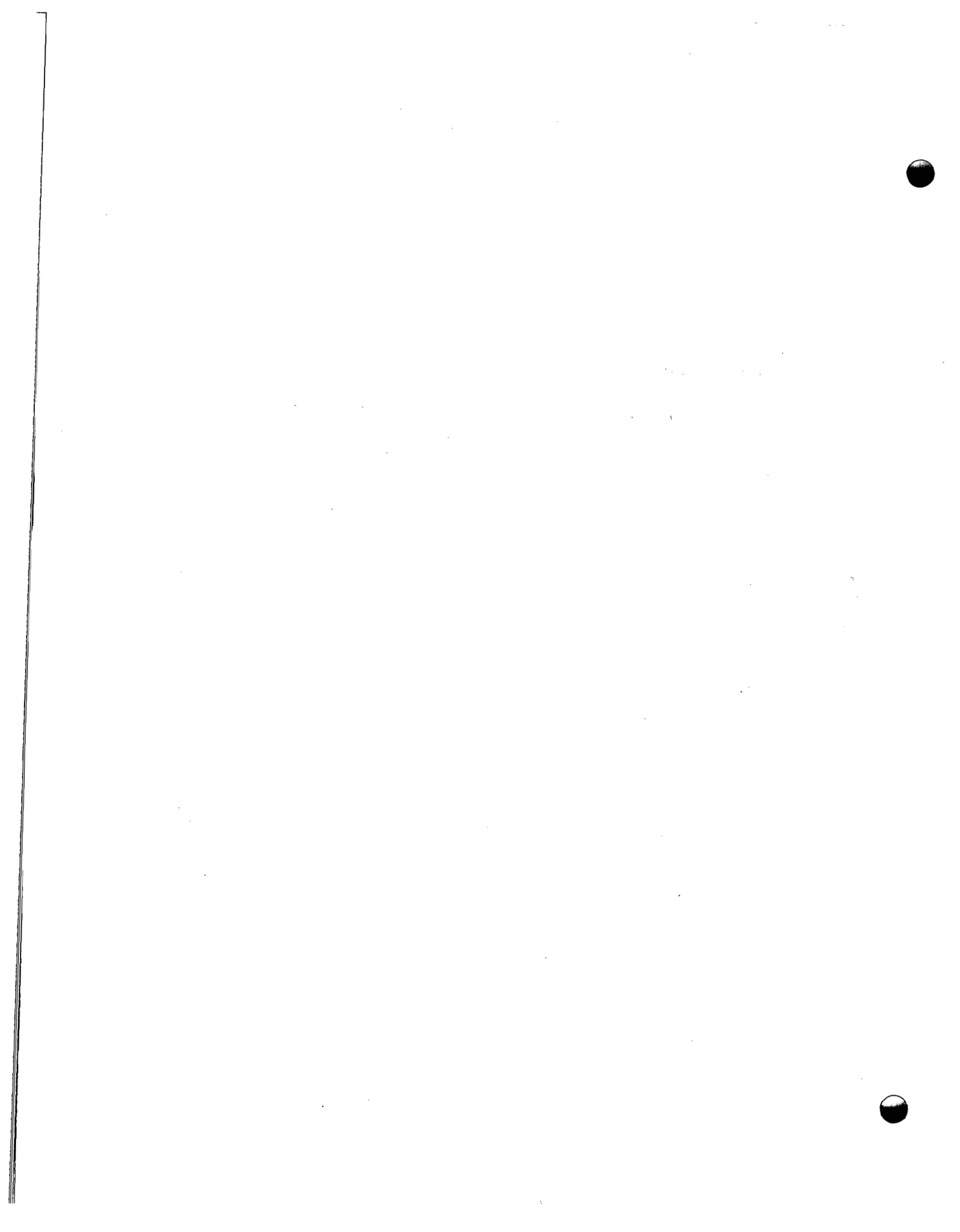
It is estimated that annealed strip material will be ready for the welding-research group by the end of October.

## A-5 and A-6

TABLE A-2. INTENDED COMPOSITIONS OF INITIAL SERIES OF CORROSION-RESISTANT WELDING ALLOYS FOR HAPO

Alloy	Intended Composition (Balance Iron) <sup>(a)</sup> , w/o						
	Cr	Ni	Mo	Cu	C	Nb	Ti
1B	22	45	6	1	0.02	2	--
2B	22	45	6	2	0.02	2	--
3B	22	45	6	--	0.02	--	0.5
4B	22	45	6	--	0.02	--	1
5B	22	45	3	2	0.02	--	0.5
6B	22	45	3	2	0.02	--	1
7B	22	45	6	3	0.02	2	--
8B	22	45	9	1	0.02	2	--
9B	22	45	3	1	0.02	2	--
10B	22	45	6	2	0.02	--	--
11B	22	45	6	2	0.02	--	1
12B	22	45	3	2	0.02	2	--

(a) Includes 0.6 w/o manganese and 0.4 w/o silicon additions.



## B-1

## B. DEVELOPMENTS FOR ALUMINUM-CLAD FUEL ELEMENTS

N. E. Daniel

In the study of aluminum-uranium fuels, 35 w/o uranium alloys with ternary additions of zirconium and tin, designed for fabrication by extrusion, are being investigated. Extruded sections from 16 ingots are being prepared for evaluation.

Preparation of Aluminum-Uranium Alloys

N. E. Daniel, E. L. Foster, and R. F. Dickerson

The objective of this research is to develop more satisfactory fuels from the aluminum-uranium system. Alloys containing 35 w/o uranium and which are amenable to extrusion fabricating techniques are being investigated. Previous experience has shown that 3 w/o additions of tin or zirconium will enhance the casting characteristics of the aluminum-35 w/o uranium alloy and will also inhibit the  $UAl_3$ - $UAl_4$  transformation. Retention of  $UAl_3$  provides greater quantities of aluminum in the matrix of the alloys and tends to improve the fabricating characteristics.

To investigate the properties of the aluminum-35 w/o uranium alloys containing tin and zirconium, and to determine the minimum quantity of each of these additions necessary for the retention of the  $UAl_3$ , 3-in. -diameter by 10-in. -long castings containing 0.5 to 3.0 w/o of each addition have been prepared. Sixteen castings were poured. Fluidity tests have been conducted on each melt. Preliminary evaluation of the fluidity tests indicates that maximum fluidity is obtained with a tin content of 1.5 w/o. All of the alloys containing zirconium exhibited fluidities approximately equivalent to that of the binary alloys. Slab specimens from the top and bottom of each 3-in. -diameter ingot have been radiographed and sectioned to obtain specimens for hot-hardness, X-ray diffraction, and metallographic evaluation.

Six-inch-long by 3-in. -diameter sections from each of the 16 ingots have been extruded utilizing the conditions outlined below:

Billet temperature	800 F
Container temperature	800 F
Die temperature	600 F
Length of billet	6 in.
Ram speed	20 in. per min
Reduction	16/1

## B-2

Lubricant

1 part Aquadag to 16 parts lead, by weight, plus 3 oz. of water

Die

Mild steel; entrance angle, of 90 deg

Sufficient material was recovered from each extrusion to obtain specimens for subsequent evaluation. The evaluation of the extruded material will involve radiography, hot-hardness, X-ray diffraction, and metallographic examinations as well as elevated-temperature tensile, creep, stress-rupture, and corrosion tests. Specimens are being prepared.

Future work will include the evaluation of the above-mentioned extruded material. Preliminary casting studies preparatory to making enriched castings of selected ternary alloys will be made in the near future. The castings will be made in the form of hollow cylindrical extrusion billets.

C-1

## C. RADIOISOTOPE AND RADIATION APPLICATIONS

D. N. Sunderman

A continuing program is under way for the Office of Isotopes Development in the fields of radioisotope application and radiation chemistry. Studies include the development of radiotracer applications in quality control, intrinsic tracers for process control, the effect of ionizing radiation upon graft polymerization, and the nitration of hydrocarbons.

The development of the radiometric method for the determination of calcium has been completed. Levels of accuracy and precision have been established as a function of concentration of CaO and the presence of interfering elements. Neutron activation of gross cement samples will be concluded following the next series of experiments as a result of its ability to produce only semiquantitative results.

In the intrinsic-tracer study effort is being concentrated on an iron-removal process common to many nonferrous-mineral beneficiation processes. Radioassay efficiencies for process solutions containing iron tracer have been studied over a range of sample volumes to establish optimum conditions and minimize tracer concentrations.

Graft-polymerization experimentation has shown that several previous investigators may have been confused by the presence of monomer in measurement of the hyperfine structure of irradiated material by electron paramagnetic resonance. With carefully purified material and a dose of  $5.75 \times 10^5$  r,  $1.5 \times 10^{-3}$  site was found per monomer unit. The chemical method of free-radical measurement indicates  $8.5 \times 10^{-4}$  site per monomer unit.

Experiments are under way to separate the thermal and radiation effects in the nitration of hydrocarbons. The composition of the reaction vessel may also affect yields of nitrocompounds. The interaction of these effects will be studied to allow optimization of nitrocompound yield and oxidation effects.

Development of Radioactive-Tracer Quality-Control Systems

C. W. Townley, C. T. Brown, and D. N. Sunderman

The development of a radiometric method for the determination of CaO in portland cement has been completed. The procedure involves the precipitation of  $\text{Ca}_3(\text{PO}_4)_2$  from alkaline solution with  $(\text{NH}_4)_2\text{HPO}_4$  labeled with phosphorus-32. The reduction of radioactivity in the solution due to the precipitation of  $\text{Ca}_3(\text{PO}_4)_2$  is a measurement of the CaO present. The complete experimental method and a sample calculation were given in BMI-1377.

## C-2

The development of the CaO procedure has been concluded during this report period with a study of the effects of CaO concentration and interfering ions on the accuracy of the method. The results of determinations made with CaO concentrations ranging from 3 to 33 mg per 50 ml of solution are summarized in Table C-1. In all of these runs the ratio of ammonium phosphate to calcium was held constant. The precision and accuracy were within 1 per cent for the determination made with CaO concentrations of 13 mg per 50 ml and above. The error increased with decreasing concentration below 13 mg CaO per 50 ml.

TABLE C-1. PRECISION AND ACCURACY OF CaO DETERMINATIONS  
AS A FUNCTION OF CaO CONCENTRATION

Theoretical	CaO Concentration, mg per 50 ml		Standard Deviation, mg of CaO	Absolute Error, per cent
	Experimental	Experimental Average		
3.33	2.94 2.83	2.88	±0.08	13.5
8.33	7.86 7.98	7.92	±0.08	4.9
10.00	9.31 9.91 9.89	9.70	±0.34	3.0
13.32	13.36 13.30 13.17	13.28	±0.10	0.3
16.66	8 determinations <sup>(a)</sup>	16.67	±0.08	0.06
33.32	33.26 33.92 33.39	33.52	±0.35	0.6

(a) Data presented in BMI-1377.

The effect of interfering elements on the calcium determination has been investigated with CaO concentrations of 16.66 mg per 50 ml and concentrations of contaminant at approximately the same order of magnitude as in portland cement. The elements found to interfere were aluminum, iron, and magnesium. Iron yielded results 6 per cent high when present at a concentration of 1 mg per 50 ml. In the 50 ml of solution, 1 mg of magnesium and 1 mg of aluminum gave results 13 per cent and 9 per cent high, respectively. Manganese did not interfere even at a quantity 20 times that found in a cement sample (0.2 mg per 50 ml).

Work has begun on the development of a radiometric method for analyzing for aluminum and iron in portland cement. Some preliminary work has been done on an EDTA titration of aluminum using  $\text{Ag}^{110}\text{IO}_3$  as an indicator. Results thus far indicate that the titration must be done in a basic solution in order to form the EDTA complex of

## C-3

silver. Thus a chelating agent such as tartaric acid must be employed to prevent the precipitation of the aluminum. Also, the solution must be heated to assist in the formation of the EDTA complex of aluminum.

During the next report period additional studies will be made of the optimum conditions for the radiometric titration of aluminum. Similar work will be done on the EDTA titration of iron, and an attempt will be made to determine the aluminum and iron in the same solution by a radiometric titration.

Another activation analysis will be attempted during the next report period to determine the effect of improved dosimetry and measurement of photopeak areas and to place a limit of accuracy on the method.

#### Use of Intrinsic Radioactive Tracers for Process Control

J. L. McFarling, H. B. Brugger, J. F. Kircher, and D. N. Sunderman

During the month of September laboratory work on radiotracer control of the copper-stripping operation was de-emphasized in favor of the iron-removal-control study. Those experiments already under way were completed but no further work with the copper-stripping operation is planned.

The results of the evaluation of the three methods for concentrating the copper activity mentioned in BMI-1377 are as follows:

- (1) Adsorption of copper-64 on a chelating ion-exchange resin does not appear to be feasible because little separation takes place among copper, cobalt, and nickel ions at the pH of the process solutions.
- (2) Precipitation of copper-64 with adsorption on a carrier would probably accomplish the desired activity concentration, but this method would not be continuous.
- (3) Isotopic exchange with inactive CuS suggested by the  $\text{Cu}^{64++}$ -CuS exchange studies would probably be possible but it is not continuous nor is it as accurate as (2).

Based on the work done so far, no good method can be recommended at this time for concentrating the copper-64 activity and increasing the precision of the radioassay. Further work along these lines is not contemplated at the present time.

Experiments were attempted to define more accurately the problem of exchange between copper-64 in solution and CuS precipitate under simulated process conditions. These experiments were unsuccessful. The conditions present in the process could not be duplicated with the present equipment. However, based on the available evidence it is felt that the exchange is severe enough to seriously limit the planned application of radiotracers to control of the copper-stripping operation.

Laboratory experiments have begun on radiotracer control of iron removal from the cobalt-nickel stream in the ammonia-leach nickel-refining process. The detection efficiency of the dip counter, a Nuclear Chicago 2 by 2-in. NaI(Tl) scintillation probe, for iron-59 in solution has been determined for volumes up to 33 liters. The results are given in Table C-2.

TABLE C-2. RADIOASSAY EFFICIENCY IN VARIOUS VOLUMES OF IRON-59 SOLUTION

Effective Counting Volume, liters	Iron-59 Activity, dpm/l	Net Counting Rate, cpm	Efficiency, $\frac{\text{cpm}}{\text{dpm/l}} \times 100$ , per cent
1	50,000	3,210	6.4
3.75	50,000	5,780	11.6
9	50,000	9,730	19.4
14	50,000	12,480	25.0
33	50,000	18,040	36.1

Experimental loops are being built for study of the radioisotope detection methods under conditions closely simulating those of an actual process. These experimental loops, which are nearly completed, will duplicate the process conditions before and after iron removal. An experimental program has been designed to study effects of changes in temperature, concentration in solution, and flow rate.

Next month effort will be concentrated on the experimental-loop program. The contamination and radiation-hazards study will also be undertaken soon.

#### Graft-Polymerization Studies

I. S. Ungar, R. A. Markle, J. F. Kircher, and R. I. Leininger

During this month free-radical studies utilizing the Varian electron-paramagnetic-resonance (EPR) apparatus were continued. Samples of pure polymethylmethacrylate (PMMA) produced by radiation polymerization and treated at 100 C in vacuo did not produce the seven-line hyperfine structure reported in the literature. However, a rod of commercial PMMA gave a spectrum which coincided exactly. In order to determine the source of the reported spectrum, samples of purified PMMA were contaminated with benzoyl peroxide and monomeric methylmethacrylate. The spectrum of the specimen containing benzoyl peroxide was no different from the pure PMMA. However, the sample contaminated with monomer produced a spectrum in which the line width was intermediate between the commercial polymer and the polymer prepared at Battelle. The contaminated sample also showed evidence of the hyperfine structure reported by previous investigators. The best estimate of unpaired spins that can be made from EPR studies at this time is  $1.5 \times 10^{-3}$  site per monomer unit. This increases to  $4.25 \times 10^{-3}$  site per monomer unit upon the admission of air to the sample tube. These values were obtained at a dose of  $5.75 \times 10^5$  r.

C-5

The chemical method for free-radical measurement was further refined and the procedure for handling the samples standardized. The average of four samples of PMMA was  $8.5 \times 10^{-4}$  site per monomer unit for a dose of  $5.75 \times 10^5$  r. One cannot say which of the two methods utilized for active-site measurement produces the better value, since the possibility exists that the same active center is not being measured in each case.

Further study was undertaken to determine the extent of thermal grafting which occurs during the separation procedure used in radiation-induced grafting. Samples of polymethyl- and polybutylmethacrylate were deactivated by heat in a vacuum to preclude the presence of residual peroxide or free radicals. The polymer was heated for 2 hr at 100 C under vacuum after being sealed in tubes. Half the samples were treated with freshly distilled vinylpyrrolidone without irradiation and half with irradiation to a dose of  $5.75 \times 10^5$  r. The samples were carefully fractionated and extracted to remove vinylpyrrolidone and its polymer. Nitrogen analysis showed that the unirradiated polymer contained one-third to one-half the nitrogen found in the irradiated samples. In addition, only one-third as much grafted polymer was formed from the unirradiated samples.

Radiation-polymerized PMMA has been fractionated into relatively narrow molecular-weight fractions. The fractions with molecular weights of approximately 6,000 and 13,000 have been chosen for further study. These samples will be irradiated, grafted, and fractionated. It is hoped that the separation of grafted from ungrafted polymer will be more sharply defined. During the preparation of the samples having the narrow molecular-weight range the polymers were precipitated several times. This would remove any slight traces of monomer remaining in the polymer. EPR studies will be made on irradiated samples of this highly purified polymer to determine if the spectrum previously obtained for PMMA was influenced by slight traces of monomer.

During the next month work will continue along the lines described above. In addition, any promising results obtained with polymethylmethacrylate will be expanded to other polymers.

#### Nitration of Hydrocarbons

M. J. Oestmann, R. E. Fulmer, G. A. Lutz, and J. F. Kircher

In the study of radiation-induced nitration of hydrocarbons, a series of thermal and irradiation runs was completed in the liquid phase of the nitric acid-cyclohexane system.

Reaction mixtures containing a 5-to-1 or 10-to-1 mole ratio of cyclohexane and nitric acid were studied in both glass and stainless steel vessels. Analytical results from nine runs are reported in Table C-3. Gas chromatography and infrared analysis were the chief techniques used to identify the reaction products. These products include nitrocyclohexane, a polynitro compound, cyclohexyl nitrate, cyclohexanol, cyclohexanone, dicyclohexyl, and adipic acid. The polynitro compound has not been positively identified. Current work indicates that this latter compound contains two or more  $-\text{NO}_2$  groups and one or more cyclohexane rings.

TABLE C-3. PRODUCT ANALYSIS OF NITRIC ACID-CYCLOHEXANE RUNS

Run	C <sub>6</sub> H <sub>12</sub> /HNO <sub>3</sub> Mole Ratio	Vessel	Tempera- ture, C	Reaction Time, hr	Gamma Dose, rads	Yield of Reaction Products, w/o of cyclohexane charge						
						C <sub>6</sub> H <sub>11</sub> NO <sub>2</sub>	(C <sub>6</sub> H <sub>11</sub> ) <sub>M</sub> (NO <sub>2</sub> ) <sub>N</sub>	C <sub>6</sub> H <sub>11</sub> ONO <sub>2</sub>	C <sub>5</sub> H <sub>11</sub> OH	C <sub>5</sub> H <sub>10</sub> C=O	(C <sub>6</sub> H <sub>11</sub> ) <sub>2</sub>	(CH <sub>2</sub> ) <sub>4</sub> (COOH) <sub>2</sub> and Tar
1	5 to 1	Stainless	30	92	--	0.06	--	--	--	--	Trace	--
2	5 to 1	Stainless	60	168	--	3.8	0.17	--	0.03	0.05	0.21	1.15
6	5 to 1	Glass	60	4.7	--	0.04	--	--	--	--	--	--
				21.5	--	0.85	--	--	--	--	--	--
				28.2	--	1.5	--	--	--	--	--	--
				46.6	--	2.7	--	--	--	--	--	--
				52.3	--	2.8	--	--	--	--	--	--
4	5 to 1	Stainless	110	68	--	9.0	Trace	0.14	0.49	0.08	0.74	1.3
3	5 to 1	Stainless	140	144	--	11.2	Trace	--	0.72	0.67	Trace	0.6
7	10 to 1	Stainless	60	166	--	4.2	--	--	0.13	0.04	--	0.66
5	10 to 1	Stainless	60	136	2 x 10 <sup>7</sup>	1.9	Trace	Trace	0.21	0.09	0.19	--
9(30W)	10 to 1	Glass	<60 <sup>(a)</sup>	117	2 x 10 <sup>7</sup>	0.10	--	--	--	--	--	--
(30D)						0.10	--	--	--	--	--	--
(30CW)						0.10	0.01	--	Trace	Trace	0.02	--
(30CD)						0.13	0.01	--	Trace	Trace	0.01	--
8(28W)	10 to 1	Glass	<60 <sup>(a)</sup>	168	3 x 10 <sup>7</sup>	0.89	0.21	0.13	0.18	0.15	0.27	--
(28D)						0.95	0.21	0.08	0.22	0.18	0.27	--

(a) Poor temperature control.

C-6

## C-7 and C-8

Oxidation reactions, producing alcohols, ketone, and adipic acid, compete with the nitration reaction. Yields of these oxidation products are generally smaller than those from the nitration reaction. However, in Run 3, a thermal run made at the highest temperature (140 C), the yield of nitrocyclohexane (11 w/o) was the highest observed so far. Higher temperatures increase the extent of oxidation and nitration.

In a kinetic study of the nitration reaction, the formation of nitrocyclohexane at 60 C was found to reach a maximum at 50 to 70 hr. This may be due to the thermal decomposition of the product. This, in turn, may be a limiting factor on the yield of compound for a given dose rate. Thus the maximum yield will be a function of dose rate as well as total dose and temperature. These parameters will be investigated in future runs.

The effect of vessel material on the nature and yield of products is not well defined in Table C-3. When more runs are completed, the effect of this parameter will be clarified.

Results from two thermal runs (2 and 7) indicate that a 10-to-1 mole ratio of hydrocarbon to nitric acid gives a slightly higher yield of nitrocyclohexane than a 5-to-1 mole ratio. The evidence for lower yields of nitrocyclohexane at 60 C in a radiation field (Runs 5, 8, and 9) compared with the yield of thermal runs (Run 7) at this temperature is not firm because of poor temperature control in two of these runs. In addition, results from Runs 8 and 9 are questionable due to breakage of a glass-covered metal stirring bar which exposed the reaction mixture to a metal surface.

To check the analytical techniques, the reaction mixture in Run 9 was separated into four different fractions. Fraction 30W was water washed and dried over  $\text{Na}_2\text{SO}_4$ . Fraction 30D was similarly treated but was washed with a  $\text{BaCO}_3$  solution prior to drying. Fractions 30CW and 30CD were treated by the same method as the corresponding 30W and 30D but concentrated by removal of most of the unreacted cyclohexane by fractional distillation. In each case, except for Fraction 30CD, the product yields were reproducible. It is concluded that satisfactory analytical techniques are now available for analyses of future runs.

To prove that radiation decomposition of nitrocyclohexane is not important in the interpretation of the results in Table C-3, samples of this compound were irradiated up to  $1 \times 10^8$  rads. Less than 1 w/o was decomposed.

During October, additional thermal and irradiation runs will be made. These runs will be carried out using a 10-to-1 mole ratio of hydrocarbon to acid in a glass container. Reaction times will be about 70 hr, and the total dose will be about  $1 \times 10^7$  rads. For the liquid-phase experiments, the temperature will be increased, possibly up to 200 C. Runs in the vapor phase will also be initiated. Work on the identification of the polynitro compound will be continued.



F-1

## F. RESEARCH FOR AEC REACTOR DEVELOPMENT DIVISION PROGRAM

S. J. Paprocki and R. F. Dickerson

REACTOR MATERIALS AND COMPONENTS

R. F. Dickerson

Ternary oxide samples are being prepared for studies of uranium oxide stabilization by means of valence compensation. High-pressure high-temperature studies of uranium oxides are also in progress, with principal effort being devoted to  $U_3O_8$ . The gamma high-pressure modification of  $U_3O_8$  has been found to contain the same oxygen content as normal  $U_3O_8$ . The combined effect of high pressure and high temperature is to reduce  $U_3O_8$  to lower oxides. Results suggest that  $U_4O_9$  can be retained under high pressure to oxygen contents associated with the  $U_3O_8$  phase field and that the excess oxygen enters uranium vacancies to produce an antistructure disorder.

Three groups of capsules containing tensile, fatigue, or impact specimens of Type 347 stainless steel are being irradiated in or awaiting insertion into the ETR. Two groups of capsules are being irradiated at 120 F. Specimens from one group of these capsules are to be annealed at 600 F prior to postirradiation testing. The third group of capsules is to be irradiated at 600 F; irradiation of these capsules has not begun due to the lack of suitable space in the ETR.

Tensile data at 650 and 800 C have been obtained for niobium-base alloys being studied as possible cladding materials in the EBR. Inability to cold roll some of these alloys may have been caused by oxygen contamination during processing; increases in oxygen content of 200 to 820 ppm over that in unalloyed niobium have been determined by vacuum-fusion analysis. Tensile data at 1200 and 1500 F are also reported for niobium-base alloys being developed for pressurized-water reactor operation along with corrosion-test data obtained in 600 and 680 F water and 750 F steam. Binary niobium-vanadium alloys appear to offer the optimum combination of cross section, strength, and corrosion resistance for the desired application. Corrosion tests of unalloyed niobium, being performed as part of a cooperative program with KAPL, BAPD, and Battelle, showed that after 28 days in 680 F water samples continued to gain weight, while after 28 days in 750 F steam samples began to flake and lose weight.

Design studies are under way for an investigation of in-pile creep of Zircaloy-2. Specimens for use in creep and also in strain-aging studies of Zircaloy-2 have been fabricated, and methods of producing thin sections of zirconium and Zircaloy-2 for study by transmission electron microscopy are being investigated.

A program is in progress to develop techniques for the continuous monitoring of oxygen in sodium at concentrations of less than 10 ppm oxygen to a sensitivity of  $\pm 1$  ppm. A sodium purification system for the production of sodium test samples is under construction. The test samples will be used in evaluating the sensitivity, reproducibility, and speed of detection of the various techniques under consideration.

Valence Effects of Oxide Additions to Uranium Dioxide

W. B. Wilson, A. F. Gerds, and C. M. Schwartz

Solid-state studies are continuing on the effect of oxide additions to uranium oxide. Previous research has shown that valence compensation may be employed to stabilize the fluorite structure of  $\text{UO}_2$  under both oxidizing and reducing conditions. Current effort has been directed toward reduction of the amount of additive required for stable materials by partial substitution of divalent oxides for trivalent oxides. A final series of ternary oxides has been fabricated. The analytical results and evaluation of the oxidation characteristics of this series have not been completed.

A sample of uranium oxide containing 2 mole per cent  $\text{La}_2\text{O}_3$  has been fabricated for evaluation of the effects of the  $\text{La}_2\text{O}_3$  additions on the thermal conductivity. Previous results have shown this composition to have very high electrical conductivity.

Specimens are being prepared to evaluate the electrical and thermal conductivities of solid solutions of  $\text{U}_3\text{O}_8$  containing 40, 50, and 60 mole per cent  $\text{La}_2\text{O}_3$ . These fully oxidized solid solutions have not been previously investigated.

High-Pressure High-Temperature Solid-State Studies

W. B. Wilson and C. M. Schwartz

An exploratory investigation is being conducted to determine the effects of ultra-high pressure and high temperature on uranium oxides and on reactions of uranium oxides with mixed oxides. Emphasis has been placed in current work on study of the effect of pressure on  $\text{U}_3\text{O}_8$ .

Samples of  $\text{U}_3\text{O}_8$  previously subjected to high pressure and high temperature were analyzed for oxygen content using a microbalance technique. This work was performed to further establish the oxygen content of the new gamma  $\text{U}_3\text{O}_8$  produced under pressure. In addition, when  $\text{U}_3\text{O}_8$  was subjected to pressures in excess of 60,000 atm at temperatures of 400 and 500 C, gamma  $\text{U}_3\text{O}_8$  was found to coexist with a cubic structure having a lattice parameter, 5.40 A, nearly identical to that of  $\text{U}_4\text{O}_9$ . Thus, it was of interest to establish if this cubic structure was  $\text{U}_4\text{O}_9$  or represented the  $\text{U}_4\text{O}_9$  structure containing a large excess of oxygen over that which occurs at normal pressure. The results of the microbalance analysis are contained in Table F-1.

The table shows that the gamma high-pressure modification of  $\text{U}_3\text{O}_8$  has the same oxygen composition as normal  $\text{U}_3\text{O}_8$  within the limits of accuracy of the microbalance equipment. Samples 112, 113, and 114 contained an estimated 25 w/o  $\text{U}_4\text{O}_9$  based upon diffraction analyses, yet their composition was still within the limits of the normal-pressure  $\text{U}_3\text{O}_8$  phase field. This result further suggests that the cubic structure of  $\text{U}_4\text{O}_9$  can be retained by pressure to much higher oxygen content. The samples run in the internally heated die at higher temperatures show an oxygen loss, as has been previously observed.

## F-3

TABLE F-1. MICROBALANCE ANALYSES OF  $U_3O_8$  SAMPLES SUBJECTED TO HIGH TEMPERATURES AND PRESSURES

Sample	Pressure, atm	Temperature, C	Analyzed Composition, x in $UO_x$	Phases Present
58	16,600	400	2.66	Gamma $U_3O_8$
59	16,600	500	2.66	Ditto
60	25,000	500	2.65	Ditto
61	25,000	600	--(a)	Ditto
62	37,500	400	2.65	Ditto
63	37,500	500	--(b)	Ditto
112	60,000	500	2.63	Gamma + $U_4O_9$
113	60,000	400	--(c)	Gamma + $U_4O_9$
114	60,000	300	2.65	Alpha, gamma, $U_4O_9$
100	50,000	~800	2.61 <sup>(d)</sup>	Gamma
97	50,000	~1300	2.38 <sup>(d)</sup>	$U_3O_7$

(a) Mixed with Sample 60.

(b) Mixed with Sample 62.

(c) Mixed with Sample 112.

(d) Run in internally heated die.

Samples 97, 112, 113, and 114 appeared to evolve gas, probably oxygen, during the initial heating in vacuum. In addition, particles were ejected from the platinum bucket at a temperature near 400 C. This necessitated weighing to obtain an accurate assay of oxygen content. The unusual behavior of these samples on heating suggests that the  $U_4O_9$  and  $U_3O_7$ -like phases underwent a rapid transformation, causing the ejection of some particles.

The table also confirms the previous result that the combined effect of pressure and high temperature is to reduce  $U_3O_8$  to lower oxides, since the high-pressure apparatus is not gastight. The terminal product of this reduction may have a direct relationship on the normal-pressure oxidation mechanism of uranium dioxide.

Recent diffraction results and electrical studies of the  $U_4O_9$  phase suggest the possibility that the excess oxygen enters uranium vacancies to produce antistructure disorder. Previous work had considered that the excess oxygen occupied the body-centered position of the fluorite structure. Since the body-centered position is surrounded with a cubic array of oxygen ions, the radius of an interstitial ion in this position must be less than that of an oxygen ion. If the oxygen is assumed to enter as an interstitial atom, the decrease in lattice parameter is difficult to explain since the uranium ion should not change to the smaller (+6) valence state.

The assumption that the oxygen enters as an ion in the uranium position would require expansion of the lattice parameter. This, however, is offset by the change in valence in the uranium. Thus, the 1.05-A-radius  $U^{+4}$  ion is replaced by the average of an oxygen ion and a  $U^{+6}$  ion. These are nominally 1.32 and 0.80 A in radius, respectively, and yield an average of 1.06 A which is very close to the  $U^{+4}$  size. Such "averaging" of ion sizes occurs in the stabilized solid solutions of  $UO_2$  containing  $La_2O_3$  and  $Y_2O_3$ .

If antistructure disorder occurs for the  $U_4O_9$  phase the density of the phase should be less than that of  $UO_2$ . Since the effect of pressure should be to produce the most dense phase, the terminal product of reduction at high pressure should yield information on the oxidation mechanism. Recent experiments in which thermocouples were directly inserted into the sample region, allowing oxygen to readily escape, have shown  $UO_2$  to be the terminal product. It must be confirmed, however, that this occurred as the result of pressure and not of chemical reduction.

The calibration of the new die to beyond 100,000 atm has been completed. The previously determined calibration using barium has been shown to be in error; a minor transition at 60,000 atm having been detected instead of the required 80,000-atm transition. A number of  $U_3O_8$  samples and other reactions have been run at 100,000 atm at temperatures above 1000 C. Analyses of these are not complete.

#### Irradiation-Surveillance Program on Type 347 Stainless Steel

W. E. Murr, F. R. Shober, J. E. Howes, and J. F. Lagedrost

The objective of this program is to determine the changes produced in the mechanical properties of Type AISI 347 stainless steel by fast-neutron bombardment (energies greater than 1 Mev) at specimen temperatures of 120 and 600 F. The surveillance program is being performed in connection with the KAPL C-33 loop and other loops employing Type 347 stainless steel in their construction.

Three groups of capsules containing tensile, fatigue, or impact specimens have been prepared and shipped to the ETR, where they are being irradiated or are waiting to be inserted in the reactor. One group of eight capsules will be irradiated at process-water temperature (120 F). A second group will operate at 600 F, and a third group will operate at 120 F but will be annealed at 600 F before postirradiation testing. It is believed that postirradiation annealing at 600 F will produce an intermediate condition between that produced by irradiations at 120 and 600 F. Irradiation data have been reported for Type 347 stainless steel at exposures up to  $3.76 \times 10^{21}$  n per  $cm^2$ . The main objective of the surveillance program is to determine mechanical properties of this material after exposures between this exposure and an exposure of  $1.6 \times 10^{22}$  n per  $cm^2$ , which is ultimately expected in the KAPL C-33 loop after 3 years of service. In order that the irradiation program may be of use, the exposures obtained in the irradiation program must lead those experienced by the loop by a minimum of 6 months.

The total neutron accumulation for the eight "cold" capsules (irradiated at process-water temperature) as of the end of Cycle 19 (September 7) is given in Table F-2, along with a list of proposed irradiation parameters of the remaining capsules in the program. The capsules operated the equivalent of 13.8 days at full power during Cycle 19, and are currently nearing the end of Cycle 20.

The three capsules to be given postirradiation annealing studies, BMI-24-18, BMI-24-20, and BMI-24-22, were loaded into the reactor during the shutdown for Cycle 19. The fluxes accumulated by these capsules during this cycle are reported in Table F-2.

TABLE F-2. CAPSULES PREPARED FOR THE 347 STAINLESS STEEL IRRADIATION SURVEILLANCE PROGRAM

Capsule	Type of Specimens in Capsules	Proposed Irradiation Temperature, F	Approximate Removal Date(a)	Approximate Exposure at Time of Removal(b), nvt	Total Exposure as of September 7, 1959, nvt		Location	Remarks
					Top	Bottom		
BMI-24-1	Tensile and fatigue	600	January, 1959	$1.55 \times 10^{20}$	--	--	BMI	Examined at BMI Hot-Cell Facility for melting
BMI-24-2	Tensile and fatigue	120	January, 1962	$1.31 \times 10^{22}$	$2.680 \times 10^{21}$	$3.521 \times 10^{21}$	ETR K-8-NE	Being irradiated
BMI-24-3	Tensile and fatigue	600	--	--	--	--	ETR	To be irradiated
BMI-24-4	Tensile and fatigue	120	January, 1963	$1.78 \times 10^{22}$	$1.733 \times 10^{21}$	$2.956 \times 10^{21}$	ETR K-8-SE	Being irradiated
BMI-24-5	Tensile and fatigue	600	--	--	--	--	ETR	To be irradiated
BMI-24-6	Tensile and fatigue	120	June, 1961	$1.08 \times 10^{22}$	$3.631 \times 10^{21}$	$2.801 \times 10^{21}$	ETR K-8-NE	Being irradiated
BMI-24-7	Tensile and fatigue	600	--	--	--	--	ETR	To be irradiated
BMI-24-8	Tensile and fatigue	120	June, 1962	$1.54 \times 10^{22}$	$1.987 \times 10^{21}$	$2.925 \times 10^{21}$	ETR K-8-SE	Being irradiated
BMI-24-9	Tensile and fatigue	600	--	--	--	--	ETR	To be irradiated
BMI-24-10	Tensile and fatigue	120	January, 1961	$0.84 \times 10^{22}$	$2.938 \times 10^{21}$	$3.140 \times 10^{21}$	ETR K-8-SE	Being irradiated
BMI-24-11(c)	Tensile and fatigue	600	--	--	--	--	ETR	Damaged at ETR
BMI-24-12	Tensile and fatigue	120	June, 1960	$0.61 \times 10^{22}$	$3.894 \times 10^{21}$	$3.260 \times 10^{21}$	ETR L-8-SE	Being irradiated
BMI-24-13	Impact	600	--	--	--	--	ETR	To be irradiated
BMI-24-14	Impact	120	June, 1962	$1.54 \times 10^{22}$	$3.411 \times 10^{21}$	$3.486 \times 10^{21}$	ETR K-8-NW	Being irradiated

51

TABLE F-2. (Continued)

Capsule	Type of Specimens in Capsules	Proposed Irradiation Temperature, F	Approximate Removal Date(a)	Approximate Exposure at Time of Removal(b), nvt	Total Exposure as of September 7, 1959, nvt		Location	Remarks
					Top	Bottom		
BMI-24-15	Impact	600	--	--	--	--	ETR	To be irradiated
BMI-24-16	Impact	120	June, 1960	$0.61 \times 10^{22}$	$3.459 \times 10^{21}$	$3.200 \times 10^{21}$	ETR K-8-NW	Being irradiated
BMI-24-17(c)	Tensile and fatigue	600	October, 1958	$3.25 \times 10^{20}$	--	--	BMI	Examined at BMI Hot- Cell Facility after high temperature observed
BMI-24-18	Tensile and fatigue	120	--	--	$1.66 \times 10^{20}$	$2.8 \times 10^{20}$	ETR	Being irradiated for postirradiation an- nealing studies
BMI-24-19(c)	Tensile and fatigue	600	--	--	--	--	ETR	Fabricated to replace BMI-24-17
BMI-24-20	Tensile and fatigue	120	--	--	$2.26 \times 10^{20}$	$3.26 \times 10^{20}$	ETR	Being irradiated for postirradiation an- nealing studies
BMI-24-21	Tensile and fatigue	600	--	--	--	--	ETR	Fabricated to replace BMI-24-1
BMI-24-22	Tensile and fatigue	120	--	--	$2.26 \times 10^{20}$	$3.8 \times 10^{20}$	ETR	Being irradiated for postirradiation an- nealing studies

(a) Based on 6-month lead on loop, plus 2 months for examination.

(b) Based on maximum fast flux at tube of  $1.7 \times 10^{14}$  nv for 6-month periods.

(c) Thermocouple lead capsules.

## F-7

The group of capsules designed to operate at a temperature near 600 F has not been inserted into the ETR since space of suitable quality is not available. Should the lack of suitable space in the ETR continue to exist, an alternate test reactor having the necessary flux requirements will be considered for the "hot" capsule experiment.

Recent information from the ETR indicates that a proposed rearrangement of fuel elements in the immediate vicinity of the stainless steel surveillance capsules will cause a lowering of the instantaneous flux seen by the capsules. If this should occur, it is expected to produce changes in the capsule removal dates reported in Table F-2, with more pronounced changes expected in the removal dates of capsules scheduled for the higher exposures.

#### Development of Niobium-Base Alloys

J. A. DeMastry, F. R. Shober, and R. F. Dickerson

Reactors operating at elevated temperature (800 C) require that the fuels be clad with a material which will possess sufficient strength and corrosion resistance to preserve the integrity of the encased fuel. The high melting point and elevated-temperature strength of niobium and niobium-base alloys should satisfy these requirements. Being studied for possible use as cladding materials in the EBR are niobium-1 w/o chromium, niobium-2 w/o chromium, niobium-4.5 w/o zirconium, niobium-10 w/o tantalum-2 w/o chromium, niobium-20 w/o titanium-1.5 w/o chromium, niobium-40 w/o titanium-10 w/o aluminum, unalloyed niobium, and an alloy containing vanadium-10 w/o titanium-1 w/o niobium.

Melting, determination of hot and cold fabricability, metallographic examinations, chemical analyses, and a short heat-treatment study have been completed. The niobium-1 w/o chromium, niobium-4.5 w/o zirconium, niobium-20 w/o titanium-1.5 w/o chromium, and vanadium alloys have been cold rolled to 0.035-in. sheet. Although the center of the sheet was sound, severe edge cracking was present in all cases.

Tensile and corrosion specimens have been prepared from the center portion of the sheet. The corrosion specimens have been sent to ANL. Determination of the mechanical properties at 650 and 800 C has been initiated and the results obtained to date are shown in Tables F-3 and F-4.

The unalloyed niobium and the niobium-40 w/o titanium-10 w/o aluminum alloy failed to cold roll. In order to determine if the alloys had been contaminated during processing, vacuum-fusion analyses for oxygen and hydrogen were performed. Table F-5 lists the results of these analyses. The unalloyed niobium showed an increase in oxygen content from 200 to 820 ppm, which may account for its failure to fabricate. However, the oxygen contents of the remaining alloys do not explain the poor fabrication results which were obtained.

The niobium-2 w/o chromium and niobium-10 w/o tantalum-2 w/o chromium alloys were placed in evacuated stainless steel packs and rolled at 2000 F. Both alloys failed to fabricate under these conditions.

TABLE F-3. TENSILE DATA AT 650 C (1200 F) FOR NIOBIUM-BASE ALLOYS

Analyzed Alloy Composition, w/o	0.2 Per Cent Offset Yield Strength, psi	Tensile Strength, psi	Elongation, per cent
Nb-1.84 Cr	107,000	115,000	4
Nb-4.33 Zr	--	82,400	4
Nb-20.5 Ti-4.28 Cr	75,500	92,200	11
Type 347 stainless steel	41,000	51,200	46

TABLE F-4. TENSILE DATA AT 800 C (1472 F) FOR NIOBIUM-BASE ALLOYS

Analyzed Alloy Composition, w/o	0.2 Per Cent Offset Yield Strength, psi	Tensile Strength, psi	Elongation, per cent
Nb-1.84 Cr	68,700	81,600	14
Nb-4.33 Zr	69,000	76,700	4

TABLE F-5. RESULTS OF VACUUM-FUSION ANALYSES OF NIOBIUM-BASE ALLOYS

Melting stock contained 200 ppm oxygen and 20 ppm hydrogen.

Analyzed Alloy Composition, w/o	Analyses, ppm	
	Oxygen	Hydrogen
Niobium	820	5
Nb-1.83 Cr	90	43
Nb-3.21 Cr	60	82
Nb-4.33 Zr	392	61
Nb-9.95 Ta-3.31 Cr	300	92
Nb-39.8 Ti-10.6 Al	313	146
Nb-20.5 Ti-4.28 Cr	350	54
V-11.7 Ti-3.07 Nb	680	98

## F-9

In order to make a thorough evaluation of the fabrication characteristics of these alloys, additional ingots are being prepared. Sections will be cut from these alloys, and an attempt to fabricate these sections will be made.

Development of Corrosion-Resistant Niobium Alloys

D. J. Maykuth, W. D. Klopp, E. F. Adkins, R. I. Jaffee,  
W. E. Berry, and F. W. Fink

The evaluation of selected niobium-base alloys for service in pressurized-water reactors was continued. The results of current work show that binary niobium-vanadium alloys offer the greatest advantage as a base material over the other binary-alloy systems investigated. The present work is concerned with optimizing alloy compositions to improve fabricability while maintaining adequate hot strength and corrosion resistance.

The corrosion results obtained to date in 600 and 680 F water and 750 F 1500-psi steam are summarized in Table F-6. The results continue to indicate that:

- (1) Unalloyed niobium does not possess adequate corrosion resistance.
- (2) The most corrosion-resistant alloys are those containing more than 40 a/o zirconium or a ternary alloy containing 28 a/o titanium-6 a/o chromium.
- (3) Niobium alloys with 7 to 12 a/o vanadium offer the optimum combination of low neutron cross section, high strength, and adequate corrosion resistance.
- (4) Addition of a third alloying agent to the 2.5 or the 5 a/o vanadium alloys does not improve their corrosion resistance.

Included in Table F-6 are results for tests started recently on additional screening alloys. After 7 days of exposure in 680 F water, niobium alloys containing 2.5 a/o zirconium, 10 a/o iron, or 2.5 a/o nickel-2.5 a/o vanadium were losing weight or exhibited large weight gains. A 5 a/o iron alloy and a 2.5 a/o vanadium-2.5 a/o zirconium alloy appear resistant at this stage of exposure.

The cooperative corrosion-testing program with BAPD and KAPL is continuing. Unalloyed niobium specimens have now been exposed 56 days in 680 F water and 750 F 1500-psi steam. Weight gains in 680 F water average 116 mg per dm<sup>2</sup>, with a range of 111 to 126 mg per dm<sup>2</sup>. Specimens have been slowly losing weight since the 42-day exposure, at which time the average weight gain was 121 mg per dm<sup>2</sup>. Specimens in 750 F steam exhibit weight losses ranging from 612 to 756 mg per dm<sup>2</sup>, with an average of 671 mg per dm<sup>2</sup>.

All corrosion tests except those noted in Table F-6 are being continued.

## F-10

TABLE F-6. SUMMARY OF CORROSION RESULTS OBTAINED ON NIOBIUM ALLOYS EXPOSED IN HIGH-TEMPERATURE WATER AND STEAM

Alloy Addition (Balance Niobium), a/o	600 F Water		680 F Water		750 F Steam	
	Exposure Time, days	Total Weight Change, mg per cm <sup>2</sup>	Exposure Time, days	Total Weight Change, mg per cm <sup>2</sup>	Exposure Time, days	Total Weight Change, mg per cm <sup>2</sup>
<u>Commercial-Niobium, Rocking-Hearth Melts</u>						
Unalloyed Nb	196	-18.6	42(a)	Disintegrated	28(a)	Disintegrated
10.5 Zr	--	--	196(a)	0.67	112	-17.2
26.1 Zr	--	--	196(a)	0.07	--	--
35.7 Zr	--	--	196(a)	0.66	--	--
45.7 Zr	--	--	196(a)	0.55	--	--
1.08 W	--	--	196(a)	-2.60	112	-27.0
4.67 W	--	--	196(a)	-29.3	--	--
9.56 W	--	--	7(a)	Cracked	--	--
2.45 Mo	--	--	196(a)	-7.10	98	Disintegrated at 98 days
5.20 Mo	--	--	196(a)	-1.30	112	-62.0
7.40 Mo	--	--	196(a)	0.62	--	--
4.42 V	--	--	196(a)	0.42	112	-1.48
6.59 V	--	--	196(a)	0.73	112	1.28
8.93 V	--	--	196(a)	0.59	112	1.04
10.7 V	--	--	196(a)	0.78	--	--
13.7 V	--	--	196(a)	0.50	--	--
24.2 V	--	--	196(a)	0	--	--
4.90 Fe	--	--	196(a)	0.10	98	Disintegrated at 98 days
9.41 Ti	--	--	196(a)	0.65	112	1.32
18.8 Ti	--	--	196(a)	0.48	--	--
24.3 Ti	--	--	196(a)	0.52	--	--
30.5 Ti	--	--	196(a)	0.40	--	--
33.8 Ti	--	--	196(a)	0.33	--	--
12.0 Ti-0.5 Cr	--	--	196(a)	0.66	--	--
20.2 Ti-2.1 Cr	--	--	196(a)	0.39	--	--
28.2 Ti-1.1 Cr	--	--	196(a)	0.20	--	--
12.0 Ti-4.2 Mo	--	--	196(a)	0.64	--	--
17.4 Ti-6.2 Mo	--	--	196(a)	0.54	--	--
23.1 Ti-7.8 Mo	--	--	196(a)	0.45	--	--
10.4 Ti-5.0 V	--	--	196(a)	0.56	--	--
16.1 Ti-8.4 V	--	--	196(a)	0.40	--	--
22.6 Ti-11.0 V	--	--	196(a)	0.48	--	--
<u>High-Purity Niobium, Consumable-Electrode Melts</u>						
Unalloyed Nb	196	0.79	196	-4.88	196	-43.7
7.18 Mo	196	0.67	196	-0.03	70(a)	Cracked
12.5 V	196	0.37	196	0.58	196	0.80

## F-11

TABLE F-6. (Continued)

Alloy Addition (Balance Niobium), a/o	600 F Water		680 F Water		750 F Steam	
	Exposure Time, days	Total Weight Change, mg per cm <sup>2</sup>	Exposure Time, days	Total Weight Change, mg per cm <sup>2</sup>	Exposure Time, days	Total Weight Change, mg per cm <sup>2</sup>
<u>High-Purity Niobium, Consumable-Electrode Melts (Continued)</u>						
46.8 Zr-5.06 Ti	196	0.32	168	0.90	168	2.55
11.2 Ti-3.2 Mo	168	0.44	168	0.57	168	0.70
18.8 Ti-8.7 Mo	168	0.22	168	0.46	168	0.60
9.9 Zr-9.4 V	84	0.25	84	0.25	70	-2.02
5.7 Zr-11.4 V	84	0.22	84	0.22	70	-0.24
9.1 Ti-6.3 Cr	84	0.25	84	0.25	70	-1.81
<u>High-Purity Niobium, Rocking-Hearth Melts</u>						
Unalloyed Nb	--	--	112	1.27	--	--
Unalloyed Nb	--	--	84 <sup>(a)</sup>	Disintegrated at 84 days	--	--
Unalloyed Nb	--	--	84	0.77	--	--
1 Zr	--	--	112	-137.0	--	--
2.5 Zr	--	--	7	-0.25	--	--
5 Zr	--	--	84	-3.35	--	--
10 Zr	--	--	84	-0.04	--	--
40 Zr	--	--	84	0.61	--	--
65 Zr	--	--	84	0.75	--	--
75 Zr	--	--	84	0.94	--	--
90 Zr	--	--	84	0.85	--	--
2.5 Ti	--	--	112	-1.06	--	--
10.0 Ti	--	--	112	0.57	--	--
25.0 Ti	--	--	112	0.38	--	--
1 Cr	--	--	112	1.02	--	--
5 Cr	--	--	112	0.54 <sup>(b)</sup>	--	--
10 Cr	--	--	84	-0.72	--	--
1 Fe	--	--	84	-0.22	--	--
5 Fe	--	--	7	0.22	--	--
10 Fe	--	--	7	-0.25	--	--
10 Zr-5 Ti	--	--	84	0.50	--	--
25 Zr-5 Ti	--	--	84	0.31	--	--
25 Zr-15 Ti	--	--	84	0.57	--	--
25 Zr-25 Ti	--	--	84	0.41	--	--
35 Zr-5 Ti	--	--	84	0.47	--	--
35 Zr-15 Ti	--	--	84	0.45	--	--
45 Zr-5 Ti	--	--	84	0.58	--	--

TABLE F-6. (Continued)

Alloy Addition (Balance Niobium), a/o	600 F Water		680 F Water		750 F Steam	
	Exposure Time, days	Total Weight Change, mg per cm <sup>2</sup>	Exposure Time, days	Total Weight Change, mg per cm <sup>2</sup>	Exposure Time, days	Total Weight Change, mg per cm <sup>2</sup>
<u>High-Purity Niobium, Rocking-Hearth Melts (Continued)</u>						
10 Zr-5 Mo	--	--	84	0.32	--	--
35 Zr-5 Mo	--	--	84	0.51	--	--
45 Zr-5 Mo	--	--	84	0.52	--	--
35 Zr-5 Al	--	--	84	0.57	--	--
45 Zr-5 Al	--	--	84	0.49	--	--
10 Zr-5 Cr	--	--	84	0.47	--	--
45 Zr-5 Cr	--	--	84	0.41	--	--
10 Zr-5 Fe	--	--	84	0.36	--	--
2.5 V	--	--	112	0.68	--	--
2.5 V-2.5 Ti	--	--	84	0.67	--	--
2.5 V-2.5 Mo	--	--	84	0.77	--	--
2.5 V-2.5 Fe	--	--	84	0.74	--	--
2.5 V-2.5 Cr	--	--	84	0.54	--	--
2.5 V-2.5 Al	--	--	84	0.82	--	--
2.5 V-2.5 Zr	--	--	7	0.19	--	--
2.5 V-2.5 Ni	--	--	7	0.96	--	--
5 V-2.5 Zr	--	--	84	0.38	--	--
5 V-25 Zr	--	--	84	0.20	--	--
5 V-35 Zr	--	--	84	0.58	--	--
5 V-45 Zr	--	--	84	0.40	--	--

(a) Off test.

(b) Losing weight.

## F-13

Evaluation is in process on the series of commercial-purity niobium-base alloy samples which were exposed in 680 F water for 196 days. The results of this work show that tungsten, molybdenum, vanadium, titanium, and zirconium, in the approximate order listed, result in significantly decreasing the diffusion rate of oxygen into niobium. The depth of contamination in most of these alloys was less than 4 mils after the 196-day exposure. Generally, the tungsten and molybdenum additions were less effective in reducing the depth of contamination than were additions of titanium, vanadium, and zirconium.

The results of tensile tests on several alloys at 1200 or 1500 F are summarized in Table F-7. As in earlier room-temperature tests, the tensile ductilities of the alloys containing large ternary additions of vanadium and zirconium or titanium and chromium were quite low. For the vanadium- and zirconium-containing alloys, this lack of ductility appears associated with the presence of significant amounts of a second phase which exists in these alloy structures. The two ternary alloys of lower alloy content, on the other hand, show appreciable ductility and moderate strengths at 1500 F.

TABLE F-7. ELEVATED-TEMPERATURE TENSILE PROPERTIES OF SELECTED NIOBIUM-BASE ALLOYS

Alloy	Alloy Content (Balance Niobium), a/o	Test Temperature, F	Tensile Properties		Elongation in 1 in., per cent
			0.2 Per Cent Offset Yield Strength, psi	Ultimate Strength, psi	
NL-8	9.4 V-9.9 Zr	1200	--	65,000	2
NL-9	11.4 V-5.7 Zr	1200	--	38,000	1
NL-10	9.1 Ti-6.3 Cr	1200	62,000	74,000	3
N-17	4.0 V-2.3 Zr	1500	30,000	46,000	9
N-49	2.0 V-2.5 Ti	1500	19,000	35,000	18

The preparation and evaluation of an additional series of 50-g ingot screening alloys are being continued.

Investigation of the Creep Properties of Zircaloy-2  
During Irradiation at Elevated Temperatures

F. R. Shober, P. B. Shumaker, A. P. Young,  
and R. F. Dickerson

The influence of fast neutrons, neutrons having energies greater than 1 Mev, on the creep properties of Zircaloy-2 at elevated temperature is important to designers of reactor components. Data obtained before and after irradiation indicate that mechanical properties are changed by irradiation and that annealing of the material below its recrystallization temperature after irradiation will remove approximately 95 per cent of the effects of fast-neutron exposure. However, there are reasons to believe that the properties as determined during irradiation in a fast-neutron flux may differ from the properties determined after irradiation. Diffusion rates are known to be accelerated by a neutron flux. Diffusion rates under irradiation are similar to rates obtained in the absence of neutrons at a higher temperature. It would appear that the rates of processes

involving atom movements are accelerated by a fast-neutron flux. Since creep of metals entails atom movements, one might expect creep data obtained during irradiation to differ from data obtained in the absence of irradiation. It is planned to compare the deformation of Zircaloy-2 in a reactor with the deformation under similar condition out of a reactor.

Another portion of the study will involve tests to provide further evidences of strain aging in Zircaloy-2. Tensile tests and internal-friction tests at room and elevated temperatures are planned as part of this program to detect and describe the strain-aging phenomenon. If evidences of strain aging are found it is planned to investigate and identify the mechanism responsible. As part of this study a technique is being investigated to make thin films for electron-transmission work with Zircaloy-2. This technique is expected to be helpful in the study of identification of dislocations and their movements in Zircaloy-2.

The execution of the in-reactor portion of the Zircaloy-2 creep tests requires an instrumented capsule. Preliminary capsule-design studies based on a fast-neutron flux of at least  $10^{14}$  nv have been initiated. Parameters include a specimen temperature of 700 F, three stress levels, the maximum being about 25,000 psi, and an exposure period of approximately two reactor cycles. The amount of creep occurring during the irradiation will be obtained from postirradiation specimen measurements. The influence of irradiation on the creep behavior may be deduced from data obtained from unirradiated creep specimens at similar temperatures and stresses.

The specimen geometry receiving primary attention thus far is a tube subjected to an internal inert-gas pressure. In one approach, a relatively short tube having a single test section (approximately 1-1/2 in. long) would be the test specimen with an individual capsule. In another approach, a longer tube would be machined with two or three 1-1/2-in. test sections and encapsulated. In either of these cases, the ID of the tube would be about 3/8 in. with wall thicknesses of 20, 40, and 60 mils. These dimensions are dictated by an internal pressure of 2000 psi, the stresses desired, and a 1-1/8-in. -OD capsule. In addition to the approaches involving pressurized tubes, the possibility of using a pressurized bellows to exert an axial load on a tensile specimen is being evaluated.

The capsule configuration being considered is based on maintaining the desired temperature level by a combination of gamma heating and external heat provided by heaters surrounding the specimen. Appropriate insulation will be provided to conserve heat. Thermocouples will be located in close proximity to the test sections. Good reliability and fast response are prime temperature-sensing requirements because of the need to regulate the auxiliary heat input in a way so that close temperature control is possible.

The Zircaloy-2 to be used in the creep and strain-aging studies has been fabricated. All material has been prepared from one lot of Zircaloy-2. Samples for chemical analysis were taken before and after fabrication.

Methods for making thin sections of zirconium and Zircaloy-2 are being studied for that portion of the program pertaining to transmission electron microscopy.

## F-15

Unalloyed zirconium has been included in the initial studies in order to minimize interference from alloy elements. Thin sections transparent to 80-kv electrons have been prepared.

Future work includes the completion of a conceptual design for the in-reactor capsule, tensile tests on Zircaloy-2 at room and elevated temperature, and internal-friction studies of annealed and strain-aged Zircaloy-2 wire.

Determination of Oxygen in Sodium at Concentrations Below 10 PPM

D. R. Grieser, P. M. Steinback, and W. H. Goldthwaite

The feasibility of continuous monitoring of oxygen concentration in a large sodium system is being investigated. Methods capable of sensitivity of  $\pm 1$  ppm of oxygen for concentrations below 10 ppm and amenable to rapid and preferable continuous determination are being sought. Since previously developed methods do not completely satisfy both specifications, new approaches are being investigated.

Five techniques have been selected for detailed experimental evaluation. These are based on (1) mass spectrography, (2) polarography, (3) ellipsometry, (4) electrical resistivity, and (5) plugging indicators. The preliminary investigations are to be conducted initially with sodium samples containing relatively large oxygen concentrations (from 20 to 100 ppm). Each technique will be judged on the basis of sensitivity to the relatively large differences in oxygen content, reproducibility of results, and speed of detection. The results obtained will be extrapolated in order to estimate the potential reliability and sensitivity at extremely low oxygen levels. Those methods showing the most promise will be selected for advanced study using sodium containing low levels of oxygen.

A sodium-purification system is being constructed for the production of sodium test samples of desired oxygen contents for the various evaluations. Standard detection methods will be used for determining the level of oxygen in the sample batches. The system is designed to handle sodium with both high and low levels of oxygen.

STUDIES OF ALLOY FUELS

R. F. Dickerson

Alloys for a study of the gamma-immiscibility gap in the uranium-niobium system and of the effect of oxygen on the composition limits of the gap have been cast and are being homogenized. Corrosion-test data for niobium-10 to 60 w/o uranium alloys show that the specimens begin to lose weight between 112 and 126 days in 600 F water and exhibit a black oxide coating; samples exposed to 680 F water for the same period are also losing weight and exhibit a brown oxide coating which appears to be spalling slightly. Specimens exposed to NaK at 1600 F for 656 hr generally show weight gains.

Thorium-uranium-alloy studies show that with increasing amounts of uranium and zirconium additions a continuous grain-boundary phase around thorium-rich grains replaces the microstructure in which uranium-phase particles are contained in a thorium matrix. Hot-hardness data indicate that ternary additions of zirconium to thorium-uranium alloys and quaternary additions of zirconium and niobium produce maximum hardness at 600 C, while at 800 C ternary additions of niobium and molybdenum produce maximum hardness. Thorium carbide and thorium carbide-uranium carbide castings have been found to exhibit improved resistance to atmospheric corrosion when arc melted in graphite molds as compared with a copper hearth; a reduction in stresses due to the lower cooling rate in graphite is believed responsible. The cast ternary carbides showed evidence of coring.

#### Development of Niobium-Uranium Alloys

J. A. DeMastry, S. G. Epstein, A. A. Bauer,  
and R. F. Dickerson

Niobium-uranium alloys appear promising for high-temperature reactor applications. In order to determine if niobium-rich uranium alloys possess properties which are desirable for elevated-temperature use in a reactor, an investigation of mechanical and physical properties, fabrication characteristics, and behavior in various corrosive media is being made. Since previous work with the uranium-rich uranium-niobium alloys has indicated that the properties are affected by the purity levels of the alloying constituents, the effects of the major impurities in niobium, notably oxygen and zirconium, are being determined.

Alloys were prepared using three separate grades of niobium as melting stock. The oxygen and zirconium content of each grade varied as follows: one contained 0.7 w/o zirconium and 600 ppm oxygen; a second contained 0.17 w/o zirconium and 700 ppm oxygen; and a third contained 0.02 w/o zirconium and 300 ppm oxygen. Alloys containing 10 to 60 w/o uranium have been prepared from each grade of niobium. These alloys are being used in the determination of physical, mechanical, and corrosion properties.

A study of the gamma-immiscibility loop in the niobium-uranium alloy system with particular regard to the effects of oxygen on the composition limits of this loop is in progress. Alloys containing 10, 20, 30, 40, 50, 52, 54, 56, and 58 w/o niobium (balance uranium) have been cast into wire bars. The charges were arc melted seven times to produce homogeneous alloys. In order to reduce any segregation that may have occurred during the casting of the alloys, the wire bars are being homogenized in vacuum for 8 hr at temperatures that range from 1200 to 1500 C; the temperature of homogenization is varied depending on the niobium content of the alloy, the temperature being increased with increased niobium content.

The niobium-10 and -20 w/o uranium alloys have been successfully fabricated by forging. No successful fabrication of alloys containing more than 20 w/o uranium has been made to date. Construction of a furnace which will permit hot working above 3000 F has been completed. Ingots of the niobium-30 and -40 w/o uranium alloys will be fabricated using this furnace for preheating of the alloys as soon as electrical connections can be made to the furnace.

## F-17

Table F-8 lists the results of corrosion testing for 112 and 126 days in 600 and 680 F water for all of the niobium-uranium alloys being studied. At between 112 and 126 days in 600 F water, specimens of all of the alloys started to lose weight. The alloys in 600 F water still have a black oxide coating. All alloys tested in 680 F water exhibit a brown oxide which appears to be spalling slightly. After 140 hr of exposure, specimens being tested in 680 F water will be removed from test and analyzed for hydrogen content by vacuum-fusion techniques.

In Table F-9 the results of a compatibility study in NaK at 1600 F are shown. These alloys have been tested a total of 656 hr and will be tested for an additional 344 hr. After examination the surfaces will be machined and pickled to remove any oxide which may have formed, and tests in sodium will be started.

In order to better evaluate the corrosion results, analyses for carbon, nitrogen, and oxygen are being obtained on the material prior to corrosion testing. Carbon and nitrogen analyses have been obtained. An evaluation of the data will be made when the oxygen analyses are complete.

A limited number of creep specimens have been prepared and tests have been started. The stress necessary to produce rupture in 100 hr will be determined. The creep properties of wrought material will be investigated at 1600, 1900, and 2400 F in vacuum in tests 1000 hr in duration.

Specimens for thermal-conductivity, thermal-expansion, and electrical-resistivity measurements are ready to be tested.

#### Development of Thorium-Uranium Alloys

M. S. Farkas, A. A. Bauer, and R. F. Dickerson

Thorium-uranium-base alloys are being studied with the aim of developing alloys of improved irradiation stability and corrosion resistance. The effect of thorium purity, casting methods, and fabrication on the size and distribution of uranium-rich particles is being investigated. Thorium-5 to 25 w/o uranium-base ternary alloys that have been and are now being studied contain either 5 to 25 w/o zirconium or small amounts of niobium or molybdenum. Some quaternary compositions contain additions of both zirconium and niobium. The preparation of thorium and thorium-uranium carbides and nitrides is also being investigated.

Metallographic examinations of as-cast alloys show that microstructures consisting of a thorium-rich matrix containing particles of a uranium phase are present in the following thorium-10 w/o uranium-base compositions: 2 w/o niobium, 1.5 w/o molybdenum, 10, 15, and 20 w/o zirconium, 10 w/o zirconium-2 w/o niobium, and 15 w/o zirconium-3 w/o niobium. Other compositions containing greater quantities of uranium and zirconium exhibit two-phase structures in which thorium-rich grains are surrounded by a continuous grain-boundary constituent.

TABLE F-8. CORROSION DATA FOR NIOBIUM-URANIUM ALLOYS<sup>(a)</sup> IN 600 AND 680 F WATER AFTER 112 AND 126 DAYS

Alloy Content (Balance Niobium), w/o	Impurity Content		Specimen Condition	Total Weight Change, mg per cm <sup>2</sup>			
	Oxygen, ppm	Zirconium, w/o		After 112 Days		After 126 Days	
				600 F Water	680 F Water	600 F Water	680 F Water
10 U	600	0.74	Fabricated	0.70	-0.20	0.61	-0.49
	700	0.17	Fabricated	0.90	-13.6	0.55	-15.0
	300	0.02	Fabricated	0.62	-42.5	0.38	-45.0
20 U	600	0.74	Fabricated	1.20	0.60	1.06	0.08
	700	0.17	Fabricated	1.34	-1.38	1.34	-5.47
	300	0.02	Fabricated	0.84	0.93	0.71	0.60
30 U	600	0.74	As cast	0.87	-0.77	0.80	-0.89
	700	0.17	Fabricated	0.54	-1.03	0.10	-1.78
	300	0.02	As cast	1.02	-2.48	1.26	-2.50
40 U	600	0.74	As cast	0.75	1.60	0.63	-0.03
	700	0.17	As cast	0.75	1.29	0.56	1.01
	300	0.02	As cast	0.89	1.61	0.73	-2.52
50 U	600	0.74	As cast	1.00	-0.97	0.93	-1.58
	700	0.17	As cast	0.92	-1.43	0.81	-1.95
	300	0.02	As cast	0.59	-6.57	0.46	-7.20
60 U	600	0.74	As cast	-1.21	(b)	-1.60	(b)
	700	0.17	As cast	0.03	-13.0	-0.46	-14.5
	300	0.02	As cast	-0.38	-9.07	-0.12	-10.17
Zircaloy-2				0.25	0.90	0.30	1.40
Niobium	500	0.03	Fabricated	-1.47	(c)	--	--

(a) Average of two specimens.

(b) Both specimens taken off test.

(c) Disintegrated after 42 days.

TABLE F-9. CORROSION DATA FOR NIOBIUM-URANIUM ALLOYS<sup>(a)</sup> IN NaK AT 1600 F

Alloy Content, (Balance Niobium), w/o	Impurity Content		Specimen Condition	Total Weight Change After 656 Hr in 1600 F NaK, mg per cm <sup>2</sup>
	Oxygen, ppm	Zirconium, w/o		
10 U	600	0.74	Fabricated	0.17
	700	0.17	Fabricated	0.05
	300	0.02	Fabricated	-0.03
20 U	600	0.74	Fabricated	0.37
	700	0.17	Fabricated	0.14
	300	0.02	Fabricated	0.25
30 U	300	0.02	As cast	0.52
40 U	300	0.02	As cast	0.38
50 U	300	0.02	As cast	0.55
60 U	300	0.02	As cast	1.15

(a) Average of duplicate tests.

Hot-hardness tests were performed as an indirect measure of strength and resistance to irradiation swelling. Good strength above 600 C is deemed necessary for fuels that may be used in high-temperature reactors. The highest hot-hardness values obtained at 600 C were exhibited by alloys of thorium-10 w/o uranium-10 w/o zirconium-2 w/o niobium, thorium-15 w/o uranium-25 w/o zirconium, and thorium-10 w/o uranium-10 w/o zirconium. However, at 800 C the alloys that showed the greatest strength were thorium-10 w/o uranium-1.5 w/o molybdenum and thorium-10 w/o uranium-2 w/o niobium. These alloys were tested in the as-induction-cast condition, and all contained Ames thorium. Thorium-15 w/o uranium-25 w/o zirconium, thorium-10 w/o uranium-25 w/o zirconium, and thorium-20 w/o uranium-20 w/o zirconium alloys exhibited an increase in hardness with increasing temperature to 400 C. This behavior is believed to be caused by age hardening.

Future studies of the thorium-uranium-base alloys will include corrosion testing in 200 C water and heat treatment at various temperatures to determine the effect of thermal history on uranium particle size and distribution, and upon the phases present. Tensile and creep properties at 600 and 700 C of thorium-uranium binary alloys and of the ternary and quaternary alloys exhibiting the greatest hot hardness will be investigated to define their high-temperature-strength properties more clearly. Also, the recrystallization behavior of several ternary alloys will be studied for comparison with the behavior of binary thorium-uranium alloys.

Cylindrical castings of ThC and ThC-20, -40, and -60 mole per cent UC have been prepared by casting arc-melted buttons in graphite molds. These castings exhibit resistance to atmospheric corrosion greater than that of the arc-melted buttons. This improvement is believed to be related to reduced stresses resulting from the lower cooling rate effected by use of graphite molds. Metallographic examinations of these castings showed that single-phase structures of (Th,U)C were obtained, although small amounts of ThC<sub>2</sub> were identified in the ThC specimen. The (Th,U)C samples all show evidence of coring which is believed to be a result of the large difference in melting points between ThC and UC. Homogenization treatments will be employed in an attempt to provide a more uniform structure.

The preparation of ThN and (Th,U)N will be attempted by arc-melting techniques.

#### FISSION-GAS RELEASE FROM REFRACTORY FUELS

J. B. Melehan, D. A. Vaughan, R. H. Barnes,  
S. D. Beck, and F. A. Rough

The objective of this program is to understand the important causes of fission-gas release in UO<sub>2</sub>. At present, considerable effort is being devoted to consideration of the characterization of sintered UO<sub>2</sub> and to the model for gas release from sintered UO<sub>2</sub>. In addition, a major effort is devoted to completion of specialized equipment for in-pile and out-of-pile study of gas release.

Characterization of Sintered UO<sub>2</sub> and Model of Gas Release

An equivalent-sphere model for the characterization of fission-gas release by diffusion has been proposed by Booth\* for porous fuel elements. It is assumed that the diffusion release from porous fuel media is equivalent to that from an equivalent sphere, that sphere for which the ratio of surface area to volume is the same as that of the fuel material. Since the major contribution to the surface area is from the pore surfaces, the surface area-to-volume ratio is a characteristic of the fuel material and is essentially independent of the nominal dimensions of the fuel element.\*\* The fission-gas release and accumulation may then be determined in terms of four parameters: the radius of the equivalent sphere, the decay constant, the diffusion coefficient, and time.

It is convenient to express the results in terms of a unit volume of the solid. The accumulation refers to the quantity released reduced by the amount which has decayed. In the analysis, it has been assumed that the isotope is a primary fission product and that it has been produced at a constant ratio from the beginning of the operation. It is further assumed that the sphere size and diffusion coefficient are constant.

The following symbols are used:

D = diffusion coefficient

$\lambda$  = decay constant

a = radius of equivalent sphere

t = time

B = production rate of isotope in a unit volume

R = release rate from a unit volume

N = accumulation of nondecayed isotope from a unit volume

$\mu = \lambda a^2 / D$

$T = Dt / a^2$ .

The following formulas for the release rate and accumulation are found.

$$R/B = 3 \left\{ (1/\sqrt{\mu}) \coth \sqrt{\mu} - 1/\mu - 2 \exp(-\mu T) \sum_{n=1}^{\infty} [1/(n^2\pi^2 + \mu)] \exp(-n^2\pi^2 T) \right\}. \quad (F-1)$$

\*Booth, A. H., "A Method of Calculating Fission Gas Release and Its Application to the X-2-f Loop Test", AECL-CRDC-727 (1957).

\*\*Eichenberg, J. D., Frank, P. W., Kistel, T. J., Lustman, B., and Vogen, K. H., "Effects of Irradiation of Bulk UO<sub>2</sub>", WAPD-183 (1957).

$$N/B = (3/\lambda) \left\{ \left[ (1/\sqrt{\mu}) \coth \sqrt{\mu} - 1/\mu \right] [1 - \exp(-\mu T)] - (2\mu/\pi^2) \exp(-\mu T) \sum_{n=1}^{\infty} \left[ 1/n^2(n^2\pi^2 + \mu) \right] [1 - \exp(-n^2\pi^2 T)] \right\}. \quad (F-2)$$

Equations (F-1) and (F-2) are exact formulas. However, in each case the series become very slowly convergent for small values of T. This difficulty is overcome by using the following approximations.

$$R/B = 3 \left\{ (1/\sqrt{\mu}) \operatorname{erf} \sqrt{\mu T} - (1/\mu) [1 - \exp(-\mu T)] \right\}. \quad (F-3)$$

$$N/B = (3/\lambda) \left\{ (1/\sqrt{\mu}) \operatorname{erf} \sqrt{\mu T} - 2\sqrt{T/\pi} \exp(-\mu T) - (1/\mu) [1 - (1 + \mu T) \exp(-\mu T)] \right\}. \quad (F-4)$$

The approximations are increasingly accurate as T becomes small, approaching the exact formulas asymptotically. They remain accurate for values about as large as  $T = 0.1$ . For larger values of T, the approximations become incorrect, but in this region the exact formulas are readily evaluated.

It is recognized that the equivalent-sphere model is not an exact representation of the structure of a porous medium. It is not proposed here that it is appropriate to apply it indiscriminately to all porous media. However, it is worthwhile, in many cases, to investigate data in terms of the equivalent-sphere model, both as a means of correlating data and as an examination of the validity of the model. As research progresses, a more realistic model may be evolved.

Thus, characterization studies are in progress to better understand the nature of the pore structure of sintered  $UO_2$  and the effects of irradiation upon it. In the study of pore structure, the number, size, and distribution of pores in sintered  $UO_2$  is being determined for comparison with density measurements. In addition, it is planned to use transmission microscopy as an aid in studies where it is desired to understand the relation between surface-area measurements obtained by gas adsorption and the internal porosity. Since irradiation may have significant effects upon internal porosity or internal surfaces, preliminary experiments are also in progress to detect the effects of fission recoils upon surfaces.

#### Diffusion in $UO_2$

The diffusion studies of fission gas in the series of single-crystal  $UO_2$  samples have not yet begun. Special equipment for such studies by irradiation and post-irradiation heating is being assembled.

F-23

Preparation for In-Pile Study

Equipment which will provide for irradiation of refractory fuels and simultaneous collection and analysis of the fission gas that is released is being assembled. The equipment will provide for any desired ratio of fission and supplementary heat and will operate up to temperatures of 2000 F.

GENERAL FUEL-ELEMENT DEVELOPMENT

S. J. Paprocki

Fabrication techniques are being developed for the preparation of cermet fuel materials containing 60 to 90 volume per cent ceramic fuel. When they are prepared under proper control of the fabrication process, these materials possess superior thermal conductivity, thermal-shock resistance, and structural strength in comparison with ceramic uranium dioxide fuel.

The gas-pressure-bonding technique is being investigated for the preparation of niobium- and molybdenum-base fuel elements and assemblies. Techniques have been developed for the self-bonding of niobium. The bonds are ductile and possess grain growth across the interface. The self-bonding of molybdenum has been more difficult; however, recent specimens prepared by a modified technique appear to possess satisfactory bonding.

An investigation is being conducted to obtain a fundamental understanding of the processes involved in the solid-phase bonding of metals by the application of heat and pressure. The results of this study are of practical application to all of the programs utilizing the gas-pressure-bonding process.

Fabrication of Cermet Fuel ElementsS. J. Paprocki, D. L. Keller, G. W. Cunningham,  
and D. E. Kizer

Techniques of fabricating cermets containing 60 to 90 volume per cent fuel to densities of 90 per cent of theoretical or higher by hot pressing and gas-pressure bonding are being studied in this program. Mechanical and physical measurements as well as metallographic techniques are being used to evaluate fabrication procedures.

Thermal-conductivity measurements have been completed on an 80 volume per cent  $\text{UO}_2$ -molybdenum cermet rod fabricated by pressure bonding green-pressed pellets. The cermet rod was 91.1 per cent of theoretical density. Thermal-conductivity values of 0.140, 0.121, 0.114, and 0.110 w/(cm)(C) were measured respectively at 100, 300, 500, and 700 C. Electrical-resistivity measurements were made simultaneously, but

calculations have not been completed. The electrical-resistivity measurements will be used in studies to develop a mathematical relationship between thermal conductivity and electrical resistivity.

Electrical-resistivity measurements have also been made on other cermet rods for which the thermal-conductivity measurements were reported previously. A straight-line relationship was found to exist between 100 and 900 C for a cermet containing 70 volume per cent  $\text{UO}_2$  in molybdenum and having a density of 91.5 per cent of theoretical. Values of 75 and  $269 \times 10^{-6}$  ohm-cm were measured at 100 and 900 C, respectively. Values of 3155, 3460, 3720, and  $3880 \times 10^{-6}$  ohm-cm were measured at respective temperatures of 100, 300, 500, and 700 C on a cermet rod of 95.5 per cent of theoretical density containing 80 volume per cent  $\text{UO}_2$  dispersed in Type 302B stainless steel. Also, electrical-resistivity measurements were made on a cermet rod containing 70 volume per cent  $\text{UO}_2$  dispersed in Type 302B stainless steel. Values of 1275, 1400, 1505, and  $1570 \times 10^{-6}$  ohm-cm were measured respectively at 100, 300, 500, and 700 C. When measurements were repeated a second time, lower electrical-resistivity values were measured at each temperature. Repeating the measurements a third time resulted in values of 1235, 1365, 1475, and  $1560 \times 10^{-6}$  ohm-cm respectively at 100, 300, 500, and 700 C.

A series of 1 by 1 by 0.100-in. 80 volume per cent  $\text{UO}_2$ -molybdenum powder compacts has been prepared for pressure bonding at temperatures between 2200 and 2400 F. In addition, niobium component frames are being machined to pressure bond a series of 80 volume per cent  $\text{UO}_2$ -niobium powder cores 1 by 1 by 0.100 in.

#### Gas-Pressure Bonding of Molybdenum- and Niobium-Clad Fuel Elements

S. J. Paprocki, E. S. Hodge, and P. J. Gripshover

Cermet and ceramic-type fuels are being clad with molybdenum and niobium by the gas-pressure-bonding technique. These cladding materials possess desirable properties for nuclear applications due to their high-temperature strength and favorable cross sections.

The self-bonding of molybdenum and niobium has been investigated as a function of surface preparation, bonding technique, and bonding parameters. A satisfactory method of preparing surfaces for pressure bonding has been developed for both materials. Bonding technique as a function of bond strength, ductility, integrity, and consistency is being studied for both materials. Bond parameters are being established for each material with each bonding technique investigated.

Three bonding techniques are presently being considered for the bonding of niobium-clad fuel plates: bonding in a protective container at temperatures low enough to sufficiently minimize reaction between the container and the niobium cladding, bonding fusion-edge-welded niobium-clad fuel plates at higher temperatures, and bonding at a low temperature by edge brazing in a container followed by bonding of the bare fuel element at higher temperatures to diffuse the braze metal away and obtain a metallurgical bond.

## F-25

Bonding parameters of 2100 F at 10,000 psi for 3 hr produce good niobium-to-niobium bonds; however, at this temperature, reactions of the container or barrier layers between the can and specimen with the niobium are encountered. Attempts were made to bond in a container at lower temperatures with niobium prepared by optimum surface-preparation methods. Bonding at the lower temperatures without a barrier layer between the stainless container and the niobium fuel plate resulted in reaction between the container and cladding, and no evidence of a niobium-to-niobium bond was discovered. As a result, two specimens were pressure bonded at 1900 F for 3 hr at 10,000 psi with spacers between the container and the niobium cladding. Iron-chromium-aluminum spacers were used in one of these specimens, while the second specimen contained niobium spacers between the cladding and container. Examination of these specimens revealed that very little grain growth had occurred across the original bond interface. Since no visible bond-line contamination was present, it appears that a bonding treatment of 1900 F is too low to promote the necessary grain growth across the original interface. Further examination revealed that no apparent reaction had occurred between the iron-chromium-aluminum spacers and the niobium cladding. These barrier materials do react, however, at 2100 F; consequently, it appears that to obtain self-bonding of niobium in a container a more suitable barrier layer will have to be developed, or it may not be possible to bond in a container at these temperatures.

Efforts are being made to develop techniques for pressure-bonding niobium-clad elements without use of a bonding container. Earlier efforts to produce a specimen edge brazed with zirconium have proven successful. This specimen showed excellent bonds and ductility. More recently a specimen has been successfully fusion edge welded. This was accomplished in a helium-atmosphere welding tank. The specimen was clamped tightly between copper cooling blocks to avoid overheating and to minimize the helium that would be entrapped between the two plates. Although a gastight, ductile weld was obtained, enough helium was entrapped between the plates to prevent complete bonding during pressure bonding. Bend tests made on this specimen after bonding at 2100 F and 10,000 psi for 3 hr showed the specimen to be completely ductile even in the weld areas. Metallographic examination revealed that, although there were areas of complete grain growth across the interface, a number of large voids were present along the interface. A comparison of this specimen and the edge-brazed specimen, which was evacuated before bonding, indicates that the voids are probably due to helium which was entrapped during welding. It is believed that the use of electron-beam welding could eliminate this problem completely.

A small-scale subassembly consisting of three niobium-clad  $\text{UO}_2$  fuel plates separated by 0.040-in.-thick channels has been prepared. Each fuel plate consists of one 0.870 by 0.870 by 0.040-in. core in a pieced component frame with two 0.010-in.-thick cover plates of niobium. The coolant channels were formed by two strips of 0.040-in.-thick niobium which were separated by an insert of  $\text{UO}_2\text{-Al}_2\text{O}_3$ . The  $\text{UO}_2\text{-Al}_2\text{O}_3$  is to be pickled out, leaving channels between each fuel plate. This specimen was pressure bonded at 2100 F and 10,000 psi for 3 hr.

Molybdenum fuel plates bonded in protective jackets are normally brittle. Since this lack of ductility may be due to reaction of the molybdenum with bonding container, emphasis has been directed toward the development of edge-sealing techniques. Two specimens have been prepared which contained zirconium foil around the periphery of the two plates forming the specimen. These specimens were bonded in a protective

container at 1800 F and 10,000 psi for 3 hr. The bonding containers were then removed and one of the specimens was destructively tested. This specimen revealed that the molybdenum had retained its ductility and that a gastight bond had been formed around the periphery of the specimen. Bend tests made through this area showed the bond to be weak, however, and separation occurred along the bond interface. The second specimen was pressure bonded at 2300 F and 10,000 psi for 3 hr. Bend tests made on this specimen indicated the cladding had been embrittled during the duplex bonding cycle. Metallographic examinations are being conducted at the present time to determine the cause of the embrittlement.

Two additional molybdenum specimens were fusion edge welded and pressure bonded at 2300 F and 10,000 psi for 3 hr. The first of these consisted of two 0.015-in.-thick plates which had been cold rolled 4 to 1 before assembly. The second specimen was prepared from two cold-rolled 0.040-in.-thick plates. Both specimens were fusion edge welded between copper cooling blocks in a helium-atmosphere welding tank. Examination of these specimens after bonding revealed the edge welds did not fail during bonding of these specimens. Bend tests indicated that the specimens had retained their original ductility. These specimens are being examined metallographically for bond integrity.

#### Factors Affecting Pressure Bonding

G. W. Cunningham and J. W. Spretnak

Although a study is being made of the complete bonding process, it is desirable when possible to isolate and study the mechanism and kinetics of particular steps in the solid-phase bonding of metals by application of heat and pressure. At the present time, an attempt is being made to determine the effect of pressure on the elimination of excess vacancies present at the interface.

One method which appears to offer promise for studying the effect of pressure consists of bonding the specimen under conditions which will give a bond interface with no macroporosity but with no grain growth across the interface and then subsequently annealing sections of the specimen in a vacuum and under various hydrostatic loads. Comparison of the microstructures should then provide a basis for measuring the effect of pressure. The feasibility of this procedure has been demonstrated by bonding OFHC copper (previously annealed 2 hr at 1400 F in hydrogen) for 3 hr at a pressure of 20,000 psi and a temperature of 1100 F in a vacuum hot-press unit. The specimen, which contained three bond lines, was then sectioned and one section was annealed 24 hr in vacuo at 1800 F while a second section was subjected to a helium pressure of 10,000 psi for 3 hr at 1800 F.

Although no void areas were visible in the as-bonded specimens, voids nucleated and grew along the bond interfaces in both of the annealed sections. In the vacuum-annealed specimen, voids approximately 0.6 mil in diameter were spaced along the interface at a concentration of approximately 1.2 voids per mil of interface length. Little or no grain growth across the interface could be detected, and no voids were visible except at the interface. In the pressure-annealed specimen, voids approximately

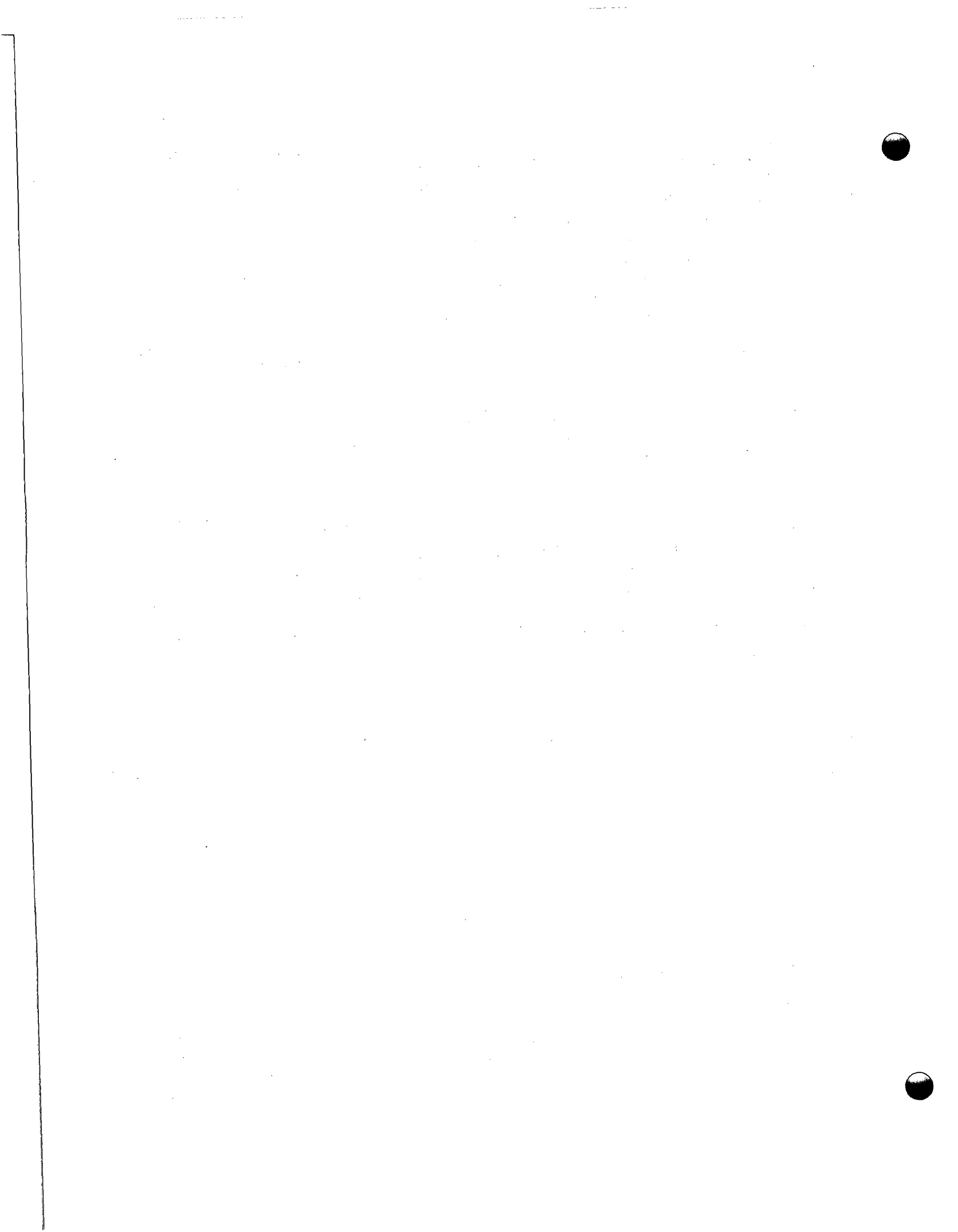
## F-27 and F-28

0.07 mil in diameter were spaced along the interface at a concentration of approximately 8 voids per mil of interface length. In addition, in some areas the voids were heavily concentrated for short distances away from the original interface. In these areas, it appeared as though when grain growth occurred voids left as the boundary moved until a boundary with a low concentration of voids was formed. It is not suggested that any vacancies were nucleated in sites in the bulk material. In other areas where grain boundaries ran almost perpendicular to the interface, voids could be detected for a distance of several mils along the grain boundaries. Since very few voids could be detected along similarly located twin boundaries, such behavior suggests the effectiveness of grain boundaries compared with twin boundaries as vacancy sinks.

The difference in stable void size upon the application of pressure would be expected according to work by Barnes of Harwell in which he applied the Gibbs-Thompson relation to the formation of voids due to the Kirkendall effect. However, the size of the voids in the present investigation are larger than that predicted by Barnes and no explanation can be offered at this time. The location of voids along the grain boundaries does suggest that pressure may be beneficial in promoting vacancy diffusion along grain boundaries.

An interesting observation was also made concerning grain growth across the interface. Whereas in most cases in the pressure-annealed specimens, grain growth extended across the original interface for short distances only and high concentrations of voids were left as the boundary moved, in some cases there were areas with a low concentration of voids where twins extended for long distances on either side of the boundary.

Additional specimens are being prepared to study the effect of pressure on the vacancies at the interface.



FF-1

## FF. FUEL-CYCLE PROGRAM STUDIES

GAS-PRESSURE BONDING OF CERAMIC, CERMET, AND  
DISPERSION FUEL ELEMENTS

S. J. Paprocki, D. L. Keller, E. S. Hodge, C. B. Boyer, and J. B. Fox

This program is concerned with the development of a fabrication process which will maintain or improve fuel-element quality, while reducing manufacturing costs. The gas-pressure-bonding technique was selected as the most promising method of fabrication for achieving these objectives. The ceramic, cermet, and dispersion fuel systems were selected because it is believed that these fuel systems offer the greatest potential for achieving a high burnup over a range of temperatures. They also offer an excellent opportunity, by the utilization of the pressure-bonding technique, for making substantial reductions in fabrication costs. The study is directed toward the refinement and further development of the gas-pressure-bonding process to accomplish simultaneous densification and cladding of these fuels with stainless steel.

The greatest emphasis will be placed on the development of  $UO_2$  ceramic bodies clad with Type 304 stainless steel. These materials will be used to prepare fuel elements and fuel-element assemblies of various designs. With a minimum of development work, the same techniques can be utilized for the dispersion and uranium dioxide cermet systems.

Initial studies are concerned with the utilization of high-density green-pressed  $UO_2$  ceramic cores, in place of sintered cores, to achieve specific densities while reducing costs. A value of 70 per cent of theoretical was selected in the beginning in order to prevent excessive deformation of the stainless steel cladding during pressure bonding. After further consideration of dimensional tolerances, shrinkage, warpage of plates, and deformation of the cladding, it seems desirable to raise the minimum density value to 75 per cent of theoretical.

As shown in Table FF-1 (Table 19), using a mixture of 75 w/o Spencer minus 20 plus 325-mesh fused  $UO_2$  and 25 w/o MCW minus 325-mesh ceramic-grade  $UO_2$ , green densities of 80.2, 83.0, and 82.9 per cent of theoretical were achieved using compacting pressures of 50, 45, and 40 tsi, respectively. These cores gave a very good green strength using Ceremul "C" as a binder. Compacts (Table 22) of a mixture of 75 w/o MCW minus 20 plus 325-mesh special dense  $UO_2$  and 25 w/o MCW minus 325-mesh ceramic-grade exhibited green densities of 75.7, 78.0, and 78.5 per cent of theoretical using pressures of 50, 45, and 40 tsi, respectively. This mixture gave compacts of good green strength and especially good handling and loading properties. In a series of different types of  $UO_2$  and blends of  $UO_2$ , these two aforementioned mixtures gave densities of 92.5 and 91.0 per cent of theoretical after pressure bonding at 2100 F for 3 hr at 10,000 psi. The two mixtures were superior to the other mixture in handling, loading, and densification properties.

The compacting characteristics of the seven types of uranium dioxide being studied in this program were reported previously in BMI-1366 and BMI-1377. These powders include

TABLE FF-1. DENSIFICATION OF UO<sub>2</sub> BY VARIOUS PRESSURE-BONDING CONDITIONS

Type of UO <sub>2</sub>	Compact	Compacting Pressure, tsi	Height, in.	Green Density		Pressure-Bonded Density <sup>(a)</sup>	
				G per Cm <sup>3</sup>	Per Cent of Theoretical	G per Cm <sup>3</sup>	Per Cent of Theoretical
<u>Tube 9, Pressure Bonded at 2200 F for 1 Hr at 10,000 PSI</u>							
MCW minus 20-mesh special dense	U-1132	50	0.459	8.74	79.9		
	U-1133	50	0.459	8.74	79.9	9.24	84.3
	U-1134	50	0.460	8.71	79.6		
<u>Tube 9, Rerun at 2300 F for 3 Hr at 10,000 PSI</u>							
MCW minus 20-mesh special dense	U-1132	50	0.459	8.74	79.9		
	U-1133	50	0.459	8.74	79.9	9.71	88.8
	U-1134	50	0.460	8.71	79.6		
<u>Tube 16, Pressure Bonded at 2100 F for 3 Hr at 10,000 PSI</u>							
Spencer minus 100-mesh fused	U-1155	45	0.460	8.68	79.3		
	U-1156	50	0.454	8.82	80.6	9.35	85.4
	U-1157	55	0.451	8.85	80.7		
<u>Tube 17, Pressure Bonded at 2100 F for 3 Hr at 10,000 PSI</u>							
Spencer minus 20-mesh fused	U-1158	55	0.413	9.75	88.9		
	U-1159	50	0.414	9.70	88.6	9.83	89.8
	U-1160	45	0.418	9.61	87.9		
<u>Tube 18, Pressure Bonded at 2200 F for 2 Hr at 10,000 PSI</u>							
Spencer minus 20-mesh fused	U-1161	40	0.419	9.62	87.9		
	U-1162	35	0.421	9.50	87.2	9.80	89.5
	U-1163	25	0.429	9.38	85.6		
<u>Tube 19, Pressure Bonded at 2100 F for 3 Hr at 10,000 PSI</u>							
75 w/o minus 20 plus 325-mesh Spencer fused, 25 w/o MCW minus 325-mesh ceramic grade	U-1184	50	0.457	8.79	80.2		
	U-1185	45	0.440	9.10	83.0	10.12	92.5
	U-1186	40	0.442	9.07	82.9		

TABLE FF-1. (Continued)

Type of UO <sub>2</sub>	Compact	Compacting Pressure, tsi	Height, in.	Green Density		Pressure-Bonded Density <sup>(a)</sup>	
				G per Cm <sup>3</sup>	Per Cent of Theoretical	G per Cm <sup>3</sup>	Per Cent of Theoretical
<u>Tube 20, Pressure Bonded at 2100 F for 3 Hr at 10,000 PSI</u>							
75 w/o Spencer minus 20 plus 325-mesh fused, 25 w/o MCW minus 325-mesh dense ceramic grade	U-1187	50	0.470	8.50	77.6	9.55	87.2
	U-1188	45	0.458	8.75	79.9		
	U-1189	40	0.457	8.75	79.9		
<u>Tube 21, Pressure Bonded at 2100 F for 3 Hr at 10,000 PSI</u>							
80 w/o Spencer minus 20 plus 325-mesh fused, 20 w/o MCW minus 325-mesh dense ceramic grade	U-1190	50	0.452	8.84	80.6	9.63	88.0
	U-1191	45	0.457	8.76	80.0		
	U-1192	40	0.448	8.25	75.3		
<u>Tube 22, Pressure Bonded at 2100 F for 3 Hr at 10,000 PSI</u>							
75 w/o MCW minus 20 plus 325-mesh special dense, 25 w/o MCW minus 325-mesh ceramic grade	U-1193	50	0.483	8.29	75.7	9.97	91.0
	U-1194	45	0.469	8.55	78.0		
	U-1195	40	0.466	8.59	78.5		
<u>Tube 23, Pressure Bonded at 2100 F for 3 Hr at 10,000 PSI</u>							
75 w/o MCW minus 20 plus 325-mesh special dense, 25 w/o MCW minus 325-mesh dense ceramic grade	U-1196	50	0.490	8.59	78.5	9.02	82.4
	U-1197	45	0.490	8.17	74.5		
	U-1198	40	0.487	8.21	75.0		
<u>Tube 24, Pressure Bonded at 2100 F for 3 Hr at 10,000 PSI</u>							
75 w/o Spencer minus 20 plus 325-mesh fused, 25 w/o MCW minus 400-mesh high fired	U-1199	50	0.424	9.44	86.3	9.74	88.9
	U-1200	45	0.424	9.42	86.0		
<u>Tube 25, Pressure Bonded at 2100 F for 3 Hr at 10,000 PSI</u>							
75 w/o minus 100 plus 325-mesh Spencer fused, 25 w/o MCW minus 400-mesh high fired	U-1202	50	0.465	8.62	78.7	9.44	86.2
	U-1203	45	0.442	9.06	82.8		
	U-1204	40	0.446	8.99	82.0		

FF-3

TABLE FF-1. (Continued)

Type of UO <sub>2</sub>	Compact	Compacting Pressure, tsi	Height, in.	Green Density		Pressure-Bonded Density <sup>(a)</sup>	
				G per Cm <sup>3</sup>	Per Cent of Theoretical	G per Cm <sup>3</sup>	Per Cent of Theoretical
70 w/o Spencer minus 20 plus 200-mesh fused,	U-1205	50	0.465	8.60	78.5		
20 w/o MCW minus 200 plus 325-mesh ceramic	U-1206	45	0.466	8.60	78.5	10.00	91.4
grade, 10 w/o MCW minus 400-mesh high fired	U-1207	40	0.464	8.65	79.0		
<u>Tube 26, Pressure Bonded at 2100 F for 3 Hr at 10,000 PSI</u>							
MCW prepared pellets	U-1164	--	0.517	8.52	77.8		
	U-1167	--	0.509	8.56	78.2	10.60	96.9
	U-1168	--	0.508	8.55	78.0		
	U-1169	--	0.508	8.54	77.9		
<u>Tube 27, Pressure Bonded at 2200 F for 2 Hr at 10,000 PSI</u>							
MCW prepared pellets	U-1170	--	0.507	8.60	78.5		
	U-1171	--	0.520	8.51	77.7	10.85	94.5
	U-1173	--	0.511	8.54	77.9		
	U-1174	--	0.485	8.54	77.9		
<u>Tube 29, Pressure Bonded at 2100 F for 3 Hr at 10,000 PSI</u>							
MCW prepared pellets	U-1179	--	0.520	8.54	77.9		
	U-1180	--	0.507	8.54	77.9	10.55	96.4
	U-1181	--	0.511	8.59	78.4		
	U-1182	--	0.516	8.59	78.4		

(a) The over-all density of the cores contained in a tube was calculated by measurement of the tube after bonding and using the loaded weight of UO<sub>2</sub> in each tube.

## FF-5

Mallinckrodt ceramic grade, dense ceramic grade, high-fired grade, special dense grade, and spherical grade, NUMEC high-fired grade, and Spencer fused grade. Mixtures of these various powders were studied from the basis of compacting and from the densification due to pressure bonding. The results of this compacting study with the various mixtures are included in Table FF-1.

Eleven rod-type specimens containing 35 assorted  $\text{UO}_2$  compacts have been pressure bonded. The initial pressure for compacting was varied in these series. The pressure-bonding containers for these specimens were fabricated of Type 304 stainless steel tubes having an inside dimension of 0.540 in. with a wall thickness of 0.020 in. Also, three rod-type specimens containing 12  $\text{UO}_2$  compacts as pressed and dewaxed by MCW were pressure bonded in containers of Type 304 stainless steel having an inside diameter of 0.318 in. with a wall thickness of 0.010 in. The specifications for these 47 green compacts, the gas-pressure-bonding conditions, and the final densifications of the compacts are given in Table FF-1.

The seven types of uranium dioxide were analyzed chemically. The MCW spherical, MCW special dense, MCW high-fired, NUMEC high-fired, and Spencer fused  $\text{UO}_2$  exhibited an oxygen-to-uranium ratio of 2.00, or stoichiometric equivalent. The MCW ceramic and dense ceramic grades gave oxygen-to-uranium ratios of 2.08 and 2.07, respectively.

Additional surface-preparation methods for preparing Type 304 stainless steel flat plates for pressure bonding are being investigated. The effect of these different methods upon the bond quality will be studied. Specimens prepared thus far include as-rolled, belt-abraded, and vacuum-annealed surfaces. These have been gas-pressure bonded 3 hr at 2000 or 2100 F at 10,000 psi. They are being evaluated by metallographic observation and bend tests.

The fabrication of several different basic fuel-element shapes incorporating uranium dioxide fuel is being investigated. These include flat plates with and without compartments, tubular shapes, rods, and corrugated shapes. Studies are being directed to the development of these shapes for the simultaneous densification and cladding of the  $\text{UO}_2$  by pressure bonding. Methods of improving dimensional properties of the clad elements by varying container designs and using compacted stainless steel end plugs with densities equivalent to the core are being investigated.

## DEVELOPMENT OF URANIUM CARBIDE-TYPE FUEL MATERIALS

F. A. Rough and W. Chubb

The technology of uranium-carbon alloys, particularly uranium monocarbide, is being developed in the expectation that uranium carbide can be used as a low-cost fuel for nuclear reactors for the production of electrical power. An integrated program of research is being conducted with respect to techniques for preparing carbides, for shaping and densifying carbide powders, and for melting and casting of shapes. The program involves research on the properties of the uranium carbides, including their physical properties, mechanical properties, resistance to chemical attack, and diffusion rates at

temperatures above 1200 C, and the mechanism of irradiation damage to the carbide structure. The data obtained are expected to remove most of the uncertainties retarding the use of uranium carbides as fuels for nuclear reactors.

Previous reports have presented data indicating that there is no practical obstacle to the melting and casting of uranium carbide specimens in sizes up to 1 in. in diameter and 8 in. long. The densities and electrical resistivities of castings containing up to 9.2 w/o carbon have been reported as a function of carbon content. Impurity additions, such as iron, silicon, tungsten, and excess carbon were reported to have a detrimental effect upon the strength and corrosion resistance of uranium monocarbide. Uranium dioxide and uranium monocarbide, which are compatible at the melting point of uranium (1130 C), have been found to react at the melting point of uranium monocarbide (2400 C) to produce uranium metal and carbon monoxide.

During the past month, skull-melting techniques have produced uranium carbide castings of cylindrical shape 2 in. in diameter and also of rectangular shape, 1-1/2 by 1-1/2 in. in cross section. The surface quality of these castings was satisfactory, but internal porosity indicates that further development of the casting technique is required. Uranium monocarbide showed no reaction in contact with molybdenum and tantalum in 24 hr at 1200 C, with copper in 24 hr at 1000 C, and with aluminum in 24 hr at 600 C. Uranium monocarbide reacted with stainless steel, Inconel, and mild steel in 24 hr at 1000 C. The nature of this reaction will be investigated. Measurements of the rates of interdiffusion of uranium and carbon through layers of uranium monocarbide and uranium dicarbide are complete. The diffusion coefficients obtained are described by the equation,  $D = 148 e^{-79000/RT}$ , over the temperature range from 1200 to 2000 C. Metallographic structures observed in cast specimens and in diffusion couples suggest that minor revisions may be required in the uranium-carbon constitutional diagram.

#### Alternate Fabrication Methods for UC

S. J. Paprocki, D. L. Keller, G. W. Cunningham, and D. E. Kizer

Methods of producing dense UC pellets by powder-metallurgy methods are being investigated. Evaluations are being made on the quality of the material produced as well as on the proposed costs for large-quantity production. Current procedures which are being investigated include reactions of uranium metal powder with various types of carbon and the reaction of uranium metal with alkanes such as methane. In addition, sintering studies are being conducted on several types of UC powder.

A mixture of 5 w/o AGOT-type graphite and 95 w/o minus 325-mesh uranium powder mixture was prepared and hot pressed to 10.4 g per cm<sup>3</sup> at 593 C. Time and pressure at temperature were 25 min and 24,000 psi. The hot-compacted core was reacted for 4 hr in a vacuum at 1040 C. The resulting density was 7.43 g per cm<sup>3</sup>. Visual examination of the core indicated that oxidation had occurred during the reaction. Additional cores of this type are being prepared from various types of carbon powders.

## FF-7

Green-pressed powder cores of 95 w/o uranium plus AGOT-type graphite or lamp-black exhibited densities of 8.96 and 3.82 g per cm<sup>3</sup>, respectively. A pressure of 50 tsi was used in compacting. After reacting 4 hr in a vacuum at 1100 C, the densities were, respectively, 7.29 and 5.63 g per cm<sup>3</sup>. Microscopic examination of the uranium-AGOT graphite core indicated that no reaction had occurred. The uranium-lampblack core could not be examined metallographically. Additional cores of this type are being prepared using Novite-A activated charcoal. In addition, green-pressed cores of UO<sub>2</sub>-carbon are being prepared from a mixture of the stoichiometric composition of UC for reaction studies.

A sample of uranium has been reacted with methane gas in order to obtain a fine UC powder. No appreciable change in the reaction rate was noted at temperatures between 650 and 925 C. The reaction was assumed to be complete when no change in pressure was noted in the reaction vessel when cooled from 650 C to 230 C after filling the vessel with hydrogen. A chemical analysis of the powder has not been obtained. A fresh charge of uranium has been placed into the reaction chamber for additional studies in converting uranium metal to UC by the use of propane gas instead of methane.

#### Melting and Casting Techniques for Uranium-Carbon Alloys

W. M. Phillips, E. L. Foster, and R. F. Dickerson

Reliable techniques for the production of high-quality cast shapes of uranium carbide are being developed. Castings up to 5/8 in. in diameter have been made by inert-arc drop-casting techniques. Attempts to produce larger castings by inert-arc skull-melting techniques are now in progress. During the past month this technique has been employed to produce large castings of varied shapes.

The skull-melting technique employs a graphite liner in a water-cooled copper crucible. A skull or layer of uranium carbide is built up on the liner by melting a charge of uranium and carbon. Melting is accomplished at 3500 amp and 25 v, using a graphite tip on the electrode.

Charges of prealloyed uranium carbide as well as charges of uranium plus carbon have been used with no observable effect of this variation on the quality of the castings. Graphite molds have been used successfully to produce cylindrical castings 1 and 2 in. in diameter and rectangular castings of 1-1/2 by 1-1/2 in. in cross section. Radiographic examination of these castings indicated some porosity. The surface quality of the castings was satisfactory. In future work variations in the furnace atmosphere will be employed in an attempt to improve the soundness of the castings.

Additional studies of the effects of using heated molds will be made in an attempt to improve the quality of the surface of castings. The melting behavior of certain U(C,N) alloys will be investigated because of the higher uranium density of UN and alloys of UC with UN.

Metallurgical and Engineering Properties of Uranium Monocarbide

W. M. Phillips, E. L. Foster, and R. F. Dickerson

A properties study of uranium carbides is in progress aimed at both determining and improving the properties of these materials. The study is concerned with the effect of such variables as impurity content, carbon content, and heat treatment on density, resistivity, thermal conductivity, and corrosion resistance in various media.

The effects of carbon content and heat treatment were investigated by measuring densities, resistivities, and transverse rupture strengths of specimens containing from 2.2 to 9.2 w/o carbon in the as-cast state and after a 1-hr anneal at 1550 C. The results showed inconsistencies, not in agreement with data obtained previously, and are being rechecked. Metallographic examinations of the as-cast specimens indicated a eutectic and insolubility gap between UC and UC<sub>2</sub> at the solidus temperature at about 6.6 to 7.0 w/o carbon.

Metallographic examinations of compatibility capsules exposed at 1000 and 1200 C for 24 hr are complete. No reaction of uranium monocarbide with molybdenum or tantalum was observed at either temperature. However, mild steel, stainless steel, and Inconel showed some reaction at both temperatures. X-ray examination is planned to determine the composition of the reaction products. No reaction was observed between uranium monocarbide and aluminum at 600 C or with copper at 1000 C after 24 hr.

Specimens of uranium monocarbide containing niobium, tantalum, titanium, tungsten, vanadium, zirconium, Al<sub>4</sub>C, Cr<sub>3</sub>C<sub>2</sub>, Mn<sub>3</sub>C, Mo<sub>2</sub>C, NbC, TaC, TiC, VC, and ZrC have been prepared by arc melting and are presently being evaluated on the basis of rupture strength, resistivity, density, and microstructure. Specimens suitable for thermal-conductivity and specific-heat measurements are also being prepared for tests.

Uranium Monocarbide Diffusion Studies

W. Chubb, R. W. Getz, and F. A. Rough

The rates of interdiffusion of uranium and carbon in the uranium-monocarbide-dicarbide system and the rates of self-diffusion of uranium and carbon in uranium monocarbide are being investigated. During the past few months work has been concentrated on determining interdiffusion rates by measuring the rate of growth of the carbide layers formed at various temperatures between molten uranium and graphite. This work is now complete, and effort is now being directed toward determining the rates of self-diffusion of uranium and carbon in the monocarbide.

All measurements of diffusion layers formed between saturated molten uranium and graphite have been completed. Molten uranium was contained in graphite crucibles at temperatures ranging from 1600 to 2000 C for times ranging from 1 to 8 hr. The thickness of the combined layers of UC and UC<sub>2</sub> was measured and used to calculate

## FF-9

diffusion coefficients. In making these calculations it was assumed that the rate of diffusion was the same in both phases and that the interface between UC and UC<sub>2</sub> had no influence on diffusion through the two layers; i. e., that UC and UC<sub>2</sub> form a single solid solution from 4.8 to 9 w/o carbon and that diffusion rates are not concentration dependent in this system. Based on four measurements at each temperature, the following mean interdiffusion coefficients have been calculated:

Temperature, C	Interdiffusion Coefficient, D, cm <sup>2</sup> per sec
1600	1.9 x 10 <sup>-7</sup>
1800	1.2 x 10 <sup>-6</sup>
1900	1.6 x 10 <sup>-6</sup>
1980	9.6 x 10 <sup>-6</sup>

In addition, the results of similar experiments recently reported in the literature\* have been used to calculate interdiffusion coefficients between 1200 and 1400 C as follows:

Temperature, C	Interdiffusion Coefficient, D, cm <sup>2</sup> per sec
1200	2.9 x 10 <sup>-10</sup>
1300	1.5 x 10 <sup>-9</sup>
1400	4.7 x 10 <sup>-9</sup>

When these values are plotted on a graph of log D versus the reciprocal of the absolute temperature from 1200 to 2000 C, they are found to fall very nearly on a straight line having the equation:

$$D = 148 e^{-79000/RT}$$

The activation energy for diffusion in this system (79,000 cal per mole) is very high when compared with those for most metals, but it is reasonable for a material having a melting point of 2400 C.

Metallographic examination of the diffusion samples at 1600, 1800, and 1900 C shows a discontinuous increase in the solubility of uranium in UC<sub>2</sub> between 1600 and 1800 C. The solubility appears to be very high at 1800 and 1900 C and much lower at 1600 C. This suggests that the high-temperature cubic form of UC<sub>2</sub> decomposes at about 1800 C by a eutectoid reaction into a metastable mixture of UC and tetragonal UC<sub>2</sub>. Lever-law calculations show that the eutectoid is at about 7.0 w/o carbon and that the product of the reaction is UC containing about 5.2 w/o carbon and tetragonal UC<sub>2</sub> containing about 8.8 w/o carbon. The eutectoid temperature is presumed to be a few degrees below the transformation temperature of stoichiometric UC<sub>2</sub>. No U<sub>2</sub>C<sub>3</sub> was observed in any of the diffusion couples, and it can only be assumed that the proper conditions for nucleation of this stable phase were not present in the samples. It is generally accepted that U<sub>2</sub>C<sub>3</sub> requires some sort of mechanical disturbance, shock, or stress to promote its nucleation.

\*Swarts, E. L., Trans. AIME, 215, p 553.

Development of mechanical and physical techniques for determining the rate of self-diffusion of uranium in uranium monocarbide is well advanced. Depleted uranium (0.04 per cent uranium-235) has been received and is being processed into melting stock for preparing 1/2-in. rods of uranium monocarbide. These will be sectioned into 1/4-in. lengths using a diamond cutoff wheel and a kerosene coolant. Enriched uranium-metal foil (93 per cent uranium-235 and 0.001 in. thick) is on hand. This will be sandwiched between two lengths of depleted carbide and bonded and diffusion annealed. A bonding technique involving a graphite jig has been tested using normal uranium foil and normal uranium carbide. Bonding has been achieved, but it is not clear that the nature of the bond is satisfactory for diffusion annealing. One bond apparently contained  $UO_2$ , another bond apparently contained  $UC_2$  plus graphite. Further tests will be made.

After diffusion annealing at temperatures between 1200 and 2000 C, the samples will be mounted in Bakelite and ground down in the direction of the axis of the specimens, perpendicular to the plane of the uranium-235 layer. Grinding will be done on a silicon carbide block in the presence of nitric acid. Samples of uranium have been obtained from natural uranium carbide specimens in this fashion. These samples are currently being analyzed for total uranium content to determine if all the uranium is recovered in the nitric acid solution when a measured length of carbide is ground off the mounted specimen.

When samples are obtained from the diffusion couples, these will be examined for the presence of uranium-235, and those that appear to contain the diffusion zone will be irradiated for a short time at the BRR. Gamma counting of the irradiated samples will provide a measure of the uranium-235 present in each sample and can be used directly to calculate the rate of diffusion of uranium in uranium carbide. Enriched uranium standards for this "activation" analysis have been prepared. A depleted-uranium background standard will be prepared from the batch of depleted-uranium metal obtained for these experiments.

#### Irradiation Effects in UC

A. E. Austin and C. M. Schwartz

A study of the effects of neutron irradiation and fission upon the structure of UC is in progress. The necessary apparatus and shielding to permit an X-ray diffraction study of irradiated UC are being constructed. Techniques for electron-microscopic examination are being worked out, using previously irradiated specimens.

Experiments are being carried out to determine the applicability of low-angle X-ray scattering for detection of voids or gas bubbles. For this purpose, additional arc melts were made of nominal 90 w/o ZrC-10 w/o UC and 60 w/o ZrC-40 w/o UC. Solid solutions of the monocarbides were obtained. These materials are being used in attempts to prepare sections sufficiently thin for the necessary X-ray transmission experiments.

## GG-1 and GG-2

## GG. VOID-DISTRIBUTION AND HEAT-TRANSFER STUDIES

D. V. Grillot, R. Wooton, H. M. Epstein,  
D. A. Dingee, and J. W. Chastain

Subcooled-boiling heat-transfer research is being conducted for the Euratom-U. S. Joint Research and Development Board. During the past month, construction of the basic flow loop for the experimental studies was completed. Additional electric lines are being added at present to deliver the maximum power required for the later experiments.

Checkout of loop operation has continued. The loop components were hydraulically tested to pressures 50 per cent above the maximum operating pressure. The orifice plate for metering flow has been calibrated through the required flow range. All pressure gages have been calibrated with a hydraulic pressure balance.

A literature survey is being conducted in the field of subcooled void formation and heat transfer. Information on present theories and correlations is being used to help design the experiments to check present correlations or form the basis for new ones.

The remainder of the items required for the instrumentation, including the praseodymium-144  $\beta$ -ray source, should be received at the beginning of next month. Void calibrations and trial checkout tests may then be performed.



H-1

## H. PHYSICAL RESEARCH

F. A. Rough

The mechanism of hydrogen migration under the influence of a thermal gradient is under study. This research is supported by the AEC Division of Research.

Thermal Migration of Hydrogen in Zirconium

J. W. Droege, W. M. Albrecht,  
W. D. Goode, and H. H. Krause

Hydrogen migration in zirconium under the influence of a thermal gradient is being studied. Fabrication of an improved diffusion cell for the experimental study is in progress. Measurement of diffusion coefficients for hydrogen in delta zirconium hydride is also under way.

Thermal Diffusion

The initial thermal-diffusion experiments were performed on a sample of beta zirconium hydride which had been pressure bonded in a stainless steel jacket. It was found that the bonding did not provide adequate thermal contact and also permitted some leakage of hydrogen around the circumference of the zirconium hydride sample. An improved cell is now being fabricated, using a cylindrical section of zirconium hydride 1 in. in diameter and 1/2 in. thick. A cylindrical piece of iron will be placed against each face of the zirconium hydride, and copper cylinders will, in turn, be in contact with the iron. These five pieces will be enclosed in the stainless steel cladding. A test element is being prepared that can be sectioned after bonding and examined metallographically to make sure that a proper bond is obtained. Higher bonding temperatures than used previously will be employed.

A properly bonded element will then be provided with thermocouples inserted radially into the iron to determine the temperatures and the heat fluxes. Holes will be drilled axially through the copper and iron to determine the pressure at the faces of the zirconium hydride. From these measurements the steady-state concentration gradient can be determined after sufficient time in an imposed thermal gradient.

Diffusion Coefficients

The diffusion of hydrogen in beta zirconium and zirconium hydride is being investigated as part of a study of the thermal migration of hydrogen in these materials. Diffusion coefficients are being determined from permeation-rate measurements.

Diffusion coefficients of hydrogen in beta zirconium in the range 650 to 850 C have been determined. A topical report, BMI-1373, describing these experiments has been published.

## H-2

Several experiments have been made to determine the rate of diffusion of hydrogen in zirconium hydride in the range 500 to 700 C using samples 0.8 to 1.5 mm thick with average concentrations of 60 to 66 a/o hydrogen. The apparent permeation rates obtained from these experiments yield erratic values of the diffusion coefficients. This was due to procedural difficulties. The permeation apparatus was originally designed for the beta-phase zirconium study at pressures below about 100 mm of mercury. It was found that the hydrogen pressures and flow rates cannot be adequately controlled at the higher equilibrium pressures, up to 1 atm, required for the study of diffusion in the hydride phase. Therefore, the apparatus and procedures are being altered to suit the study.

I-1

## I. SOLID HOMOGENEOUS FUELED REACTORS

W. S. Diethorn and W. H. Goldthwaite

Fission-gas retention and the mechanical and physical properties of commercial fueled-graphite spheres are being studied as part of the Pebble-Bed Reactor program.

LABORATORY EVALUATIONS OF FUELED-GRAPHITE SPHERESJ. F. Lynch, M. C. Brockway, S. Rubin,  
D. J. Bowers, and W. H. Duckworth

Compression, impact, hot-oil, and self-welding studies on coated fueled-graphite spheres are continuing. In addition to spheres coated with SiC, siliconized SiC, and pyrolytic carbon, a new series of spheres coated with zirconium carbide and titanium carbide is being evaluated.

EVALUATION OF METAL-COATED UO<sub>2</sub> PARTICLES

A. F. Gerds, J. Koretzky, and F. W. Boulger

A study of carburization of UO<sub>2</sub> particles coated with nickel, nickel-chromium, niobium, or Al<sub>2</sub>O<sub>3</sub>, dispersed in a carbon matrix, is continuing. As-received particles, pressed compacts baked at 1700 F, and pressed compacts baked at 1700 F and heated at 2500 F (168 hr) or 3000 F (6 hr) have been examined metallographically. The 1700 F bake did not affect the Al<sub>2</sub>O<sub>3</sub>-coated UO<sub>2</sub>, but all the metal-coated particles reacted with carbon at this temperature. All the metal coatings lost their integrity at 2500 F. No reaction between Al<sub>2</sub>O<sub>3</sub> and carbon was observed at this latter temperature. All the coated particles showed extensive reaction at 3000 F.

Heat treatment and metallographic examination of the Al<sub>2</sub>O<sub>3</sub>-coated UO<sub>2</sub> will be continued.

FABRICATION DEVELOPMENT OF Al<sub>2</sub>O<sub>3</sub>-CLAD UO<sub>2</sub>  
FUEL PARTICLES

A. K. Smalley and W. H. Duckworth

Work during September was directed toward refining the fabrication method. Attempts are being made to optimize the type and amount of organic binder used in the

UO<sub>2</sub> particles and in the Al<sub>2</sub>O<sub>3</sub> cladding, and to develop a method of compacting the composite pellets without damaging the cladding. Pellet evaluation consists of high-temperature (1200 F) air-oxidation tests, alpha assays for uranium contamination in the cladding, and fission-gas-retention determinations.

### FISSION-PRODUCT RELEASE FROM FUELED-GRAPHITE SPHERES

W. S. Diethorn

Neutron-activation and in-pile experiments are being conducted to determine fission-gas retention and the effect of radiation on fueled-graphite spheres.

#### Neutron-Activation Studies

R. Lieberman, H. S. Rosenberg, and D. N. Sunderman

Two coated graphite spheres and Al<sub>2</sub>O<sub>3</sub>-clad UO<sub>2</sub> powder were activated and the fission-gas release determined during postirradiation heat treatment. The powder was prepared by BMI. The data are reported in Table I-1.

TABLE I-1. NEUTRON-ACTIVATION RESULTS<sup>(a)</sup>

Specimen	Coating	Postirradiation Heat Treatment Temperature(b), F	Time at Temperature(c), min	Fission-Gas Release(d), per cent of xenon-133
FA-20, 310 (graphite sphere)	Carbon, 5 mil	1500	200	0.03
		1500 (1 day)	158	0.06
FA-8, 7 (graphite sphere)	SiC, 30 mil	1200	2	0.5
Al <sub>2</sub> O <sub>3</sub> -clad UO <sub>2</sub>	Al <sub>2</sub> O <sub>3</sub> , ~400 microns	1500	30	None
		1800	30	2.4 x 10 <sup>-3</sup>
		2000 (1 day)	60	1.4 x 10 <sup>-3</sup>
		2200	30	Very small
		2450 (1 day)	30	5.5 x 10 <sup>-3</sup>

(a) Each specimen irradiated once.

(b) Time in parentheses is delay time between this heat treatment and prior heat treatment.

(c) Zero time begins when heat is applied to specimen. Heatup time is 5 to 10 min for all specimens.

(d) Number of atoms released divided by number of atoms present at beginning of heat treatment times 100.

Prior to irradiation, Sphere FA-8, 7 was impacted, producing a fine crack extending around the entire circumference of the coating.

## I-3

The fission-gas retention of the  $\text{Al}_2\text{O}_3$ -clad  $\text{UO}_2$  is encouraging. The powder consisted of 1000 to 2000- $\mu$ -OD angular particles with 25 w/o natural  $\text{UO}_2$  in the cores. Prior to irradiation, an alpha assay of the powder showed that uranium contamination in or on the cladding was negligible (<0.5 cpm per g). Calculations show that this uranium contamination cannot possibly account for the release values reported in Table I-1. The interpretation of the release rates is difficult in this preliminary evaluation because the effects of nonuniform cladding thickness and microcracks in the cladding are not known.

### In-Pile Capsule Experiments

D. B. Hamilton, D. Stahl, G. E. Raines, R. J. Burian,  
and W. H. Goldthwaite

Last month in BMI-1377 the nature and objectives of the in-pile capsules currently planned in this program were described.

#### SP-3

Postirradiation examination of Sweep Capsule SP-3 was reported last month. Metallographic examination of each type of specimen is under way. This work will complete the postirradiation examination of SP-3.

Specimen burnups estimated from wire dosimeters in this capsule are reported in Table I-2.

TABLE I-2. SP-3 BURNUPS

Specimen	Uranium-235 Burnup, per cent
FA-6, 18E	2.7
FA-6, 20E	2.2
FA-8, E4	2.7
FA-8, E5	2.9

#### SP-4

Irradiation of Static Capsule SP-4 in the BRR is continuing. Sphere-surface operating temperatures are about 300 F lower than the target temperature of 1900 F. Several of the thermocouples, located outside and adjacent to the sphere surfaces, have failed. This capsule will be left in the BRR until the scheduled four-cycle exposure is completed.

SP-5

Irradiation of this sweep capsule has been postponed and no target date has been set.

SPH-1

The target date for irradiation of this high-flux high-burnup capsule has been changed to December, 1959.

SPF Capsule Series

The first capsule in this series, SPF-1, is assembled and scheduled for BRR insertion in early October.

Fabrication of parts for SPF-2 has been completed, and capsule assembly is under way.

J-1

## J. PROBLEMS ASSOCIATED WITH THE RECOVERY OF SPENT REACTOR FUEL ELEMENTS

### Corrosion Studies of the Fluoride-Volatility Process

C. L. Peterson, P. D. Miller, W. N. Stiegelmeier, and F. W. Fink

As part of a program of assistance to the Chemical Technology Division, the corrosion of several pieces of process equipment used at ORNL in studies of the Fluoride-Volatility process is being evaluated.

The corrosion of the Mark II fluorinator was described in BMI-1377. Further study of some of the internal components of this vessel which were used for only part of the runs has permitted some correlation of the corrosion with the operating conditions.

Three phases of experiments were conducted in this fluorinator with a total exposure of about 1939 hr to molten-salt temperatures using a total sparge of 60,470 standard liters of fluorine. During these phases, the exposure to molten salts and to fluorine sparging was distributed as follows:

<u>Phase</u>	<u>Time at Temperature, per cent of total</u>	<u>Fluorine Sparged, per cent of total</u>
I	47	74
II	16	26
III	37	0

By far the greatest metal loss occurred during Phase I, while the metal loss during Phase III in which no fluorine was sparged was insignificant. This indicates that the fluorine sparge is a much more important factor in producing attack than the duration of the exposure to molten salts.

There is some indication that, as might be expected, the attack was much more severe when the temperature ranged from 690 to 700 C than when it averaged about 630 C.

On the basis of the corrosion evaluation, it appears that rather severe corrosion can be anticipated in a fluorinator constructed from "L" Nickel. If this material is used, the data indicate that the attack may be reduced by operating at as low a temperature as is compatible with other considerations. Corrosion may also be reduced by maintaining the sulfur concentration in the salt, sparging gases, and the nickel as low as possible and by avoiding an excess of fluorine sparge.

Substantial intergranular penetration had been observed on the inside walls of the Unit Operations INOR-8 hydrofluorinator. This occurred predominantly at and above the molten-salt interface. A fairly thick scale, which has not yet been identified but

which appears granular and metallic, also covers the inside wall in this region. Below the interface there is neither much scale nor intergranular penetration on the vessel wall. Deep pits occurred on the wall at the interface and over the full length of both sides of the draft tube. Scale also occurred on the inner surface of the draft tube. At present, the indications are that the scale, pitting, and intergranular attack are closely associated with the area in the hydrofluorinator where the HF sparge had easy access to the walls, with the molten-salt interface being most vulnerable. The evaluation of this equipment is being continued.

### Study of the Effect of Irradiation on Cladding- and Core-Dissolution Processes

R. A. Ewing, H. B. Brugger, D. K. Dieterly, and D. N. Sunderman

#### Sulfex Process

Dissolution of two 7-in. prototype Consolidated Edison pins was described in previous reports. Uranium concentrations in the sulfuric acid decladding solutions from these pins were 19.5 and 16.6 mg per liter. Uranium-input data are not yet available, but on the basis of approximately 1.6 g of uranium in the pins, indicated uranium losses were from 0.32 to 0.36 w/o.

Acid-insoluble filter residues from both of these tests were low, 0.2 to 0.3 g. Since uranium content of these residues was very low, 0.04 to 0.07 w/o, uranium losses to this fraction were negligible.

The next "cold" Sulfex test, to be conducted shortly at the hot cell, primarily will check the performance of the apparatus when remotely operated. In addition, the effect of prolonged contact of the decladding solution and the declad pins is to be checked. Study of this factor is also to be included in the subsequent tests of irradiated pins.

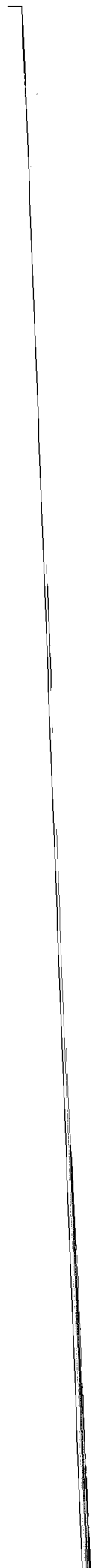
Thorium-loss data are not yet available for these first two tests. Separation of the thorium from interferences by a lanthanum fluoride carrier precipitation is being evaluated. The analytical procedure is not yet fully developed, but is expected to prove satisfactory.

#### Darex Process

Two "cold" Consolidated Edison pins have been declad by the Darex (dilute aqua regia) process. The volume of dissolvent is twice that of the Sulfex process, and construction of a larger dissolver was necessary. Due to the violence of the reaction in its early stages, it was also found advisable to add a foam trap between the dissolver and the condenser. Core dissolutions, employing the same conditions as used in Sulfex dissolutions, proceeded smoothly. Weights of acid-insoluble filter residues were a little lower, 0.10 to 0.15 g, but again contained negligible uranium, <0.1 w/o.

## J-3 and J-4

The dissolution apparatus is now at the hot cell, and remotely operated familiarization testing is under way. A few minor modifications have been shown to be necessary and are now being made. Following their completion, one cold test each of Sulfex and Darex dissolution is to be made, which will exhaust the supply of cold Consolidated Edison pins. If performance of the apparatus in these tests is satisfactory, testing of irradiated pins can begin soon thereafter.



K-1

## K. DEVELOPMENTS FOR SRE, OMRE, AND OMR

EVALUATION OF URANIUM MONOCARBIDE AS A REACTOR FUEL

F. A. Rough

Two new capsules of cast uranium monocarbide specimens have been discharged from the MTR after irradiation to about 4,000 and 10,000 MWD/T burnup. These capsules are to be examined possibly in November. Preparation of a series of cast UC cylinders for irradiation in the SRE is well under way. The study of thermal conductivity of cast UC specimens reported last month is temporarily suspended until additional specimens are available.

Irradiation of Uranium Monocarbide

D. Stahl, J. H. Stang, and W. H. Goldthwaite

The irradiation of Capsules BMI-23-3 and BMI-23-5 at the MTR was completed after Cycle 127. BMI-23-3 was irradiated in Position A-28-NE for 12 cycles at an unperturbed thermal flux of about  $1.0 \times 10^{14}$  nv; BMI-23-5 was irradiated in Position A-30-NE for 6 cycles at an unperturbed flux of about  $0.8 \times 10^{14}$  nv. The estimated burnups (obtained on the basis of reactor-quoted fluxes) for peak-flux specimens in BMI-23-3 and BMI-23-5 are about 10,000 and 4,000 MWD/T of uranium, respectively. These capsules are scheduled to arrive at the BMI Hot-Cell Facility during October.

The irradiation of Capsules BMI-23-4 and BMI-23-6 is continuing in MTR Positions A-27-SE and A-13-NE, respectively, to achieve 15,000 and 5,000 MWD/T burnup of UC, respectively. The central-core temperatures for BMI-23-4 and BMI-23-6, as estimated from thermocouples adjacent to the top specimens, were about 100 and 1300 F during Cycle 128; these levels are about 100 F lower than those observed during Cycle 127.

Postirradiation Examination of Irradiated  
Uranium Monocarbide

S. Alfant, A. W. Hare, F. A. Rough, and R. F. Dickerson

Two capsules of uranium carbide specimens (5.0 and 4.6 w/o carbon) having burnups of about 4,000 and 10,000 MWD/T UC are scheduled to arrive at the BMI Hot-Cell Facility during October. Examination of these specimens will be initiated possibly during November.

Preparation of UC Pins for Irradiation in the SRE

C. K. Franklin, W. J. Hildebrand, E. L. Foster,  
and R. F. Dickerson

In a program involving development of advanced fuels for the SRE, quantities of cast UC shapes are being evaluated for their preirradiation qualities. Two surface situations are being considered in the preparation of the UC fuel, those representing as-cast surfaces and those representing machined-ground surfaces.

Twenty-four inches of finish shapes have been completed. Ten inches of this material possesses its original cast surfaces and 14 in. has been diamond ground to final size. The cylinders measure  $0.610 \pm 0.002$  in. in diameter and vary in length from 0.9 to 2.3 in.

Compositions of the finish cylinders range from 4.9 to 5.0 w/o carbon. A metallographic examination of the cylinders has confirmed the higher-than-stoichiometric composition of carbon. Thin platelets of  $UC_2$  were observed at the grain boundaries and as a Widmanstätten pattern within each grain of UC. Radiographic examination and density measurements indicate, also, that the material is of high quality. The density of the cast UC shapes averages about  $13.5 \text{ g per cm}^3$ .

The next group will be cast to approximately 0.64 in. in diameter. This group will include about 35 in. of finished cylinders. The as-cast surfaces will be removed by machine grinding to a final diameter of 0.610 in.

## L-1

## L. TANTALUM AND TANTALUM-ALLOY STUDIES

J. H. Stang

In this section, which reports the progress of investigations under the auspices of Los Alamos Scientific Laboratory (LAMPRE Program), final metallurgical and analytical data are presented for 23 binary tantalum alloys which constitute the group which has been in preparation during the past several weeks. A complete set of strip specimens of these materials in both the cold-rolled and annealed conditions has now been forwarded to Los Alamos for plutonium-alloy corrosion testing.

Development of Container Materials for LAMPRE Applications

D. C. Drennen, M. E. Langston, C. J. Slunder, and J. G. Dunleavy

During September work on the series of binary tantalum-base alloys for which various data are presented in Tables L-1 and L-2 was completed. These data show that hafnium, tungsten, and zirconium analyses are in good agreement with the intended compositions. On the other hand, the analyses for thorium, titanium, and yttrium indicate that the recovery of these elements varied considerably. The recovery of titanium varied from 30 to almost 100 w/o and that of thorium from 65 to 75 w/o. The low values obtained for the rolled 0.025 and 0.05 w/o titanium alloys are attributed to segregation. As noted last month, the retention of yttrium was very poor.

The data in the tables also show the extent of contamination of the alloys by various elements. The high carbon content in Specimens 49 and 50 is thought to be traceable to an overheating of the Wilson seal at the top of the arc-melting furnace. No reason for the unusually high levels of nitrogen, 100 and 110 ppm in Specimen 49 and 220 ppm in Specimen 51, is apparent.

In general, it is seen that as the amount of the alloying addition - hafnium, titanium, thorium, yttrium, and zirconium - increased, the oxygen content decreased. This suggests that all of these elements were effective scavengers of oxygen in tantalum.

The grain-size data given in Table L-2 show that additions of hafnium, thorium, tungsten, and zirconium produced a finer grained structure than that of unalloyed tantalum in the cast buttons. This effect, however, was not observed in the annealed materials. The annealing treatments listed in the footnotes of Table L-2 were required to bring about the recrystallization of the various alloys. Two other contaminants, tungsten and zirconium, were present in the hafnium-containing alloys because of the grade of hafnium used as melting stock. Variable tungsten contents in unalloyed tantalum and in some of the other alloys was probably due to erosion of the tungsten electrode, even though this was not always readily apparent during arc melting.

A comparison of the analytical data for the annealed materials in Table L-2 and the rolled materials in Table L-1 shows that the vacuum-annealing treatment at 2600 F was

TABLE L-1. CHEMICAL ANALYSES OF COLD-ROLLED BINARY TANTALUM ALLOYS

Specimen	Intended Composition (Balance Tantalum), w/o	Alloying Element, w/o	Analyzed Actual Composition													
			C							Other Elements, ppm						
			C	H	N	O	Fe	Si	Cu	W	Nb	Zr	Al	Mo	Ni	Cr
44 (control)	100 Ta	--	40	1.5	20	43.5	3	1	5	3000	10	10	10	10	1	3
46	0.025 Hf	0.025	40	1.5	10	30	3	1	8	3000	10	10	10	10	1	20
47	0.05 Hf	0.046	40	1.5	<10	31	3	1	5	2000	10	10	10	10	1	3
52	0.10 Hf	0.10	40	0.5	30	38	3	1	10	350	10	10	10	10	1	3
49	1.5 Hf	1.3	150	0.3	100	28.5	3	1	15	1.1 <sup>(a)</sup>	10	110	10	10	1	3
50	3.0 Hf	2.7	150	0.6	20	20.5	3	1	10	6600	10	220	10	10	1	3
56	6.0 Hf	5.55	20	1.2	20	12.0	3	1	10	250	10	380	10	10	1	3
53	0.025 Zr	0.021	60	0.6	30	32.5	3	1	5	500	10	--	10	10	1	3
54	0.05 Zr	0.033	40	0.5	<10	23.5	3	1	8	500	10	--	10	10	1	3
55	0.10 Zr	0.071	30	0.9	10	20.5	3	1	10	<30	10	--	10	10	1	3
51	1.5 Zr	1.24	40	0.3	220	41.5	3	1	5	100	10	--	10	10	1	3
57	3.0 Zr	2.65	20	0.7	10	9.5	3	1	10	<30	10	--	10	10	1	3
59	0.025 Ti	0.015	10	0.3	40	19.5	3	1	5	<30	10	10	10	10	1	3
60	0.05 Ti	0.004	20	0.7	20	20	3	1	10	200	10	10	10	10	1	3
61	0.10 Ti	0.030	10	0.6	50	17.5	3	1	5	<30	10	10	10	10	1	3
62	0.025 Th	0.018	40	0.4	40	27.0	3	1	5	<30	10	10	10	10	1	3
63	0.05 Th	0.034	20	0.3	60	20.0	3	1	5	<30	10	10	10	10	1	3
64	0.10 Th	0.061	20	0.5	20	12.5	3	1	8	<30	10	10	10	10	1	3
65	3.0 W	2.5	20	0.6	30	22	3	1	4	--	10	10	10	10	1	3
66	0.025 Y	<0.0005	20	0.1	20	19.5	3	1	2	<30	10	10	10	10	1	3
67	0.05 Y	<0.0005	20	0.7	20	16.5	3	1	2	<30	10	10	10	10	1	3
68	0.10 Y	<0.0005	20	0.6	20	12.0	3	1	4	<30	10	10	10	10	1	3
69	0.20 Y	<0.0005	20	0.6	40	10.0	3	1	5	<30	10	10	10	10	1	3

(a) Weight per cent.

L-2

TABLE L-2. GRAIN SIZE, HARDNESS, AND CHEMICAL ANALYSES OF ANNEALED BINARY TANTALUM ALLOYS

Specimen	Intended Composition (Balance Tantalum), w/o	Hardness, VHN	Average Grain Diameter, mm		Alloying Element, w/o	Analyzed Composition						
			As Cast	Annealed		C	Other Elements, ppm					
							H	N	O	Cu	W	Zr
44 (control)	100 Ta	119 <sup>(a)</sup>	2.4	0.06	--	30	0.2	40	52	10	2000	10
46	0.025 Hf	112 <sup>(b)</sup>	2.0	0.05	0.027	40	1.2	40	60	--	6400	<200
47	0.05 Hf	102 <sup>(b)</sup>	1.6	0.04	0.043	50	0.6	20	54	--	2800	<200
52	0.10 Hf	100 <sup>(a)</sup>	1.7	0.04	0.096	50	0.2	60	36.5	80	300	10
49	1.5 Hf	170 <sup>(a)</sup>	0.8	0.04	1.20	160	0.2	110	21.5	80	1.00 <sup>(c)</sup>	250
50	3.0 Hf	150 <sup>(b)</sup>	0.35	0.04	2.70	170	0.30	30	8	--	7200	240
56	6.0 Hf	148 <sup>(a)</sup>	0.38	0.05	5.25	30	0.1	30	15	50	300	500
53	0.025 Zr	100 <sup>(a)</sup>	1.7	0.05	0.033	70	0.1	60	18.5	15	500	--
54	0.05 Zr	99 <sup>(d)</sup>	2.0	0.06	0.027	80	0.4	20	104	--	--	--
55	0.10 Zr	82 <sup>(a)</sup>	1.9	0.06	0.10	50	0.1	40	23	10	<30	--
51	1.5 Zr	196 <sup>(e)</sup>	0.35	0.04	1.26	50	0.4	220	54	--	--	--
57	3.0 Zr	168 <sup>(a)</sup>	0.39	0.04	2.75	40	0.3	50	21	80	200	--
59	0.025 Ti	82 <sup>(a)</sup>	2.0	0.14	0.024	10	0.1	40	22	15	100	10
60	0.05 Ti	72 <sup>(a)</sup>	2.2	0.14	0.027	10	0.1	10	23.5	20	200	10
61	0.10 Ti	73 <sup>(a)</sup>	3.1	0.20	0.030	20	0.2	40	20	10	100	10
62	0.025 Th	131 <sup>(f)</sup>	1.8	(g)	0.019	80	0.2	50	39	--	--	--
63	0.05 Th	132 <sup>(e)</sup>	1.5	0.10	0.031	40	1.2	70	32	--	--	--
64	0.10 Th	109 <sup>(f)</sup>	1.1	0.06	0.066	110	0.2	50	106	--	--	--
65	3.0 W	138 <sup>(a)</sup>	1.5	(g)	2.90	30	0.2	20	24	20	--	10
66	0.025 Y	89 <sup>(d)</sup>	2.9	0.10	<0.001	40	0.4	20	59	--	<50	10
67	0.05 Y	86 <sup>(d)</sup>	3.1	0.07	<0.001	40	1.5	20	66	--	<50	10
68	0.10 Y	131 <sup>(d)</sup>	2.5	0.14	<0.001	50	0.2	30	90	--	<50	10
69	0.20 Y	106 <sup>(d)</sup>	3.5	0.06	<0.001	60	1.0	40	63	--	<50	10

(a) Vacuum annealed 1 hr at 2600 F.

(b) Vacuum annealed 2 hr at 2600 F and 1 hr at 2750 F.

(c) Weight per cent.

(d) Vacuum annealed 2 hr at 2600 F, 1 hr at 2750 F, and 2 hr at 2900 F.

(e) Vacuum annealed 2 hr at 2600 F, 1 hr at 2750 F, and 1 hr at 2900 F.

(f) Vacuum annealed 2 hr at 2600 F, 1 hr at 2750 F, and 3 hr at 2900 F.

(g) Grain size not determined.

L-3

accompanied by a slight increase in carbon, nitrogen, and oxygen contamination levels and a decrease in the hydrogen contents. In general, there was a larger increase in the carbon and oxygen contamination levels as the number of annealing treatments and the temperatures were increased.

Arc melting of another large group of binary alloys of tantalum was initiated late in September. This is the final group of binary alloys in the schedule; alloying elements will include aluminum, beryllium, boron, cerium, iron, lanthanum, scandium, silicon, thorium, titanium, uranium, and yttrium.

#### Effect of Irradiation on Tantalum

J. A. DeMastry, F. R. Shober, F. A. Rough, and R. F. Dickerson

The two MTR irradiation capsules designated as BMI-25-1 and BMI-25-2 containing tantalum tensile specimens were charged into MTR Core Positions L-53 and L-57, respectively, during Cycle 122 shutdown (May 18, 1959). The former capsule was discharged after three cycles during Cycle 126 shutdown (August 10, 1959); the latter is to be discharged after seven cycles (October 12, 1959). The capsules will be shipped together back to the Battelle Hot-Cell Facility, and should arrive about November 1. The evaluation of the irradiated specimens will include tensile properties, Tukon hardness measurements, and some simplified bend tests.

The preparation of unirradiated arc-melted tantalum-tungsten specimens (1.5 and 3 w/o tungsten, representing the anticipated conversions in the irradiated specimens) for control experiments is nearly completed. The specimens have been annealed at 1150 C for 45 min. The tantalum-1.5 w/o tungsten alloy showed complete recrystallization at this temperature; however, the tantalum-3 w/o tungsten alloy was only partially recrystallized. This alloy will be annealed at 1400 C for 1 hr, which should result in complete recrystallization.

N-1

## N. DEVELOPMENTS FOR THE MGCR

W. C. Riley

Research on core materials in support of the MGCR program is in progress at Battelle. The major effort is on the development and evaluation of  $\text{UO}_2$  dispersions in  $\text{BeO}$  and dispersions of  $\text{UC}$  and  $\text{UC}_2$  in graphite, and on the cladding of  $\text{UO}_2$  particles with  $\text{BeO}$ . The evaluations include laboratory tests, examinations, and measurements, neutron-activation screening studies of comparative fission-gas-release characteristics, detailed neutron-activation studies of promising material developments, in-pile fission-product-release studies, and static capsule irradiations to high burnups.

A study of the diffusion of fission products through fuel-element cladding materials is in progress.

FABRICATION AND CHARACTERIZATION OF FUEL MATERIALS

A. B. Tripler, Jr.

Bulk densities of the graphite-matrix fuel elements were increased significantly by the use of Thermax carbon black and skeletal graphite as filler material. The room-temperature gas permeability (argon) of the specimens was approximately 20 times lower than the best obtained previously.

In some cases  $\text{BeO}$ -clad  $\text{UO}_2$  particles have shown no substantial weight increase when heated in air at 1200 F. In others the weight gain is large. Fabrication procedures that will not disrupt the  $\text{BeO}$  cladding are being studied.

Carburization studies in the  $\text{BeO}$ -graphite system are progressing using  $\text{BeO}$ -clad  $\text{UO}_2$  particles dispersed in graphite. No extensive reaction of  $\text{BeO}$  cladding with the carbon or graphite matrices was observed when the composite bodies were heated at 2500 F for 168 hr or at 3000 F for 6 hr.

Preliminary neutron-activation tests and fission-gas release studies were repeated on duplicate  $\text{UC}$ -graphite and  $\text{UC}_2$ -graphite pellets. The original results were considered unreliable because of difficulty with the carbon adsorbent. Of the 12 pellets tested (nine of  $\text{UC}$  and three of  $\text{UC}_2$ ), all but two of the  $\text{UC}$ -containing pellets and all of the  $\text{UC}_2$ -containing pellets released greater than 10 per cent of the xenon-133 present. The high gas release is attributable in part to partial disintegration of the pellets.

Neutron-activation testing and gas-release studies were also made on part of a new group of  $\text{BeO}$ - $\text{UO}_2$  pellets in which the fuel was initially present as  $\text{UO}_2$ -10 w/o  $\text{Be}(\text{OH})_2$ . The xenon-133 gas release varied from 0.88 to 1.63 per cent, which is only slightly higher than observed previously.

Further studies are being made in connection with the neutron-activation work to determine the influence of adsorbent-carbon purity on the amount of fission gas found.

UO<sub>2</sub> Dispersions in BeO

A. K. Smalley and W. H. Duckworth

Densely sintered matrices of BeO containing about 20 volume per cent of uniformly dispersed UO<sub>2</sub> particles are being developed for fuel-element applications.

Laboratory work in this program was temporarily suspended during September.

UC and UC<sub>2</sub> Dispersions in Graphite

W. A. Hedden, W. C. Riley, and W. H. Duckworth

Improved graphite-matrix fuel element cores containing UC or UC<sub>2</sub> in an amount equivalent to 20 volume per cent of UO<sub>2</sub> are being developed.

During September significant increases in the bulk density of the carbon matrix in fuel-containing compacts were achieved. Decreases in gas permeability were also observed.

Bulk densities in the range of 70 to 72 per cent of theoretical were obtained for compacts baked at 2300 F. This is an appreciable increase over the 60 per cent of theoretical which was the highest obtained previously. These compacts contained about 64 w/o of UC and a filler carbon composed of skeletal graphite, Thermax carbon black, and residue from the pitch binder.

Gas permeabilities (argon) measured at room temperature on the above type of specimens were as low as  $0.8 \times 10^{-5}$  darcy. This is about 20 times lower than the best obtained previously. Measurements made on selected nonfueled specimens showed permeability values as low as  $0.3 \times 10^{-5}$  darcy. Permeability values of about  $10^{-7}$  darcy are being sought.

In future work, the investigation of methods to increase density and decrease the permeability of fueled compacts will be continued.

Cladding of UO<sub>2</sub> Particles With BeO

A. K. Smalley and W. H. Duckworth

A method for cladding UO<sub>2</sub> fuel particles with a densely sintered shell of BeO is being developed.

Work during September was aimed at refining the method for fabricating the fueled pellets and at improving the reproducibility of the method. To date, batches have been unpredictable in the amount of UO<sub>2</sub> oxidation occurring on heat treatment in air at 1200 F. This heat treatment is the screening test by which the integrity of the claddings

## N-3

is initially evaluated. Some batches are substantially unaffected by the heat treatment, whereas in other batches made under similar conditions as much as 80 w/o of the  $\text{UO}_2$  present is oxidized to  $\text{U}_3\text{O}_8$  in less than 5 hr.

Attempts are being made to optimize the type and amount of organic binder used in the fuel particles and in the BeO cladding, and to develop a method for compacting the composite pellets without damaging the claddings. Also, experiments are in progress to determine the optimum heating schedule for removing the volatile matter from the pellets without disrupting the claddings.

Evaluations of the claddings will consist of:

- (1) Measuring the amount of  $\text{UO}_2$  oxidation as a result of heating the pellets in air at 1200 F
- (2) Measuring the alpha-particle emission to estimate the  $\text{UO}_2$  contamination in or on the claddings
- (3) Measuring the fission-product release caused by neutron-activation testing.

#### Carburization Studies in the BeO-Graphite System

A. F. Gerds, J. Koretzky, and F. W. Boulger

The effect of temperature and time on the reaction of graphite or carbon and BeO is being studied in composite bodies of BeO-clad  $\text{UO}_2$  dispersed in graphite or carbon.

BeO-clad  $\text{UO}_2$  particles were dispersed in several types of petroleum coke-pitch mixtures and in AGOT graphite-pitch mixtures. Pellets were formed at 24,000 psi and baked at 1700 F. The bodies which contained the AGOT graphite were heated additionally in helium at either 2500 F for 168 hr or at 3000 F for 6 hr. Individual clad particles and the compacts that had been heated at 1700, 2500, or 3000 F were examined in section by metallographic techniques. The results indicated that no extensive reaction between the BeO and graphite was caused by heating at 1700, 2500, or 3000 F. Apparently, heat treatment at 3000 F caused some interdiffusion between  $\text{UO}_2$  and BeO. Because of this diffusion, the amount of  $\text{UO}_2$  in the center of the BeO-coated particles was reduced.

Metallographic examination of the specimens will be continued. The reaction between other graphite matrices and BeO will be studied.

#### Preliminary Characterization by Neutron Activation

P. Gluck, R. H. Barnes, and D. N. Sunderman

The investigation of the release of fission products from  $\text{UO}_2$ -BeO, UC-graphite, and  $\text{UC}_2$ -graphite fuels is continuing.

## N-4

In September, measurements were made of fission-product release from pellets of UC-graphite, UC<sub>2</sub>-graphite, and UO<sub>2</sub>-BeO during postirradiation heat treatment at 1800 F. Studies were conducted in the same manner as described in BMI-1366. The fueled graphite pellets were duplicates of an earlier group for which release data were questionable because of difficulty with the adsorbent. The UO<sub>2</sub>-BeO pellets tested were some of those in which the fuel was initially present as UO<sub>2</sub>-10 w/o Be(OH)<sub>2</sub> (see BMI-1377, p 82). The results of the measurements on the UO<sub>2</sub>-BeO specimens are summarized in Table N-1. In addition to the xenon-133 and iodine-131, small amounts of tellurium-132, iodine-132, and xenon-133m were also detected.

In the early work in which low-purity charcoal was used as an adsorbent exclusively, low amounts of fission-product release were observed. Later work, which is based on a high-purity charcoal, indicates higher releases. In order to determine the magnitude of the difference in adsorptive capacity between the two charcoals, both charcoals were used under identical conditions with UC-graphite specimens. The results indicate lower apparent releases when low-purity charcoal was used. However, it is not clear that the difference is due solely to the adsorptive capacities. It may also be due to a partial disintegration of the specimens. All the UC-graphite and UC<sub>2</sub>-graphite pellets partially disintegrated during heat treatment, except two which were heat treated with low-purity charcoal. Pellets UC-1 and UC-4 had the lowest xenon-133 release. Further tests will be made using UO<sub>2</sub>-BeO, which has not disintegrated, to determine the difference between the two charcoals.

During the next month studies will be continued on UO<sub>2</sub>-BeO specimens fabricated by different techniques.

### STUDIES OF FISSION-GAS RELEASE FROM FUEL MATERIALS

R. H. Barnes

Design, construction, and assembly of apparatus for the neutron-activation and in-pile fission-gas release studies were continued.

#### Detailed Neutron-Activation Studies

P. Gluck, R. H. Barnes, and D. N. Sunderman

Assembly of the apparatus for the postirradiation fission-gas-release study is continuing. Completion of the assembly of the apparatus is scheduled for November.

#### In-Pile Studies

N. E. Miller and G. E. Raines

The sweep-gas and temperature-control apparatus for the in-pile apparatus are partially assembled. The thermal mock-up of the in-pile capsule that is to be used to

TABLE N-1. FISSION-GAS RELEASE FROM UC-GRAPHITE, UC<sub>2</sub>-GRAPHITE, AND UO<sub>2</sub>-BeO SPECIMENS DURING POSTIRRADIATION HEAT TREATMENT IN VACUUM AT 1800 F FOR 24 Hr

Specimen	Firing Temperature, F	Specimen Weight, g	Fuel, w/o	Thermal-Neutron Flux, 10 <sup>11</sup> nv	Decay Time (a), days	Total Uranium Burnup, 10 <sup>7</sup> a/o	Fission Gas Release (b), per cent	
							Xenon-133	Iodine-131
<u>UC-Graphite and UC<sub>2</sub>-Graphite Specimens</u>								
UC-1 (c, d)	2000	0.3930	60.3	3.52	13.25	5.19	2.0	3.3
UC-2 (e)	2000	0.3483	60.3	3.52	13.00	5.19	15.0	3.9
UC-3(e)	2000	0.3398	60.3	3.52	13.12	5.19	14.5	10.2
UC-4(d)	2350	0.3874	60.3	3.59	13.04	5.29	1.5	1.7
UC-5(e)	2350	0.4089	60.3	3.66	13.30	5.39	10.3	1.6
UC-6(e)	2350	0.4275	60.3	3.75	13.08	5.53	10.9	5.4
UC-7(e)	2700	0.3931	60.3	3.56	15.72	5.24	14.7	14.2
UC-8(e)	2700	0.3483	60.3	3.61	15.76	5.32	13.8	15.9
UC-9(e)	2700	0.3399	60.3	3.70	15.79	5.46	16.1	15.3
UC <sub>2</sub> -10(e)	2700	0.3875	61.3	3.51	15.82	5.17	12.9	18.4
UC <sub>2</sub> -11(e)	2700	0.4089	61.3	3.58	15.85	5.28	11.2	12.2
UC <sub>2</sub> -12(e)	2700	0.4275	61.3	3.68	15.89	5.43	10.4	15.9
<u>UO<sub>2</sub>-BeO Specimens</u>								
A-2(f)	2800	0.7595	48.5	5.18	17.82	7.65	1.63	2.83
A-3	2800	0.7429	48.5	5.10	17.03	7.53	1.37	2.80
B-1	3000	0.7511	48.5	5.08	17.00	7.50	1.05	1.79
B-2	3000	0.7766	48.5	5.22	16.95	7.70	1.32	2.13
B-3	3000	0.7674	48.5	5.19	16.91	7.65	0.88	1.6

(a) Radioactive decay time between irradiation and radioassay.

(b) Fission-gas release is the ratio of atoms released divided by the atoms present at the beginning of heat treatment multiplied by 100.

(c) Specimen designation, 15999-29.

(d) Specimen used with low-purity charcoal.

(e) Specimen disintegrated during heat treatment.

(f) Specimen designation, 15171-77.

N-5

provide information on the thermal and mechanical performance of the capsule is near completion.

### HIGH-BURNUP IRRADIATION EFFECTS IN FUEL MATERIALS

W. E. Murr, J. E. Gates, and R. F. Dickerson

The objective of this program is to study the radiation stability of ceramic-type fuels under conditions simulating those of the MGCR. Fuels under investigation include uranium dioxide in beryllium oxide ( $\text{UO}_2\text{-BeO}$ ), uranium monocarbide in graphite (UC-graphite), and uranium dicarbide in graphite ( $\text{UC}_2\text{-graphite}$ ). Fuel loadings are about 20 volume per cent in each type of specimen. Four capsules containing electrical heaters and thermocouples to maintain and measure specimen-surface temperatures at 1500 F in a specified neutron flux were included in the program. Each capsule contained a total of six irradiation specimens, two of each fuel material. The specimens consisted of four cylindrical fuel pellets, each 0.222 in. in diameter by 0.250 in. long, sealed in Type 316 stainless steel tubing under a helium atmosphere. The irradiation of one capsule in the BRR has been completed; the remaining three capsules are being irradiated in the MTR.

Examination of specimens from the capsule irradiated in the BRR has been performed, and results of the examination of the specimens were reported previously in BMI-1366 and BMI-1377. Specimens in the BRR capsule achieved uranium burnups ranging from 1.1 to 1.7 a/o at temperatures ranging from 1300 to 1550 F. In general, the specimens were relatively unaffected by the irradiation, although individual pellets of UC and  $\text{UC}_2$  in graphite exhibited diametral decreases of 1.2 to 2.0 per cent as well as embrittlement of the graphitic matrix. The pellets of  $\text{UO}_2\text{-BeO}$  did not exhibit density or dimensional changes, and no matrix change was observed. About 0.40 to 1.25 per cent of the krypton-85 fission gas that was produced escaped from the specimens. Fission-gas release was lowest in the  $\text{UO}_2\text{-BeO}$  specimens.

The remaining three capsules of the irradiation program have been in operation at the MTR since the beginning of MTR Cycle 125 (July 24). During the current cycle (127), the capsules are operating under the temperature and power requirement conditions shown in the tabulation below.

<u>Capsule</u>	<u>Thermocouple Temperature (a), F</u>	<u>Heater Power Consumption (b), w</u>
BMI-31-1	1400-1500	440
BMI-31-2	1370-1500	2000
BMI-31-3	1385-1490	2500

(a) Specimen-surface temperature is 25 to 30 F higher.

(b) Each capsule contains three heaters, rated for 1 kw each.

N-7

From the tabulation, it is evident that the capsules are operating at or near the intended temperatures, although the external heat requirements for Capsules BMI-31-2 and BMI-31-3 indicate that they were placed in a lower flux than anticipated. Consequently, the specimens in these two capsules are undergoing burnup at a lower rate than specimens from Capsule BMI-31-1. Currently, all three heaters in the capsules, and four of the six thermocouples in each capsule are operating satisfactorily.

### DIFFUSION OF FISSION PRODUCTS IN CLADDING MATERIALS

S. G. Epstein, A. A. Bauer, and R. F. Dickerson

An investigation of the diffusion of fission products in "A" Nickel cladding material is being conducted. Fission products were introduced into "A" Nickel foils for this study by irradiation recoil from enriched uranium in contact with the nickel.

A diffusion couple was prepared from two irradiated 5-mil "A" Nickel foils by pressing the foils together at 800 C under an applied load of 10 tons. A previous attempt to bond at a lower temperature was unsuccessful. Microscopic examination revealed that bonding was essentially complete, and extensive grain growth was evident across the couple interface. The couple was encapsulated in a quartz tube which was evacuated through an end joint and sealed at this joint. After heating to a temperature of 2000 F and maintaining this temperature for 2 weeks to allow diffusion of the fission products within the "A" Nickel, the tube was opened and the couple removed. A deposit of radioactive material was detected on the inner walls of the quartz tube and on the "A" Nickel couple surfaces by gamma scanning. The deposit was identified as consisting of mainly cerium isotopes and a small amount of zirconium.

After swabbing the surface of the diffusion couple to remove deposited materials, a plastic mask was applied, leaving exposed only the center portion of the "A" Nickel which had been in contact with the uranium foil and which should contain the fission recoils. The couple was suspended in an electrolytic cell with each "A" Nickel surface facing a lead electrode, the couple being equidistant from both electrodes. The electrolyte was a 10 w/o sulfuric acid solution containing 22 g per liter of NaCl. Etching times were selected to dissolve five equal layers from the "A" Nickel couple as previously determined on an unirradiated control sample. However, after the third time interval of 24 min the exposed metal had completely dissolved and only three equal layers of metal had been obtained. This suggests that the irradiated "A" Nickel is more active chemically than the "A" Nickel used in calibrating the etching procedure.

Aliquots of solution were taken after each etch interval for analysis. A gross fission-product analysis was performed using a gamma scintillation counter. Values of 1.4, 1.2, and  $1.8 \times 10^7$  cpm were obtained for the outer third, the center third, and the inner third layers of the couple, respectively. Since the maximum range of fission recoils into nickel is about  $10 \mu$ , roughly 0.4 mil, the fission recoils were all located in the inner third layer of the couple before annealing. This layer was expected to retain the largest fraction of the fission products. The fact that nearly as much fission-product activity was found in the other two layers, however, indicates that a great deal of fission-product diffusion took place during the 2-week anneal at 2000 F. The higher

activity shown by the outer layer as compared with the center layer etched from the couple may have been the result of incomplete removal of the radioactive deposit on the surface of the couple.

Gamma scanning revealed that the etch solutions contained relatively large amounts of isotopes of barium, cerium, niobium, and zirconium. Relative values obtained with the gamma scintillation counter for small samples of solution taken from the first, second, and third etchant solutions, respectively, were 158,000, 91,000, and 115,000 cpm of combined niobium and zirconium isotopes and 60,000, 77,000, and 123,000 cpm of cerium isotopes. Since cerium was found to be an abundant fission product present in all layers, it has been decided to analyze for this element by chemical means. This analysis is now in progress.

#### CARBON-TRANSPORT CORROSION STUDIES

N. E. Miller, D. J. Hamman, J. E. Gates, and W. S. Diethorn

Selected metal and graphite specimens have been exposed to radiation in helium-filled quartz tori designed to promote convective flow of the helium and gaseous impurities past the specimens. The initial results were reported in BMI-1366. Additional metallography and microhardness tests are under way.

O-1 and O-2

## O. ENGINEERING ASSISTANCE TO KAISER ENGINEERS

Reactor-Flow Studies

L. J. Flanigan and H. R. Hazard

Flow studies, using air, in a quarter-scale model of the Partially Enriched Gas-Cooled Power Reactor are being conducted at Battelle to provide design data for the prototype. Previously reported work includes model construction and the completion of a program to determine the effect of hole location in the core-support cylinder on core-flow distribution, mixing, and pressure drop.

In September, mixing studies were run with the final core-support cylinder in place. In a study of transition from two-loop to one-loop operation, flow was stable under all conditions and core-flow distribution varied smoothly from that for two-loop operation to that for one-loop operation. The shield flow was varied from 0 to 5 per cent with no observable difference in core-flow distribution. Tests were run at reduced flow rates to check the effect of Reynolds number on pressure drop and core-flow distribution. Upper-plenum velocities were measured and studies made of the flow patterns using  $\text{TiCl}_4$  smoke.

In early October, studies of flow in the thermal-shield flow passage will be completed and velocities in the lower and inlet plenums will be measured.



## P-1

## P. DEVELOPMENTAL STUDIES FOR THE SM-2

S. J. Paprocki

The work discussed in this section of the report is being conducted for Alco Products in support of the SM-2 program. It involves the development of fuel, absorber, and suppressor materials.

Fabrication techniques are being developed for full-scale reference fuel elements consisting of a Type 347 stainless-UO<sub>2</sub> dispersion core clad with Type 347 stainless. The UO<sub>2</sub> incorporated in the dispersion core is of spherical shape and manufactured by Mallinckrodt. A boron burnable poison is incorporated in the core in the form of a dispersion of ZrB<sub>2</sub>.

Stainless-Eu<sub>2</sub>O<sub>3</sub> is being considered as the control material and flux suppressor. Techniques are being investigated for the consolidation and spheroidization of the Eu<sub>2</sub>O<sub>3</sub> powder.

Two noninstrumented capsules containing eight fuel specimens each are being irradiated in core positions of the MTR. An instrumented (thermocouples and auxiliary heaters) capsule has been inserted in a beryllium-reflector position of the ETR. The estimated flux in both the MTR and ETR positions ranges from 3 to 5 x 10<sup>14</sup> nv.

Materials Development

S. J. Paprocki, D. L. Keller, G. W. Cunningham, D. E. Lozier,  
A. K. Foulds, W. M. Pardue, and J. M. Fackelmann

Techniques are being developed for the fabrication of fuel elements, suppressor components, and control rods for the SM-2 reactor. Selection of reference materials has been made, and specifications will be established on the basis of the fabrication studies.

Fuel Materials

The reference fuel element contains a core of approximately 26 w/o UO<sub>2</sub> and 1 w/o ZrB<sub>2</sub> dispersed in a Type 347 prealloyed stainless powder matrix (0.030 in. thick) and clad with 0.005-in. -thick Type 347 stainless steel.

The use of arc-melted high-purity ZrB<sub>2</sub> which has been crushed to minus 100 plus 200-mesh size appears to be the most desirable method of incorporating ZrB<sub>2</sub> into the core matrix. A core specimen sintered and roll clad at 2150 F contained massive ZrF<sub>2</sub> particles which were not fractured, did not contain any evidence of an oxide phase, and appeared to be uniformly distributed. Chemical analyses of the sintered compacts showed a decrease in boron content of approximately 5 w/o. However, this value is within the range of accuracy for the chemical analyses.

Small-scale specimens are being used to determine the effect of fabrication variables such as temperature and particle size of powders. Metallographic examination of a series of compacts pressed and sintered at temperatures of 2000 to 2200 F indicates that all core structures containing spherical  $\text{UO}_2$  are superior to those containing high-fired and other types of  $\text{UO}_2$  fabricated at the 2200 F temperature. However, there is a definite improvement even in the spherical  $\text{UO}_2$  dispersions as the temperature is increased to 2200 F. At 2000 F, the  $\text{UO}_2$  fractures even though it resists stringering, but at 2200 F, there is relatively little fracturing and virtually no stringering. Some improvement is noted in structures rolled at 2000 F when higher sintering temperatures are used. Chemical analyses are in progress to determine whether decreasing the rolling temperature has any pronounced effect on boron losses of the various compounds.

A series of cores containing 26 w/o  $\text{UO}_2$  dispersed in matrices of 100 w/o minus 44- $\mu$ -diameter stainless powder, 100 w/o 105 to 150- $\mu$ -diameter stainless powder, and 20 w/o 105 to 150- $\mu$ -diameter-80 w/o minus 44- $\mu$ -diameter stainless powder were fabricated by sintering, and roll cladding at 2200 F. Metallographic investigation of the roll-clad cores indicated that an improved structure was obtained with the minus 44- $\mu$  stainless powder. The use of 100 w/o 105 to 150- $\mu$ -diameter matrix powder resulted in considerable fracturing and stringering of the  $\text{UO}_2$ , while the 20 w/o 105 to 150- $\mu$ -diameter-80 w/o minus 44- $\mu$ -diameter powder exhibited slightly less fracturing and stringering of the  $\text{UO}_2$  shot.

Full-size fuel-element plates are now being produced within specified tolerances. Camber on the plates produced to date has varied from 0.004 to 0.070 in. The last three plates produced had cambers of 0.012, 0.006, and 0.004 in. The plate widths are averaging 2.635 in.

Fully enriched as well as depleted  $\text{UO}_2$  in sufficient quantity to prepare plates for welding studies and critical-assembly tests has been received, and picture-frame packs are being machined for their fabrication.

#### Fabrication of Irradiation Specimens

The specimens for the six remaining ETR irradiation capsules have been roll clad and flat annealed. These plates are presently being radiographed to locate the exact position of the cores for machining to final size of 1.506 by 0.575 in. The specimens containing the suppressor section will be 2.506 in. in length. Capsule suspension and centering holes, 0.032 and 0.025 in. in diameter, respectively, will be drilled in the frame material on both ends of the specimens followed by examination and identification procedures such as: chemical analysis of the boron content, microscopic examination of representative specimens of each type, and radiographs, photomacrophs, and leak checks of all specimens.

As each series of specimens is completed, the specimens will be further identified by file notches and preirradiation measurements will be made in preparation for encapsulation.

### Development of Control and Suppressor Materials

The use of a  $\text{Eu}_2\text{O}_3$ -stainless steel dispersion as a control material as well as a possible flux suppressor in the fuel elements of the SM-2 reactor has led to the need for  $\text{Eu}_2\text{O}_3$  of a minus 100 plus 200-mesh particle size.

Since  $\text{Eu}_2\text{O}_3$  is normally produced as a finely powdered material, a study is being conducted to determine the most satisfactory method of increasing the particle size. The material used to date has been produced by mixing the minus 400-mesh  $\text{Eu}_2\text{O}_3$  powder with Ceremul "C" and water using  $12 \text{ cm}^3$  of binder and  $40 \text{ cm}^3$  of water for each 100 g of powder. The powder is then dried for 1/2 hr at 150 F, pressed at 6 tsi, and crushed to minus 30 plus 80 mesh. The particles of this mesh fraction are then sintered in a platinum boat at 1800 C for 1 hr and screened to the final particle size of minus 100 plus 200 mesh. This process produces a dense material; however, the particles are irregular in shape and have sharp edges which have a tendency to fracture upon rolling and limit the over-all density and quality of the dispersions. The particles can be improved by tumbling before sintering. This action has a tendency to round the sharp edges and polish the particle surfaces; however, the particles remain irregular in shape. Screens or abrasive material added to the tumbling procedure tend to break the particles rather than cause them to approach the ideal spherical shape.

A commercial source has been found which will supply fired monoclinic  $\text{Eu}_2\text{O}_3$  in the desired particle size at approximately the cost of the finely powdered material. A 100-g sample of this material has been ordered for evaluation purposes.

The study will continue in an attempt to improve upon the particle shape, and an inquiry will be made of the various commercial suppliers in an attempt to find an economical source of spherical  $\text{Eu}_2\text{O}_3$  particles of satisfactory particle size, purity, and density.

### Encapsulation Studies

A. K. Hopkins, W. E. Murr, and J. H. Stang

In order to determine the radiation stability of fuel materials developed for the SM-2 program, a ten-capsule program has been initiated. Fuels of interest to the SM-2 program include dispersions of 26 to 40 w/o uranium dioxide dispersed in Type 347 stainless steel with additions of boron compounds as burnable poison. The ten-capsule program includes three noninstrumented capsules to be irradiated in the MTR and seven instrumented capsules to be irradiated in the ETR. Capsules for the ETR irradiation series contain heaters and thermocouples to maintain and monitor specimen-surface temperatures of about 650 F. The MTR capsule-irradiation series will rely upon fission and gamma heat to maintain specimen-surface temperatures.

The three MTR capsules, BMI-32-1, BMI-32-2, and BMI-32-3, arrived at the test reactor during July. Capsules BMI-32-1 and BMI-32-2 have been in operation in

## P-4

the reactor since the beginning of Cycles 126 and 127, respectively. The third capsule of the series, BMI-32-3, is scheduled for insertion into Position L-58 during the Cycle 129 shutdown (October 12). The reported thermal-neutron flux for these positions ranges from 3 to  $5 \times 10^{14}$  nv. According to present estimates, the capsules will remain in the reactor approximately seven cycles to achieve the intended burnup levels. However, the schedule may be modified when flux-perturbation data are received from three mock-up capsules that were irradiated at NRTS during September.

The first of the seven instrumented capsules, BMI-32-4, was shipped to the ETR early in August, and was placed into the reactor at the beginning of Cycle 20 (September 14). The capsule contained six stainless steel-clad fueled specimens, the top four of which were separately compartmented and provided with electrical heaters and thermocouples. Temperatures registered by thermocouples located in NaK about 1/32 in. away from each of the top four specimens are shown in the tabulation below prior to and following the addition of auxiliary heat to the capsules.

Thermocouple	Temperature Indicated, F	
	Without Auxiliary Heating <sup>(a)</sup>	With Auxiliary Heating (About 1 Kw)
1	415	400
2	430	380
3	265	300
4	Failed shortly after irradiation began	

(a) Temperatures of 400 to 425 F correspond to a specimen-surface temperature of about 650 F, the design temperature level.

After several days of operation under partial auxiliary heating, Thermocouple 3 failed, and Thermocouple 1 indicated a temperature of 650 F for a brief period of time. Thermocouple 1 then returned to a temperature reading of 400 F and has maintained a steady position. There is no explanation for the short excursion unless the couple momentarily shifted position.

A temperature drop occurs from Specimen 1 down to Specimen 4. The capsule is baffled between the heated specimens (1 through 4) and unheated region; consequently, it is believed this temperature differential is the result of a decrease in flux across the length of the capsule.

Six more instrumented capsules are scheduled for ETR irradiation. The assembly of these six capsules will be initiated during October and, according to present estimates, will be completed before the end of the calendar year.

## Q-1

## Q. GAS-COOLED REACTOR PROGRAM

D. L. Keller

Studies for Aerojet-General Nucleonics (AGN) directed toward the development of compact gas-cooled reactors are reported in this section. The activities on the various tasks are reported under "Materials Development Program" and "In-Pile-Loop Program".

MATERIALS DEVELOPMENT PROGRAM

D. L. Keller

Work has been completed on the fabrication of thin-walled  $\text{UO}_2$  pellets. It was concluded through experimental work and consultation with several commercial fabricators that 0.162-in. -OD pellets with 0.040 to 0.100-in. -diameter holes can be fabricated by conventional pressing and sintering techniques. During September a program was initiated to study the fabrication of  $\text{BeO-UO}_2$  fuel pellets. Parallel studies will investigate the irradiation effects of this material.

Progress on encapsulation and irradiation-effects studies is reported with particular attention given to the results of irradiating three solid  $\text{UO}_2$  pins and three annularly loaded  $\text{UO}_2$  pins all canned in Inconel and contained in Capsule BMI-27-2.

A hazards evaluation for the GCRE critical-assembly experiments covering the ML-1B program was completed during the past month. An interim report covering the current series of ML-1A experiments was started, and a few experiments pertinent to the evaluation of 1B fuel elements were performed.

Fabrication of  $\text{UO}_2$  Pellets

H. D. Sheets and C. Hyde

The present objective of this program is to establish the feasibility of cold pressing and sintering  $\text{UO}_2$  pellets 0.162 in. in OD with hole diameters varying from 0.040 to 0.130 in.

Pressing dies for compacting pellets with an OD of 0.200 in. and an ID of 0.050, 0.077, 0.106, 0.136, or 0.166 in. were designed and machined. These dimensions were chosen on the assumption that the  $\text{UO}_2$  pellets would have a linear shrinkage of 20 per cent during sintering.

## Q-2

Mallinckrodt ceramic-grade light  $\text{UO}_2$  was prepared for pressing by ball milling for 15 hr in a rubber-lined mill with  $\text{Al}_2\text{O}_3$  balls, adding 3 w/o of camphor dissolved in methanol, drying at room temperature, and screening through a 100-mesh screen.

For pellets having a hole diameter of 0.050, 0.077, or 0.106 in. , no difficulties were encountered in pressing at 20,000 or 40,000 psi, or in ejecting from the die. The pellets with a 0.136-in. -diameter hole, however, were quite fragile and broke readily during ejection and subsequent handling. The pellets with a 0.167-in. -diameter hole were extremely fragile, and it was necessary to press them at 60,000 psi to obtain specimens strong enough to remain sound when ejected from the mold.

The attempt to sinter the specimens in hydrogen at 3000 F was unsuccessful. An interruption of the flow of hydrogen into the furnace occurred during the run, admitting air and oxidizing all of the specimens. Normally, no difficulties would be anticipated in sintering specimens of these shapes.

Two equipment manufacturers and four fabricators were contacted to obtain their opinions on the feasibility of producing thin-walled pellets. On the basis of the laboratory work and these discussions, two problems appear to be critical in determining whether pellets of a given wall thickness can be manufactured:

- (1) Can uniform mold fill be obtained?
- (2) Is the green strength of the specimen sufficient to permit ejection and handling?

Obtaining uniform mold fill did not appear to be a problem on any of the specimens prepared. One of the equipment manufacturers stated, however, that his equipment provided for a die with a retractable pin, so that the die cavity could be filled before the pin is put into position. This technique is reported to have eliminated problems associated with nonuniform filling of the die.

The problem of ejecting and handling the pressed pellet is related to the kind and amount of temporary binder used and to the thickness of the walls. The experimental work here, in which camphor was used as the temporary binder, indicated that if the walls were less than 0.030 in. thick, the pellets were fragile and easily broken.

One of the four fabricators contacted stated that a 0.162-in. -diameter pellet with a 0.130-in. -diameter hole could be fabricated successfully by pressing. The other three were less optimistic. The most conservative estimate was that a 0.080-in. hole would be the maximum.

All of the fabricators agreed that it probably would be more economical to extrude these shapes than to press them. This might be true if a batch of 5 lb or more could be used. The people contacted were not aware of the limitations on the size of the batch imposed by nuclear considerations.

Summarizing briefly, it is believed that 0.162-in. -diameter  $\text{UO}_2$  pellets with a hole diameter in the range from 0.040 to 0.100 in. can be fabricated at the present state

## Q-3

of the art. A research program would be required to develop techniques for producing thinner walled specimens.

No further work is planned on this program.

Fabrication of BeO-UO<sub>2</sub> Fuel Pellets

A. K. Smalley and W. H. Duckworth

Fuel pellets consisting of UO<sub>2</sub> particles dispersed uniformly in a dense BeO matrix are being fabricated for a capsule irradiation test. The nominal fuel loading is 25 volume per cent of fully enriched UO<sub>2</sub>, and the desired pellet dimensions are 0.160 in. in diameter by 0.250 in. long.

Three types of pellets were prepared for the proposed capsule loading. These differed in the average diameters of the UO<sub>2</sub> particles and the BeO crystals, approximately as follows:

- (1) UO<sub>2</sub> particles about 200  $\mu$ , BeO crystals about 15  $\mu$ .
- (2) UO<sub>2</sub> particles less than 10  $\mu$ , BeO crystals about 10  $\mu$ .
- (3) UO<sub>2</sub> particles less than 10  $\mu$ , BeO crystals about 5  $\mu$ .

Bulk-density measurements on sintered pellets indicated that Groups (2) and (3), above, had average bulk densities, based on eight pellets, of about 99 per cent of the calculated theoretical density. Group (1), containing 200- $\mu$  fuel, had an average density of about 83 per cent of theoretical. Metallographic examination of a polished section of this material showed large voids and cracks in the BeO matrix in the vicinity of the UO<sub>2</sub> particles, and appreciable porosity within the UO<sub>2</sub> particles.

The cracks and voids in the BeO matrix were attributed to badly mismatched sintering shrinkages of the BeO and the fuel particles. Specimens containing the 200- $\mu$  fuel will be remade. About 10 w/o of Be(OH)<sub>2</sub> will be incorporated in the UO<sub>2</sub> prior to mixing with the BeO matrix, in an attempt to enhance the sintering shrinkage of the fuel particles. A detailed procedure for fabricating these specimens will be given in the next monthly report.

Encapsulation Studies

D. W. Nicholson, P. B. Shumaker, J. F. Lagedrost,  
and J. H. Stang

Irradiation of Clad Pin-Type Specimens Containing  
Dense UO<sub>2</sub>

Review of the irradiation history of Capsules BMI-27-1 and BMI-27-2 continued during September as a part of the over-all postirradiation studies. Each capsule contained six pins fabricated by cladding a stack of six UO<sub>2</sub> pellets (each pellet being about 100 mils in diameter and 3/16 in. long) and was designed to maintain specimen-surface temperatures at 1700 F. Actually, as reported during the irradiation period, the thermal behavior of these capsules was erratic and oftentimes unexplainable.

In the case of BMI-27-2, there was no indication from thermocouple-monitored temperatures that 1700 F was exceeded any time during its five cycles of irradiation. At the start of irradiation of BMI-27-1, the thermocouples indicated temperatures between 1700 and 1800 F, but the capsule was quickly repositioned to rectify the situation. After this, only the lower two specimens were maintained in the 1400 to 1600 F range; temperatures of the other specimens, which were located well above the peak flux in the irradiation position, ranged from 1000 to 1400 F.

Hot-cell examinations of the capsules (Capsule BMI-27-1 was opened during September) revealed that the majority of the specimens were severely damaged, possibly as a result of having been overheated during exposure. In the case of BMI-27-1, the situation is further complicated by the fact that an indeterminate amount of NaK had leaked from the inner specimen-containing capsule into the inert-gas annulus which separates this shell from the water-contacting shell. While this loss of NaK from the specimen chamber occurred, there is reason to believe that only the top two or three specimens along the capsule axis could have been completely uncovered and, consequently, required to dissipate their heat without benefit of the liquid metal. The fourth and sixth specimens along the axis as well as the top two suffered considerable damage; the third and fifth specimens were intact.

In a further study, an evaluation was made of the possibilities for high rates of fissioning at the ends of the pellet stack within individual specimens. While the problem was treated in a simplified way, the results indicate that end effects could, under some conditions, have assumed importance in the over-all picture. The investigation of such effects is continuing.

Irradiation of UO<sub>2</sub>-Graphite Specimen Assemblies  
With an Integral Corrosion-Gas-Flow System

Work continued during September on the design of capsules for the elevated-temperature irradiation of specimens formed by cladding a stack of three SiC-coated graphite-8 w/o UO<sub>2</sub> wafers with Hastelloy X (Inconel 702 has been dropped from use); the wafers are 1-3/8 in. in diameter and 1 in. long. Each specimen assembly will also

## Q-5

include two small Hastelloy X tubes run along its length to form an integral loop for the circulation of GCRE reference gas pressurized to 400 psia. Four capsules are now involved; each will contain one specimen assembly as described above. During irradiation specimen temperature control (at a nominal 1700 F) will be achieved through regulation of the helium-argon ratio in the annulus separating the Hastelloy X cladding and the outer capsule shell.

Laboratory mock-up experiments to evaluate the thermal characteristics of a simulated capsule have now been completed. In these tests the desired internal temperature of 1700 F was produced with variations in annulus-gas composition and heat input (from sheathed resistance heaters). However, experiments in which a temperature of 1700 F is maintained by gas-mixture control compensating for fluctuating heat input have not yet been conducted. These final experiments are now scheduled for early October.

Design of the capsule support equipment is nearly completed and a hazards analysis is well under way. It is anticipated that one capsule system will be ready for irradiation (at the Battelle Research Reactor) during the first week in November. This first irradiation, which will last for a relatively short time (perhaps 60 days), will provide in-pile experience concerning various operational characteristics. According to present plans, it will be followed by a long-term (nominally 5500 hr) irradiation of three capsules arranged in a vertical stack.

#### Irradiation of Specimens Contained UO<sub>2</sub> in Graphite

Capsule BMI-29-1, containing six SiC-coated graphite pins fueled with 8 w/o highly enriched UO<sub>2</sub> and clad with Inconel 702, Hastelloy X, and Carpenter-20 Cb (two each), was discharged from the MTR on September 22 after a two-cycle irradiation. It will be returned to the BMI Hot-Cell Facility about October 7 for examination.

An initial objective of this experiment was to achieve 15 per cent fission burnup of the fuel in the specimens. This burnup would have required at least three normal MTR cycles under the conditions of the irradiation. However, it was decided to remove the capsule after two cycles because recent high-temperature out-of-pile experiments with SiC-coated graphite indicate that the coating contributes to corrosion of the inner surfaces of the cladding.

It is estimated that the peak flux specimen (approximately 1775 F surface temperature) in Capsule BMI-29-1 achieved slightly over 9 per cent fission burnup during the two-cycle exposure. Individual specimen-surface temperatures were fairly constant in-pile, and ranged from approximately 1575 to 1775 F. Hot-cell examination is scheduled to start late in October.

#### Irradiation of Specimens Containing MCW Spherical UO<sub>2</sub> Dispersed in Stainless Steel

Because of scheduling difficulties, Capsules BMI-33-1 and BMI-33-2 were not inserted into MTR during September as originally expected. These capsules are equipped

## Q-6

with thermocouples and heaters, and each contains plate-type stainless steel-clad specimens fueled with stainless steel-UO<sub>2</sub> (30 w/o highly enriched material) dispersions. Two types of UO<sub>2</sub>, MCW spherical UO<sub>2</sub> and ORNL hydrothermal UO<sub>2</sub>, are involved.

It is now anticipated that the irradiations will commence in mid-October and will terminate about January 1. The target irradiation temperature is 1650 F.

#### Irradiation of Specimens Containing UO<sub>2</sub> Dispersed in BeO

Plans are under way to irradiate four to six Hastelloy X-clad pins containing UO<sub>2</sub>-BeO (25 volume per cent highly enriched UO<sub>2</sub>) pellets, 0.160 in. in diameter. The temperature specified for this irradiation, which will be conducted in the Battelle Research Reactor, is 1750 F. According to present plans, the exposure will commence about November 1 and will consist of four reactor cycles in a peak unperturbed flux of approximately  $4 \times 10^{13}$  nv.

The capsule design, which is now being formulated, will be based on the double-wall scheme in which the specimens are immersed in NaK contained in an inner sealed shell. In this design, a narrow helium annulus separates the shell from the outer water-contacting shell. Auxiliary sheathed resistance-wire heaters and thermocouples will be incorporated into the system.

#### Effects of Irradiation

J. H. Saling, J. E. Gates, and R. F. Dickerson

The study of the radiation stability of fuel-element materials for compact gas-cooled reactors includes (1) the evaluation of irradiated solid and annularly loaded UO<sub>2</sub> specimens clad with Inconel, and (2) the evaluation of in-pile-loop subassemblies containing PWR-type fuel pins of solid UO<sub>2</sub> clad with Inconel.

#### Capsule Program

Six specimens were irradiated in Capsule BMI-27-2. Four of the specimens were composed of solid UO<sub>2</sub> clad with Inconel and two were composed of UO<sub>2</sub> annularly loaded with an MgO core and clad with Inconel. The specimens were positioned end to end in a stainless steel expanded-sheet holder which was immersed in NaK inside a stainless steel capsule. The sealed inner capsule containing the specimens was positioned inside another stainless steel capsule. The outer capsule was designed to maintain a gas annulus around the inner capsule to act as a heat barrier. The experiment was designed to operate with the center of the capsule in the peak-flux position of the A-7-NW hole at the MTR. In this position the peak temperature obtained in the fuel specimens would normally be at the capsule center line. In order to reduce the temperature gradient over the length of the specimen stack, the gas annulus in approximately 5 in. of the center region of the capsule was reduced. This provided a better heat-transfer path for

## Q-7

the central region of the capsule, resulting in a smaller temperature gradient along the capsule length.

As reported earlier, the two specimens near the top and the two specimens near the bottom of the capsule failed. The top specimen was composed of solid  $\text{UO}_2$  clad with Inconel and the second specimen from the top was composed of  $\text{UO}_2$  annularly loaded with an MgO core and clad with Inconel. Both of these specimens failed apparently by melting at a point near the bottom of the fueled section of each specimen. The third and fourth specimens from the top of the capsule were both composed of solid  $\text{UO}_2$  clad with Inconel. These specimens were located in the central section of the capsule where the gas annulus has been reduced. Both of these specimens appeared to be in very good condition. Measurements indicated that there was no change in density or length of the specimens and less than 1.0 per cent change in diameter. The fifth specimen from the top of the capsule was composed of  $\text{UO}_2$  annularly loaded with an MgO core and clad with Inconel. This specimen exhibited no evidence of melting but was ruptured along the entire length of the fueled section of the specimen, exposing the MgO core. The sixth or bottom specimen in the capsule was composed of solid  $\text{UO}_2$  clad with Inconel. This specimen failed apparently by melting at a point near the top of the fueled section of the specimen.

Examination of the failed specimens revealed that with the exception of the bottom section of the top specimen, there was no  $\text{UO}_2$  remaining inside the cladding. Examination of the bottom of the capsule revealed a large quantity of fragments of  $\text{UO}_2$  mixed with melted globules of metal. The material had a very coarse granular appearance.

Fission-gas sampling of the capsule and of the two good specimens indicated that measurable quantities of gaseous fission products were released from the  $\text{UO}_2$ . The quantity of gaseous fission products obtained from sampling the capsule is considered to be unreliable, since the gas sample was obtained through the bottom of the capsule and this area was filled with fragments of  $\text{UO}_2$ . The results of fission-gas sampling of the two good specimens have been obtained, and will be reported as a fraction of the total fission gas produced in the samples as soon as burnups are determined.

The burnup of the uranium in the two undamaged specimens from Capsule BMI-27-2 is being determined by isotopic analysis. Uranium oxide from the top specimen will also be analyzed. Results of the isotopic analyses should be available in 4 to 6 weeks.

Metallographic examination of  $\text{UO}_2$  from the top specimen in the capsule and of  $\text{UO}_2$  from the fourth specimen from the top of the capsule has been completed. The  $\text{UO}_2$  appeared unaffected by irradiation.

Metallographic examinations of two sections of the cladding from each of the four failed specimens and one section of the cladding from each of the two unfailed specimens have been completed. In the case of the failed specimens, one transverse section of the cladding was removed from each of the failed areas for metallographic examination. Another transverse metallographic section was removed from these specimens about 0.75 in. from the failed area toward the top end of the specimens. This was done in order to study the structure of the cladding at and away from the melted or failed areas. One transverse section of the cladding was removed near the center of the fourth specimen from the top of the capsule, and one longitudinal section was removed from the third specimen from the top of the capsule. The longitudinal section covered an area from

## Q-8

approximately 0.25 in. above the top of the fuel section to approximately 0.25 in. below the top of the fuel section. The purpose of this examination was to determine if any differences occurred in the grain structure of the cladding adjacent to a nonfueled area as compared to that adjacent to a fueled area.

In general, there was a marked difference in the structure of the cladding in the melted area as compared to the structure occurring about 0.75 in. above the failed area. The structure of the cladding in the area of failure showed considerable grain growth with evidence of a small amount of precipitates in the grain boundaries. Very little grain growth was observed in unfailed areas except near the outer surface of the cladding.

The longitudinal metallographic sample from the third specimen from the top of the capsule showed very little evidence of grain growth in areas adjacent to or removed from fueled areas. However, there was again an indication of grain growth occurring at the outside surface of the cladding. The transverse section of the fourth specimen showed definitely larger grain structure toward the outside surface of the cladding.

These observations might indicate that either the outside surface of the cladding was maintained at a higher temperature than the inside surface which was adjacent to the fuel, which is highly improbable, or that there was diffusion of a foreign material into the cladding from the outside.

An emission spectrometer analysis was performed on a section of the cladding from a melted area of the top specimen. The results indicated that the cladding was composed of Inconel with a very high (5 to 25 w/o) silicon content. Inconel diluted with 11 w/o silicon is very similar to Nicrobrazo-30, which has a melting temperature of approximately 1900 F. Since temperatures as high as 1850 F were measured during the irradiation of the capsule, the cause of failure now appears to be related to the addition of silicon to the cladding material in amounts sufficient to lower the melting point of the cladding to a point equal to or near the nominal irradiation temperature of 1800 to 1850 F.

The source of the silicon is unknown at present, but an examination of unirradiated annularly loaded fuel pins will be conducted in order to determine whether the silicon could have come from the MgO core of the fuel pins. If the MgO core of the annularly loaded specimens contained a high percentage of silicon, the silicon from the core of the fifth specimen from the top of the capsule, which ruptured during irradiation, could have reacted with the cladding of other specimens as indicated by the grain growth observed during the metallographic examination. Apparently the temperature of the center two specimens in the capsule was low enough to prevent melting. The cause of rupture of the fifth fuel pin is unknown at this time, but a similar type of failure was recently observed when an unirradiated annularly loaded fuel pin was heat treated at 1800 F. The source of this failure is still being investigated.

### Loop Program

A postirradiation evaluation of the in-pile-loop subassembly 1B-1αT has been initiated. This element consisted of 19 fuel pins containing UO<sub>2</sub> pellets clad with Inconel.

## Q-9

Sixteen of the 19 fuel pins had spacers brazed to them in order to insure proper channel spacing. The configuration of the element was such that there were 12 fuel pins in the outer ring of the element, 6 fuel pins in the second ring, and 1 fuel pin in the center.

Channel-spacing measurements consisted of depth measurements from the surface of the center pin to a tangent to the surface of the outer ring, depth measurements from the surface of the fuel pins in the second row to a tangent to the surface of the outer ring, and spacings between the fuel pin composing the outer ring of the element. All measurements were taken at three locations along the length of the element. Difficulties were encountered in obtaining these measurements both before and after irradiation. The difficulties were caused in part by turning of the fuel pins during handling of the element which produced changes in spacings in either direction and to difficulties in making measurements tangent to the outer surface of the assembly. As a consequence it is difficult to reach any conclusions regarding changes in fuel-rod spacing as a result of irradiation.

During irradiation of the 1B-1αT subassembly, high fission-product activity was noted in gas samples taken from the loop. Subsequent leak checks of the fuel pins revealed that Pins 15 and 16 leaked at a location of corrosive attack which occurred at a point approximately 13 in. from the inlet end of the subassembly. These fuel pins were located adjacent to each other in the outer ring of the element and at approximately 12 o'clock with respect to the reactor. The cause of this attack is believed to be alloying of the Inconel with the braze material. The braze material used was Nicrobraze-30. Metallographic examination of a transverse section of the corroded spacer from Pin 16 revealed that components of Nicrobraze had diffused along the grain boundaries of the Inconel and had produced cracks which followed the grain boundaries. The cracks are believed to be caused by thermal cycling.

An emission spectrometer analysis of a section of the corroded spacer from Pin 16 as well as additional metallography on Pins 15 and 16 are planned.

#### GCRE Critical-Assembly Experiments

R. A. Egen, J. W. Ray, W. S. Hogan,  
D. A. Dingee, and J. W. Chastain

Hazards evaluation for the GCRE critical-assembly experiments covering the ML-1B program was completed during the past month. An interim report covering the current series of ML-1A experiments was started, and a few experiments pertinent to the evaluation of 1B fuel elements were performed.

The ML-1B core is fueled with elements consisting of 19 Inconel X tubes containing enriched  $\text{UO}_2$  and arranged in a hexagonal configuration. In the hazards evaluation the modifications to the present core which are required to mock-up the oxide-pin core for the experimental program were studied and the safety aspects were analyzed.

The interim report which is in preparation includes results of (1) evaluations of reactivity worth of mock-up scissor-acting safety blades for the ML-1, (2) determination

## Q-10

of the composition of production GCRE-1 fuel elements by comparison with critical-assembly elements, (3) measurements of flux and power distributions in a 1B (oxide pin) fuel element, and (4) evaluations of reactivity effects of voids at reflector surfaces in ML-1.

A program of experiments to evaluate the 19-pin 1B element was started in the past month. The fuel pins in the prototype are 0.164-in. -ID by 0.030-in. -wall Inconel X tubes containing  $\text{UO}_2$  fuel pellets. To provide data on these pins in a minimum time the oxide fuel is being mocked up with layers of enriched and natural uranium foil. The enriched foil is 0.004 in. thick by 0.10 in. wide. Two thicknesses of 0.10-in. -wide natural uranium foil were procured, 0.015 and 0.020 in. The active length of the pins is 22.75 in. Using this foil 19-pin fuel assemblies will be simulated with enrichment ratios between the inner 7 and outer 12 pins of 48/24, 93+/30, 73+/20, and 75/20. The ratio of power-production rates between various pins in the 19-pin assemblies will be measured, and data will be obtained from which thermal utilization can be calculated. Also, a comparison of reactivity worth for the different enrichment ratios will be obtained.

It is expected that the interim report will be finished during the coming month. A number of the fuel-pin studies described above will also be completed.

### IN-PILE-LOOP PROGRAM

G. A. Francis

During the period covered by this report, activity on the two in-pile recirculating-gas-loop programs was continued. At the Battelle Research Reactor an Aerojet General Nucleonic's fuel subassembly designated 1B-1 $\beta$ T was irradiated. At the Engineering Test Reactor the hot check was continued. The primary problem being encountered during the check is that of a blower operation. Details on the different phases of the loop programs are described in the following paragraphs.

### BRR Loop Program

S. J. Basham and W. H. Goldthwaite

The recirculating gas loop at the BRR has been used for testing of fuel subassembly for the GCRE program for the past 18 months. During this period five subassemblies have been irradiated. The operation of the last subassembly, the 1B-1 $\beta$ T, was initiated on September 9. The presence of fission gas in the system resulted in termination of the test after 35 hr. Subsequent to the power runs the element was irradiated for 100 min at a reactor power of 2 kw for power-generation studies.

The beta subassembly consisted of a threaded top plug which sealed the subassembly into the loop, a column to which the fuel subassembly was attached, and fuel

## Q-11 and Q-12

pins which were arranged concentrically and surrounded by an insulation liner. The casing of the 19 fuel pins was made of Inconel 702 tubing with integral longitudinal fins on the outside surface. The fins on the outer surface constitute the major difference between the alpha and beta elements.

During initial irradiation of the specimen, steady-state operation was achieved at a coolant flow rate of 1000 lb per hr and a peak pin surface temperature of 1400 F. Loop gas activity during the first 11 hr of operation was in the 1-millicurie range. After 14 hr of operation, a total gas activity of 42 millicuries was observed. The major isotopes present were identified as xenon-133, xenon-135, and krypton-85m.

After a shutdown at 2-1/2 days, loop operation was continued. Steady-state runs were made at peak pin-surface temperatures of 1500, 1600, and 1650 F. The activity level ranged from 9 to 14 millicuries during the final period of operation. Shortly after cycling the peak specimen-surface temperature from 1000 F to 1600 F to 1000 F in 30 min, the loop gas activity increased to 150 millicuries and the experiment was terminated.

During the next normal reactor down period, the beta subassembly was irradiated in the BRR at a reactor power level of 2 kw. The blower was not operating during the run and temperatures in the system reached equilibrium 53 min after reactor startup. The purpose of this run was to allow comparison of the element temperatures with the predicted power generation based on flux measurements.

During October, plans call for removal of the subassembly from the loop and transfer to the hot cell for examination. The future loop use will be for irradiation of specimens now being fabricated by Aerojet General Nucleonics.

ETR Loop Program

J. V. Baum and E. O. Fromm

During September, the hot check of the loop was continued. The hot check consists of loop operation with the reactor at full power and a dummy specimen in the loop test section. The major problem being encountered during the check is the blower operation. During September, the bearings of all three blowers were replaced due to excessive temperatures during normal operation. Subsequent study of the bearings and lubricant show that bearings on two of the blowers were not damaged. Damage to bearings on the third blower might be the result of loosening of the impeller on the shaft. Some change in character of the grease lubricant was observed, but its lubricating quality had remained. It appeared that the change was a result of either excessive temperature or mechanical working of the lubricant. Subsequent to the bearing change, the Blower 1 has operated 274 hr. A period of high-temperature operation occurred early in the run. A second blower was started late in the month. Some difficulties are being encountered in the operation of this blower also.

Plans call for operation of all three blowers for at least 300 hr before insertion of the first test subassembly.

RWD/CRT:all